3

UCID- 21044

PROGRESS REPORT ON THE RESULTS OF TESTING ADVANCED CONCEPTUAL DESIGN METAL BARRIER MATERIALS UNDER RELEVANT ENVIRONMENTAL CONDITIONS FOR A TUFF REPOSITORY

R. D. McCright
W. G. Halsey
R. A. Van Konynenburg

December 1987

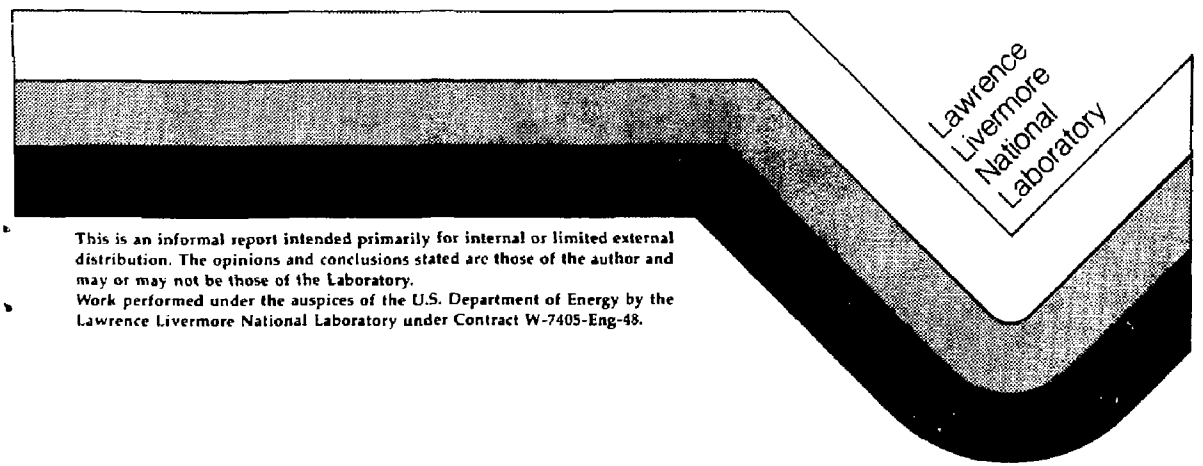

Printed in the United States of America
Available from
National Technical Information Service
U.S. Department of Commerce
5285 Port Royal Road
Springfield, VA 22161

Price Code	Page Range
A01	Microfiche
Papercopy Prices	
A02	001 - 050
A03	051 - 100
A04	101 - 200
A05	201 - 300
A06	301 - 400
A07	401 - 500
A08	501 - 600
A09	601

Prepared by Nevada Nuclear Waste Storage Investigations (NNWSI) Project participants as part of the Civilian Radioactive Waste Management Program. The NNWSI Project is managed by the Waste Management Project Office of the U.S. Department of Energy, Nevada Operations Office. NNWSI Project work is sponsored by the Office of Geologic Repositories of the DOE Office of Civilian Radioactive Waste Management.

UCID--21044

DE88 005272

Contents

(continued)

(continued)

EXECUTIVE SUMMARY

Performance requirements of waste packages at the candidate high level radioactive waste repository located at Yucca Mountain, Nevada are provided in NRC regulation 10CFR60. This regulation specifies that containment of radionuclides will be "substantially complete" for a period of time yet to be determined, but between 300 and 1000 yrs, followed by a "controlled release" for up to 10,000 yr. The goal of the metal barrier task is to test candidate materials, select a material for advanced design activities, and provide performance models and data on that material to provide reasonable assurance that the waste package will meet the requirements. The approach taken by the task is to identify the categories of material degradation and failure that might occur in the repository environment and establish modeling and testing activities to determine which do occur, which are performance limiting, and which candidate materials will best assure meeting the requirements.

This report discusses potential degradation modes for candidate materials being considered for use in waste package containers, and summarizes the results of metal barrier testing activities conducted at LLNL and subcontractor facilities. This work was performed by the Nuclear Waste Management Program at LLNL for the Nevada Nuclear Waste Storage Investigations project of the Department of Energy's Office of Civilian Radioactive Waste Management.

Although the waste package design is not yet final, a typical conceptual design is a closed metal cylinder approximately 65 cm in diameter and 300-500 cm long with walls approximately 1 cm thick. The container body might be made from rolled and welded plate, or it might be cast or extruded. The top and bottom might be forged and welded. All joints except the final closure can be readily annealed to relieve stress. The final closure has been identified as a point of potential limitation in long-term container performance, and steps to alleviate the residual stress and microstructural inhomogeneities at the closure weld are discussed.

The waste package will be placed in a mined geologic environment which is below the surface of Yucca Mountain and well above the water table in a stratum of welded devitrified tuff rock. This location results in a relatively dry condition without hydrostatic or significant lithostatic loads. Decay heat from the spent fuel will raise the temperature of the container surface to a maximum of 250°C after the repository is closed. The temperature will slowly drop and the containers will eventually be cool enough to allow condensation, dripping, or flow of water onto the surface. The corrosion environments anticipated are therefore "warm" air-steam, and "cool" aqueous contact. The groundwater associated with the repository site is near neutral in pH and fairly low in ionic content. The gamma radiation from the waste decay will produce radiolytic alterations in the local environment in the early time period.

A variety of metals have been considered for the container over a 5-yr period. A list of six current candidates has emerged which spans a range of composition/cost/performance in two alloy families. The candidates are: (a) austenitic alloys: AISI 304L and SISI 316L stainless steel and nickel-based alloy 825, and (b) copper-based materials: CDA 102 high purity copper, CDA 613 aluminum bronze, and CDA 715 cupro-nickel. Electrochemical tests such as measurement of anodic polarization curves have been run on the candidate materials, more extensively on the austenitic materials, but to some extent on the copper-based materials also. The tests have been run with and without gamma radiation exposure in environments that are conservative with respect to those anticipated for the repository. Immersion tests in

anticipated and more severe environments have been conducted with visual examination for pitting attack. It appears that under expected conditions the candidate materials are sufficiently resistant to these forms of attack to meet the performance requirements. The tests do indicate however, that if critical ionic species become concentrated in the environment, pitting attack could become more severe. Tests conducted on AISI 304 and 304L revealed TGSCC under accelerated conditions of stress, gamma flux, and water chemistry. These results indicate TGSCC might be possible under actual repository conditions. In response, an approach is being taken to identify critical parameters (such as chloride ion concentration), and to quantify critical values at which localized corrosion modes become limiting.

Relatively little testing work has been performed in the area of phase stability and embrittlement effects. Literature information indicates that under expected material and environmental conditions the candidate materials should not be performance-limited by these effects, but unexpected fabrication, handling, and thermal processes might make some of the candidates susceptible to phase segregation, precipitation of undesirable phases, or embrittlement. The metastable austenitic materials (AISI 304L and 316L), and the aluminum bronze (CDA 613) appear to have more potential for these effects. Further study in this area is being pursued.

In summary, testing of candidate waste package materials has been directed toward sorting the potential degradation modes for the various materials into those which are potentially performance-limiting and those which do not appear to be limiting. This testing is intended to support the process of selecting one (or two) of the candidate materials for use in advanced design activities. One of the major criteria for material selection is expected to be the number and severity of operable degradation modes of the as-fabricated container in the expected environment. The material selected will be further tested to demonstrate adequate performance, determine critical parameters, and provide data for long-term waste package performance modeling.

ABSTRACT

This report discusses the performance of candidate metallic materials envisioned for fabricating waste package containers for long-term disposal at a possible geological repository at Yucca Mountain, Nevada. Candidate materials include austenitic iron-base to nickel-base alloys (AISI 304L, AISI 316L, and Alloy 825), high-purity copper (CDA 102), and copper-base alloys (CDA 613 and CDA 715). Possible degradation modes affecting these container materials are identified in the context of anticipated environmental conditions at the repository site. The proposed location of the repository is above the permanent water table. Low-temperature oxidation is the dominant degradation mode over most of the time period of concern (minimum of 300 yr to a maximum of 1000 yr after repository closure), but various forms of aqueous corrosion will occur when water infiltrates into the near-package environment. The results of three years of experimental work in different repository-relevant environments are presented. Much of the work was performed in water taken from Well J-13, located near the repository, and some of the experiments included gamma irradiation of the water or vapor environment. The influence of metallurgical effects on the corrosion and oxidation resistance of the material are reviewed; these effects result from container fabrication, welding, and long-term aging at moderately elevated temperatures in the repository. The report indicates the need for mechanisms to understand the physical/chemical reactions that determine the nature and rate of the different degradation modes, and the subsequent need for models based on these mechanisms for projecting the long-term performance of the container from comparatively short-term laboratory data.

1. INTRODUCTION

The Department of Energy's Office of Civilian Radioactive Waste Management (OCRWM) is engaged in the development of a geological repository for the storage of U. S. high-level nuclear waste, as directed by the Nuclear Waste Policy Act of 1982. The Nevada Nuclear Waste Storage Investigations (NNWSI) Project is evaluating one of three sites designated by the Department of Energy (DOE) as leading candidates. This site is located in tuff rock at Yucca Mountain in Bullfrog County (formerly part of Nye County) in southern Nevada. Lawrence Livermore National Laboratory (LLNL) has the responsibility for design, testing, and performance analysis of waste packages for the tuff site.

The Environmental Protection Agency (EPA) and the Nuclear Regulatory Commission (NRC) have promulgated regulations that set limits on the release of radionuclides from geological repositories. NRC regulation 10CFR60 specifies that containment of radionuclides will be "substantially complete" for a period of time yet to be determined, with a minimum period of 300 yr and a maximum of 1000 yr. Following this containment period, the regulation limits the release rate of any radionuclide from the engineered barrier system to one part in 100,000 per year of the inventory of that radionuclide present at 1000 yr after permanent closure of the repository. EPA regulation 40CFR191 sets limits for the cumulative releases of specific radionuclides to the "accessible environment" over a period of 10,000 yr after disposal. In addition to requirements for containment and limited release rates and cumulative release, 10CFR60 also specifies that the waste must be retrievable for a period of 50 yr after emplacement. The waste packages therefore must play a role in providing for handling and retrieval capability as well as waste containment and later, release rate limitation.

NNWSI proposes to locate the repository above the water table in the unsaturated zone. The expected waste package environment in this zone has been described by Glassley (1986). We plan to design the repository with a sufficient areal density of radioactive decay heat output that the temperatures at the surfaces of most of the waste packages will remain above the boiling point of water for the first part of the 300- to 1000-yr containment period. The pressure will remain at approximately 1 atm, and the peak temperature will be limited to approximately 270°C (it should be noted that the actual peak temperature will depend on detailed design features that are not yet firmly established). During the containment period, the package environment will thus consist of gamma-irradiated moist air and tuff rock. The initial gamma dose rate will be in the 10^4 rad/hr range for spent fuel and in the 10^3 rad/hr

range for borosilicate glass (Van Konynenburg, 1986). After the packages cool to below the boiling point of water, liquid water in small amounts can be expected to be present as a result of condensation and infiltration (estimated at less than 1 mm per yr), but by then the gamma dose rate will have decayed by at least a factor of 1000. Based upon analysis of water from the saturated zone in the same rock member (the Topopah Spring member of the Paintbrush tuff), it is expected that the water that will be present after the containment period will be a sodium bicarbonate groundwater with its pH buffered near neutral or slightly alkaline, with small concentrations of dissolved salts (e.g., chlorides and sulfates) and silica, and with dissolved atmospheric gases (e.g., oxygen).

Although this environment is expected to be fairly benign, it still appears that corrosion and oxidation are most likely to be the processes that will determine the ultimate containment life of the waste packages. Accordingly, we have entered upon a fairly comprehensive experimental and theoretical effort to study the corrosion and oxidation behavior of candidate materials in this environment in order to be able to narrow the field to one or two materials and to develop a predictive capability for them over the long term.

The two waste forms that are planned to be emplaced in the repository are spent reactor fuel from commercial nuclear power plants and borosilicate glass made from the reprocessed fuel at the West Valley Demonstration Project in New York and the Savannah River Plant in South Carolina. Conceptual waste package designs have been developed for these two waste forms. Both involve a welded outer container having a relatively thin wall (1 cm for most of the candidate materials) since high pressures (internal or external) will not be present.

Candidate materials have been selected for advanced conceptual designs of the waste packages. They include austenitic iron to nickel-base alloys and copper-base materials. This report reviews our progress up to June 1987, in corrosion and oxidation testing of these candidate materials under environmental conditions believed to be relevant to a high-level nuclear waste repository in unsaturated Topopah Spring tuff. We discuss results under both anticipated and non-anticipated conditions. Non-anticipated conditions have been used to accelerate particular degradation modes and to serve as bounding cases.

In order to prevent failure of a container material by corrosion or oxidation, it is important to understand the possible degradation modes. Which modes will be operable will depend on a number of factors, including the specific material, the processes by which the

containers are fabricated and closed, stresses introduced in the material by internal and external loads, details of the environment, the duration of time involved, and other possible factors. Our research and development activities are directed toward discerning which degradation modes will apply, and in what time periods after repository closure. We then plan to model the important modes in order to predict the material performance.

2. FUNCTIONS OF THE METAL BARRIER

The functions of the metal barrier or waste package container will change from the first 50 yr of repository operation through the 300- to 1000-yr "containment period" and the 10,000 yr "controlled release period." The metal barrier will function as the vessel for transporting, handling, emplacing, and retrieving (if necessary) the waste form during the operational period. It will then serve (together with the temperature-engineered dry tuff environment) as the containment barrier for a period of at least 300 yr after the repository is permanently closed. The period of substantially complete containment might be as long as 1000 yr post-closure, the exact period of containment time being determined by the NNWSI Project's position in its license application and ultimate approval by the NRC. In the controlled release period, many containers might remain unbreached. Containers that are breached will most likely have cracks or pits penetrating their walls. Though breached, they will nonetheless provide a partial barrier to the transport of water to the waste form and the transport of radionuclides out of the waste packages.

From this consideration of the metal barrier function, it can be seen that the chemical stability of the metal container in the repository environment will be important in determining the suitability of the candidate materials proposed for the container over all of the time periods. The mechanical properties are of importance, too, especially for the earlier time periods. The metallurgical stability of the container material is also of importance, particularly if potentially embrittling phases are formed as an ageing phenomenon (especially during the repository operational and containment periods), and these phases are less fracture-tough than the phase distribution of the starting material.

3. CANDIDATE MATERIALS FOR WASTE PACKAGE CONTAINERS

The set of materials selected as candidates for waste package containers in the tuff repository has undergone some evolution over the course of the NNWSI Project, and it is helpful to review the history of selection.

Initially, the NNWSI Project selected AISI 304L stainless steel as its reference material and a relatively thin-walled design for its containers. A number of factors contributed to these choices. First of all, it was known that there would be no significant lithostatic or hydrostatic pressure on the containers if emplaced in tuff above the water table. Therefore, thick walls would not be necessary for the prevention of buckling, as is the case for most other proposed deep geologic sites. This situation seemed to lend itself to use of a thin, corrosion-resistant material rather than a thicker, corrosion-allowance material. Secondly, the Savannah River Plant had already selected AISI 304L stainless steel as the reference material for borosilicate glass pour canisters for its defense waste. It appeared likely at that time (and has since been established as policy by the Federal government) that defense waste and commercial waste would be emplaced in the same repository. NNWSI's initial proposal was thus to use the pour canisters as the containment barriers for defense waste, and to fabricate containers of the same material (AISI 304L stainless steel) for the spent fuel. Past experience with austenitic stainless steels in hot air and dry steam environments had been very satisfactory, and it appeared that this material would serve well in the unsaturated tuff environment at temperatures above the boiling point.

The process by which AISI 304L stainless steel was selected as the reference material also resulted in the selection of three other alternatives: AISI 321, AISI 316L, and Alloy 825. These were chosen for their increased resistance to particular types of corrosion, should this be found necessary after more detailed testing, particularly if extensive contact with an aqueous phase was found to be likely, or if the environment turned out to be more severe than anticipated. We also selected AISI 1020 carbon steel as a candidate for borehole liners, should they be found to be necessary to enhance retrievability.

Initially, the selection process involved the evaluation of 17 commercial alloys (Russell et al., 1983) according to the criteria of mechanical properties, weldability, corrosion resistance, and cost. We considered all four to be equally important. Using projections of available corrosion data to the repository environment as we understood it, we ranked the 17

candidates and arrived at the selection of the four austenitic alloys AISI 304L, 321, 316L, and Alloy 825 for further consideration. Meanwhile, screening tests had been started and included these alloys and some others. Thus, these tests produced data on some materials that had been eliminated from consideration by the time the tests were completed.

As the project proceeded, it became clear that the AISI 304L stainless steel of the borosilicate glass pour canisters (such as those proposed for the Savanah River plant) would have been subjected to a thermal history that might lead to sensitization of the material to intergranular stress corrosion cracking and that differential thermal expansion during cooling of the poured glass and the canister would put the canister walls into hoop tension, aggravating this situation. We therefore decided to modify the waste package design for the glass waste forms to include an outer container surrounding the pour canister. The thermal history and the stress state in this container could be better controlled, so as to reduce the threat of intergranular stress corrosion cracking.

In 1984 at the request of OCRWM, NNWSI began to investigate the feasibility of using copper-base materials for waste package containers. After consultation with the Copper Development Association, Inc. and the International Copper Research Association, Inc., we selected three copper-base materials for further consideration: CDA 102 (oxygen-free copper), CDA 613 (aluminum bronze), and CDA 715 (70-30 copper-nickel). Copper-base materials appeared to offer several potential advantages. First of all, among the available engineering metals, copper alone is able to co-exist thermodynamically with water (under some conditions). The driving force for corrosion and oxidation is thus smaller for copper than for materials such as Fe-Cr-Ni alloys that depend on passive film formation for their corrosion resistance. Localized and stress-assisted forms of corrosion are thus generally less severe for copper-base materials. Evidence for survivability of copper materials can be seen in the existence of native copper deposits and in copper and bronze artifacts recovered from the ruins of earlier civilizations.

Another potential advantage of the copper-base candidates we selected is that they are generally simpler metallurgical systems. The principal solute elements are soluble over a wide temperature range, and copper itself undergoes no phase transformations; these materials should thus exhibit higher alloy stability over long time periods.

The primary performance concerns with the copper-base materials were the corrosion and oxidation rates in a high gamma radiation field, which would exist in the early part of the containment period. As experimental work later indicated, these rates were not excessively high, and a partial explanation for this result is the catalytic decomposition of hydrogen peroxide (chief radiolysis product in aqueous systems) by copper. This might turn out to be an advantage for the copper-base materials (see discussion in Sections 10.4 and 10.5). A further advantage of the copper-base materials compared with the iron-base austenitic materials is their apparent greater resistance to attack in environments modified by microbiological organisms. This advantage might be due to the toxic effect of copper corrosion products on some biological entitities or the inherent greater resistance of copper and its alloys to localized corrosion in acidic, concentrated, electrolytic environmental conditions created by the microbiological organisms. The high-nickel austenitic material would also be expected to be resistant to microbiological attack, primarily because of the greater stability of the protective passive films on the nickel-base, as opposed to the iron-base, austenitic alloys.

After it was decided to include copper-base materials as candidates for further consideration, it became necessary to reduce the number of the other candidates in order to bring the scope of the testing program within the range of our available resources. We therefore decided to eliminate AISI 321 from further consideration. Alloy 825 offers the same benefits as AISI 321, as well as additional benefits, so that the range of qualities has been preserved within the austenitic family.

As a result of the selection process we just described, we have arrived at six candidate materials for the waste package: AISI 304L and 316L stainless steels, high-nickel austenitic Alloy 825, oxygen-free copper CDA 102, 7% aluminum bronze CDA 613, and 70-30 copper-nickel CDA 715. The nominal compositions of these materials are shown in Tables 1 and 2. Representative mechanical properties of the candidate materials are listed in Tables 3 and 4. Within this field of candidates we have materials based upon three different metals: iron, nickel, and copper. We have corrosion-resistant materials, and we also have one (CDA 102) that can be viewed as somewhat of a corrosion-allowance material (CDA 102 would likely be used with a greater wall thickness than the others anyway because of its lower strength).

Table 1. Alloy compositions for candidate container materials (austenitic alloys)[a].

Common alloy designation	UNS[b] designation	Chemical composition (wt.%) C (max)	Mn (max)	P (max)	S (max)	Si (max)	Cr (range)	Ni (range)	Other element
304L	S30403	0.030	2.00	0.045	0.030	1.00	18.00-20.00	8.00-12.00	N: 0.10 max
316L	S31603	0.030	2.00	0.045	0.030	1.00	16.00-18.00	10.00-14.00	Mo: 2.00-3.00 N: 0.10 max
825	N08825	0.05	1.0	not specified	0.03	0.5	19.5-23.5	38.0-46.0	Mo: 2.5-3.5 Ti: 0.6-1.2 Cu: 1.5-3.0 Al: 0.2 max

[a] Information adapted from ASTM specifications A 167 and B 424; refer to ASTM (1984).
[b] Unified Numbering System; refer to SAE (1977).

Table 2. Representative mechanical properties for candidate container materials (austenitic alloys)[a].

	Tensile strength (min)		Yield strength (min)		Elongation (min)	Reduction of area (min)
	(MPa)	(psi)	(MPa)	(psi)	(%)	(%)
304L (annealed)	483	70,000	172	25,000	30	40
316L (annealed)	483	70,000	172	25,000	30	40
825 (annealed)	586	85,000	241	35,000	30	not specified

[a] Information adapted from ASTM specifications A 167 and B 424; refer to ASTM (1984).

Table 3. Alloy compositions for candidate container materials (copper and copper-base alloys)[a].

Common alloy designation	UNS[b] designation	Chemical composition (wt.%) Cu	Fe	Pb	Sn	Al	Mn	Ni	Zn	Other
CDA 102 (oxygen-free copper)	C10200	99.95 (min)	--	--	--	--	--	--	--	--
CDA 613 (aluminum bronze)	C61300	92.7 (nom)	3.5 (max)	--	0.2-0.5	6.0-8.0	0.5 (max)	0.5	--	--
CDA 715 (70-30 cupronickel)	C71500	69.5 (nom)	0.4-0.7	0.5 (max)	--	--	1.0 (max)	29.0-33.0	1.0 (max)	--

[a] Compiled from CDA Standards Handbook Data Sheets, Copper Development Association, Greenwich, CT.
[b]Unified Numbering System; refer to SAE (1977).

Table 4. Representative mechanical properties for candidate container materials (copper and copper-base alloys).

Common alloy designation/condition	Yield strength[a] (ksi)	Tensile strength (ksi)	Elongation (%)
CDA 102			
Hot rolled	10	34	45
Hard	45	50	4
CDA 613			
Soft anneal	40	80	40
Hard	58	85	35
CDA 715			
Hot rolled	20	55	45
Half hard	70	75	15

[a] 0.5% extension under load. Compiled from CDA Standards Handbook Data Sheets, Copper Development Association, Greenwich, CT.

Our present thinking is that the borehole liners, if any are used, might have to be made of a material from the same alloy family as the containers to avoid galvanic interactions and to avoid introducing additional chemical elements (corrosion products from the less noble material in the galvanic couple) that could complicate the analysis of radionculide behavior. It should be noted that galvanic attack of the liners could have an impact on retrievability of the containers.

As part of the container material selection process, we intend to re-examine the selection criteria and their relative importance. Decisions about these criteria and their weighting factors will be submitted to peer review by a panel of experts, as will the choice of the container material for advanced design work.

4. DEGRADATION MODES OF AUSTENITIC MATERIALS UNDER REPOSITORY CONDITIONS

This section analyzes the degradation modes that can occur for the austenitic materials considered as candidate container materials under anticipated repository conditions. The analysis also includes some non-anticipated conditions, especially those conditions that have some degree of credibility of occurring over the long time periods: the 300- to 1000-yr containment period and the 10,000-yr controlled release period.

Different forms of corrosion and oxidation attack by the environment on the metal container constitute the most likely degradation modes; the process by which the container is fabricated and closed and the strains imposed by these processes and by internal and external stresses on the container can further affect the different degradation modes. Research and development activities for metal barriers are centered around these different degradation modes with the purpose of discerning which of these degradation modes are applicable and in which time period after permanent closure of the repository particular degradation modes are operable.

4.1 Environmental and Metallurgical Considerations

The waste package environment is described in Glassley (1986). The more important environmental features that would affect the stability of austenitic stainless steels and high-nickel alloys in functioning as a containment barrier are: (1) the amount of water that could gain

access to the container surface and (2) the nature and concentrations of dissolved species in the water. The water that enters the repository will be conditioned by percolation through layers of tuff rock above the repository horizon and is expected to be moderately oxidizing, low in salinity, and essentially neutral in pH. Water from the nearby Well J-13 has been conditioned by the Topopah Spring tuff member and has the characteristics indicated in Table 5. Imposition of the radiation field will cause some chemical changes in the species present in the environment. As a class of materials, the austenitic alloys perform well in mildly to moderately oxidizing chemical environments, which would be the expected situation in radiolyzed air, water vapor, and near neutral, non-saline water. Differences in corrosion behavior among the austenitic materials, particularly the resistance to localized and stress-assisted forms of corrosion, occur when the pH moves from the neutral range and when the salinity of the water increases. The more highly alloyed materials (especially in the Cr, Ni, and Mo contents) are usually more resistant than the leaner alloys.

The environment is expected to be gaseous until the container surface temperature cools below 96°C (boiling point of water at the repository elevation). As discussed in O'Neal et al. (1984) on the thermal factors in the environment, some of the spent fuel waste packages would remain above the boiling point for the entire 1000-yr containment period, while other waste packages would remain above the boiling point for several hundreds of years. Depending on the areal power loading and the age of the waste, the waste package containers holding borosilicate glass waste forms might cool below the 96°C isotherm in 50-150 yr (O'Neal et al., 1984), but it is possible to co-mingle these with the spent fuel packages to ensure that a maximum number of container surfaces remain above the boiling point for at least the minimum 300-yr containment period. When cooled below 96°C, liquid water in small quantities could enter from the outside or could form by condensation and reside in the near-package environment. Even when cooled to 96°C, the containers would be hotter than the rock wall and other surfaces where steam would be expected to condense first. The absence of an aqueous electrolyte during much of the containment period translates into the absence of a rapid mechanism for localized, stress, or enhanced general corrosion; therefore, the only operating degradation mechanism would be a low rate of general oxidation (<0.1 μm/yr) occurring uniformly over the surfaces exposed to steam and air in the expected waste package container surface temperature range.

Table 5. Average composition of Well J-13 water. (All values except pH are in mmol/L.) From Ogard and Kerrisk (1984).

	Well J-13
Na	1.96
K	0.14
Ca	0.29
Mg	0.07
HCO_3^-	2.34[a]
SO_4^{-2}	0.19
Cl^-	0.18
SiO_2	1.07
pH	6.9

[a] Measured alkalinity.

Austenitic materials are generally corrosion resistant because of the formation of a protective, passive film on the surface. The passive film is characteristically 50-100 A thick; structurally, the film is an amorphous chromium-rich iron oxide when the austenitic material is in contact with aqueous environments; at higher temperatures, a more stable chromium-nickel spinel structure forms. The passive film is generally stable in mildly to moderately oxidizing environments and over a wide range of pH. The low corrosion and oxidation rates of passive austenitic materials are controlled by solid-state diffusion through the passive film; continuous dissolution and reformation of the film occur. Breakdown of the passive film exposes the thermodynamically active substrate to the environment and is the first stage of rapid general corrosion or of initiation of localized corrosion and stress corrosion cracking. The mechanical properties of the film influence the stress-rupture of the film and initiation of corrosion, which propagates quickly when the chemical environment does not favor rapid repassivation of the alloy. Projections of long-term satisfactory performance of austenitic containers depend on maintenance of the passive film. Modeling of the corrosion behavior under a variety of expected and possible (though unlikely) environmental conditions is therefore based on the chemical and mechanical stability of the passive film. Further discussions on passivity of austenitic materials can be found in several texts on the subject of corrosion such as Fontana and Greene (1978), Uhlig (1963), and Evans (1976).

AISI 304L, as well as the other austenitic materials, is expected to show excellent general (uniform) corrosion resistance in aerated dry steam environments (less than saturation at the relevant temperatures and pressures) as well as in wet steam and in vadose water with a composition similar to Well J-13 water. Radiolysis products, such as hydrogen peroxide, oxides of nitrogen, and even dilute nitric acid, are not expected to increase the general corrosion rate by a significant factor provided that the material is not sensitized (see Section 6). The degradation mode limiting the use of AISI 304L and the other austenitic materials is rarely general corrosion, but rather much more rapid penetration via localized or stress-assisted forms of corrosion. The objective of the metals testing activities is to identify those modes and to determine to what extent these forms of corrosion would occur during the containment and controlled release periods. Corrosion modes that will receive particular attention are summarized in the following three classifications.

(1) Corrosion forms favored by a sensitized microstructure.

A sensitized microstructure could develop during the fabrication and welding thermal cycle of the container or possibly during the very long times (decades to centuries) in the containment period because of the heat output resulting from radioactive decay of the waste form. A sensitized microstructure is one in which chromium-rich carbides ($M_{23}C_6$ where M denotes a metal atom, primarily Cr) have precipitated from solid solution and have produced a chromium-depleted zone around the carbides. Precipitation of carbides occurs preferentially at grain boundaries. Such a sensitized microstructure might lead to intergranular corrosion or intergranular stress corrosion cracking if a suitable aqueous environment (liquid water intrusion or condensation of wet steam on the container surface) were to come into contact with the sensitized region. These forms of corrosion are favored by oxidizing, aqueous conditions.

(2) Corrosion forms favored by the presence of different chemical species in Well J-13 water.

Continuous evaporation of water infiltrating downward might leave a residue of ionic salts in the rock pores. Later dissolution of these salts in a smaller volume of new water could produce higher ionic concentrations in water now able to penetrate the repository horizon after the 96°C isotherm had retreated to within the container. Another way of concentrating ionic species is by flow through fractures above the repository of episodic surges of water that then contact the hot container surface and evaporate, concentrating the solute species. Concentration factors from these mechanisms (Morales, 1985) are not expected to exceed 20x. The chloride-ion concentration is of paramount concern with regard to resistance of stainless steels to pitting, crevice, and transgranular stress corrosion cracking. The other ions present in the Well J-13 water might favor or retard these kinds of corrosion attacks. Oxygen and other oxidizing species in the water, including production of radiolytically generated oxidizing species, would be expected to increase the stress corrosion susceptibility of candidate austenitic stainless steels (transgranular path predominant if annealed material; intergranular path predominant if sensitized material).

(3) Corrosion and embrittlement phenomena favored by transformation products from metastable austenite.

This classification includes problems that are partly related to corrosion and partly related to mechanical embrittlement. The austenite in some candidate materials (AISI 304L and AISI 316L) is metastable and might transform to martensite, ferrite, sigma, or other phases because of mechanical (cold work) or thermal effects. Transformations such as austenite-to-ferrite phase and ferrite-to-sigma phase might reduce the fracture toughness (Gordon, 1977). Similarly, transformation of austenite to martensite reduces fracture toughness, and the martensite is more susceptible to hydrogen absorption and subsequent embrittlement. These metallurgical transformations would be most likely to occur in heavily deformed sections (caused by improper handling) and in and around welds.

Brittle phases such as sigma reduce the fracture toughness, so that residual and operating stresses can initiate cracks if the brittle transformation product is more or less continuous. Other transformation products such as martensite and possibly ferrite might be more susceptible to hydrogen absorption and embrittlement. Hydrogen will be generated from radiolysis of water vapor or water, or from the electrochemical cathodic reaction on a corroding metal surface. Oxidizing conditions in the external container environment should preclude long residence time for atomic hydrogen on the outside container surface. Because some population of spent fuel rod cladding will be water-logged from reactor operations and the internal environment of the container is assumed to be argon (or other inert gas) and therefore non-oxidizing, it is assumed that some hydrogen could be generated inside the container by radiolysis of the water vapor. This hydrogen could be transported to the inside surface of the container. Austenite is normally resistant to detrimental hydrogen effects (low permeation for atomic hydrogen). Martensite formation is favored by high plastic deformation. These effects are most likely to occur in and around welds. Localized deformation could also result from improper handling of the waste container during the filling or emplacement operations. Gamma radiation is the only significant radiation that the container will encounter. The rates of atomic displacement caused by electromagnetic (as opposed to particle) radiation are too low to cause metallurgical reactions such as austenitic transformation or carbide precipitation.

Other candidate materials were chosen on the basis of their known superiority (over that of AISI 304L) in resistance to specific forms of corrosion -- indeed the reason for development of the more highly alloyed stainless steels is their improved resistance to

aggressive chemical conditions. The rationale of alloying additions to the basic 18 Cr - 8 Ni stainless steel composition to overcome susceptibility to various kinds of corrosion is discussed in greater detail elsewhere (Sedricks, 1979).

Premium grades of AISI 304 material with even lower carbon contents than AISI 304L (0.03 wt.%, maximum) would be expected to have greater resistance to sensitization. Addition of nitrogen (as in the LN grades and in certain "nuclear grades") generally in excess of 0.06 wt.% also appears to be beneficial in retarding sensitization. Cowan and Gordon (1977) review the relationship between sensitization and stress corrosion cracking behavior of the stainless steels and give metallurgical and compositional approaches to reduce such behavior. In the presence of chloride ions and resulting pitting/crevice corrosion, AISI 316L is more resistant than AISI 304L since molybdenum additions are known to combat these forms of corrosion. Published work by Pessall and Nurminen (1974) indicates quantitative effects of molybdenum and other alloy additions in promoting pitting and crevice corrosion resistance in chloride environments. Chloride-induced transgranular stress corrosion cracking (TGSCC) concerns can be overcome by high-nickel additions, such as in Alloy 825. [Alloy 825 is resistant to TGSCC in boiling 155°C (approximately 44%) $MgCl_2$, which is the standard test solution (ASTM G 36, 1973) for detecting susceptibility to this form of corrosion.] Alloy 825 also contains 2-3% molybdenum and is titanium-stabilized to combat localized and intergranular forms of corrosion as well. In addition, Alloy 825 possesses an austenitic structure stable over the entire range of temperatures of interest.

Recent discussions on potential degradation modes have revealed the occurrence of severe localized and stress corrosion cracking of stainless steel due to the action of microbiological organisms that alter the chemical nature of the environment. Microbiologically induced corrosion has occurred under circumstances where it was quite unexpected, a recent example being cited in the paper by Stoecker and Pope (1986). In assessing whether or not microbiological organisms could influence the aqueous environment in the Yucca Mountain repository, it appeared that the long dry period with temperatures in excess of 100°C and the initially high radiation field would preclude the propagation of these organisms later, when environmental conditions were more favorable to their existence. This conclusion might be premature, and more research into whether the microorganisms can survive in a dormant state during the hot, dry period and then revive at a later period is warranted. One environmental condition that the microorganisms could produce and that could lead to severe corrosion problems for the austenitic materials is a decrease in pH (sulfuric-acid-producing

microorganisms). Some of the work on localized corrosion (Section 7) is concerned with low pH solutions as an accelerating mechanism to study this kind of attack.

In Sections 5-8, the degradation modes affecting the austenitic materials are discussed in greater detail and are accompanied by presentations of published results appropriate to each degradation mode. Some of the testing has been performed under environmental conditions that are anticipated; however, many tests have been performed under unanticipated environmental and metallurgical conditions. The reasons for conducting tests under unanticipated conditions are: (1) the particular set of environmental and metallurgical conditions accelerates the corrosion mode, thus making quantitative assessment of the long-term effect possible in relatively short-term laboratory tests; and (2) the set of environmental and metallurgical conditions (in certain cases) presents a possible worst case scenario of credible, although unlikely, conditions for comparison of the performance of different candidate materials under adverse conditions.

4.2 Design, Fabrication, and Emplacement Considerations

The environmental and metallurgical considerations on the various degradation modes that the container material can undergo are influenced by several aspects of the waste package design, the fabrication of the waste package container (including joining processes for closing it), and the way that the waste packages are handled and emplaced in the repository. Operational factors in the repository will also influence the performance of the waste package container.

The conceptual design of the waste package has been extensively discussed in the report by O'Neal et al. (1984), and many of the design considerations and design options are discussed there. Nearly all of these design and waste package emplacement options affect the resulting thermal environment around the container and, in many cases, they affect the radiation field that will be produced. Figure 1 shows the dimensions and general configuration of the two types of waste packages (spent fuel and vitrified, or glassy, waste from fuel reprocessing). Many factors of the design are undergoing review and revision, so that the information in the figure should be regarded as only an example of one possible arrangement. These particular design options show vertical emplacement of single waste packages in boreholes; horizontal emplacement of multiple waste packages is also under consideration. A common outside diameter for the disposal container for both types of waste package is an important

consideration. The length of the container will vary according to the type of waste package and, possibly, according to the particular dimensions of spent fuel elements. Additionally, the internal configuration will differ according to the reactor fuel type and whether the fuel assemblies will be disassembled and consolidated or remain intact. Several internal configurations are under study. The waste packages containing reprocessed waste consist of an inner pour canister (recipient for the molten glass) provided by the waste form producer and an outer container provided at the disposal site. The length of the outer container depends on the dimensions of the inner pour canister.

In all cases, the NNWSI Project is considering thin-walled containers for both types of waste packages. The container wall thickness is on the order of 1 cm. This thickness might be increased for a high-purity copper container (discussed in Section 10) because of the lower strength of this material. Also, it might be more feasible to produce somewhat thicker containers by different fabrication processes; therefore, a range of thicknesses (approximately 1 to 3 cm) should be considered for the range of materials and processes currently being considered.

Different processes for fabricating the container are being considered by another task (Design, Fabrication, and Prototype Testing) in the NNWSI Project. Different processes might be used to fabricate the "body" of the container (e.g., rolled and welded plate) and the "ends" (e.g., forged bottom and forged top and pintle). Such choices could result in thicker end sections than the container body. Also, these choices could produce quite different microstructures in the different components. The components are assembled by welding, and the welding process introduces a number of metallurgical considerations (discussed in Section 8). The NNWSI Project (particularly the Design, Fabrication, and Prototype Testing Task) is looking at several fabrication options to eliminate some of the assembly welds, including extrusion of the container body.

Figure 1. Representation of a spent fuel waste package (left) and a reprocessed glass waste form package (right), showing container dimensions.

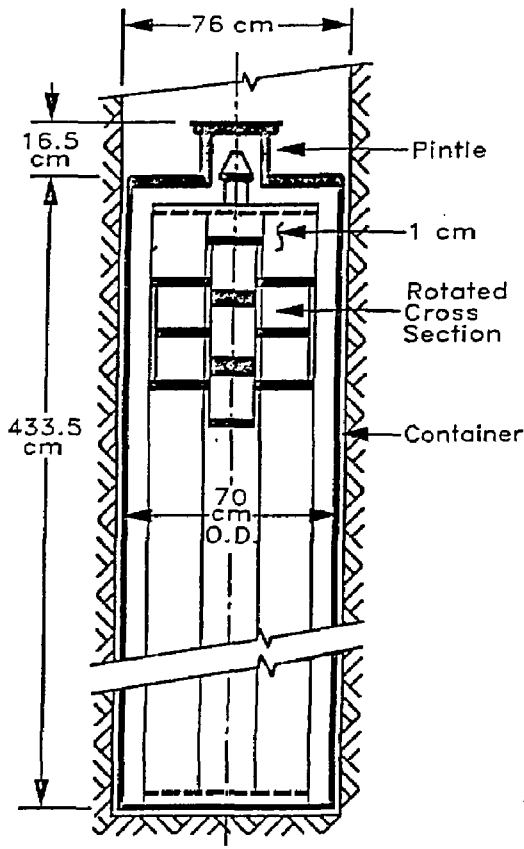

BWR (boiling water reactor) spent fuel waste package emplaced in vertical borehole PWR same except for 3 holes instead of 7.

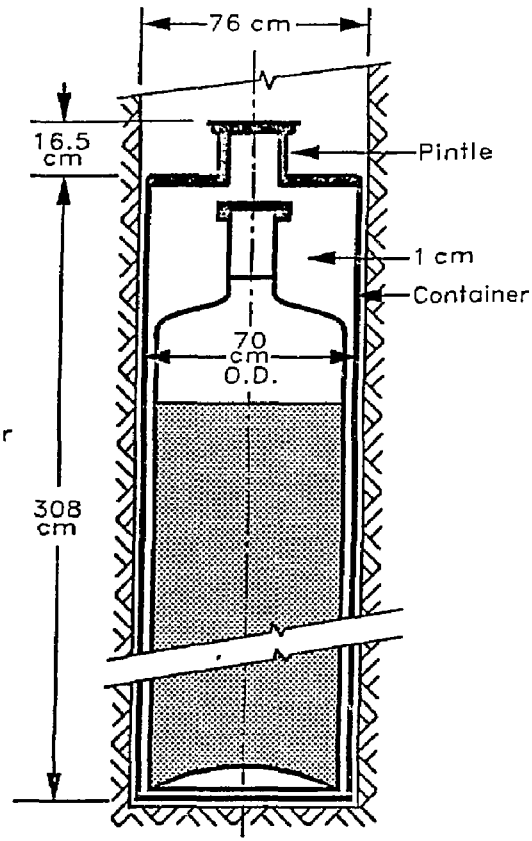

WV/DHLW (defense high-level waste) package emplaced in vertical borehole.

Figure 2 gives the reader a graphic representation of the implications of the design, handling, and emplacement considerations on the performance of the metal container. These implications are mentioned in Section 4.1 and are discussed more fully in Sections 5-8 for the austenitic candidate materials; many of the same implications apply to the copper-base materials as well, which are discussed in Section 10. A horizontal emplacement is shown in Fig. 2, as there are possibly more corrosion and degradation considerations for this arrangement than for the vertical emplacement. It should be emphasized that care will be taken during the handling and emplacement operations to avoid some of the problems indicated in Fig. 2. For instance, badly deformed, scratched, dented, or otherwise damaged containers would not be emplaced. Similarly, undercut or cracked welds would be rejected. However, there is the finite probability that inspection of the fully assembled and closed container will not reveal all significant flaws that could later cause problems. The Metal Barrier and Design Tasks are both evaluating potential container fabrication and welding processes in terms of their performance implications. The goal is to produce reasonably homogeneous material, to minimize residual stresses, and to eliminate crevices and surface defects when possible; however, there are practical and economic limitations to the degree to which these can be fully attained.

To emplace (and retrieve, if required) the containers in horizontal boreholes, a "sled" or other mobile platform is needed. This introduces a possible galvanic corrosion effect if the construction metals for the container, platform, and borehole liner are dissimilar and an aqueous environment intrudes. Also, a crevice is produced between the container and its supporting platform. The repository construction and operation also introduces changes in the environment that can have significant implications on the performance of the container during later periods. These changes range from modification of the rock properties to the introduction of "foreign" materials (for example, drilling fluids and lubricants) during the construction and operation period that might modify the natural environment. Human and possibly microbiological activity during this period of time can also introduce some changes to the environment. Discussion of these is largely beyond the scope of this report, but consideration of these effects will need to be addressed in some later work as more details of envisioned repository construction and operation processses become available.

Figure 2. Schematic representation of an emplaced waste package container. Possible corrosion and degradation problems are indicated.

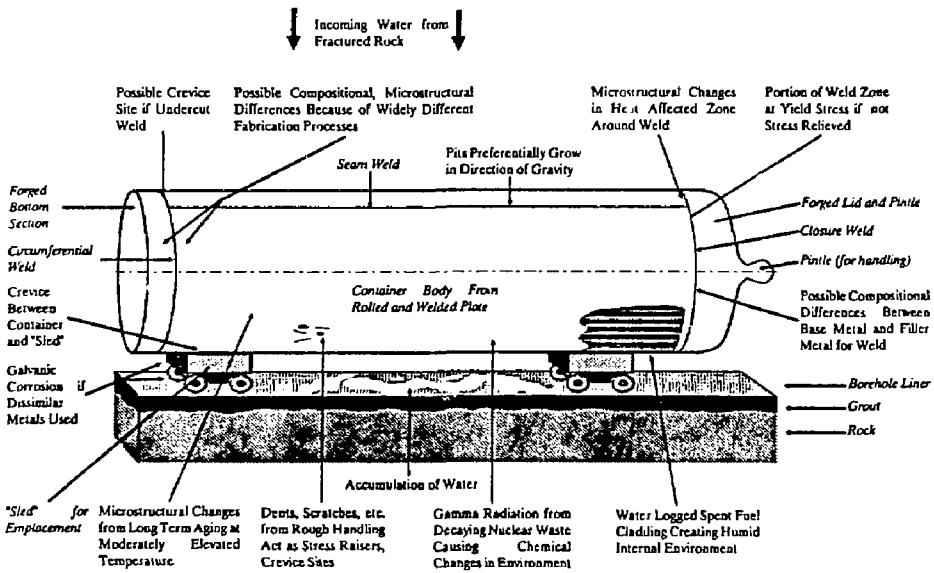

5. GENERAL CORROSION AND OXIDATION OF AUSTENITIC MATERIALS

Low temperature oxidation will occur from the time that the waste packages are emplaced in the repository. Depending on several features of the waste package and repository design, peak surface temperatures in the approximate range of 130-270°C might occur. General aqueous corrosion can occur when liquid water is present in the environment, either from intrusion of groundwater to the container surface or from condensation of steam on the container surface. Depending on several conditions related to the absolute humidity and surface condition, aqueous corrosion effects can occur at or somewhat above the 96°C boiling point.

Coupons of the candidate materials have been exposed to environments that approach those that might be expected in the repository during the containment period and the controlled release period. Test environments included Well J-13 water, wet steam, and dry steam at various temperatures. In other cases, test environments were more aggressive than expected conditions in order to accelerate the rates. A good example is exposure to irradiated Well J-13 water and steam (tests conducted in a Co-60 gamma radiation facility). The tests have been described by McCright et al. (1983), Juhas et al. (1984), and Westerman et al. (1987) and followed a planned interval principle whereby multiple coupons were initially emplaced in the test environment and were removed from the environment after certain intervals for examination. The corrosion penetration rate was calculated from the weight loss experienced during the exposure interval, and the exposed surface was examined for the pattern of corrosion attack (uniform, localized, or edge). Standard ASTM procedures were followed in preparing and cleaning the coupons (ASTM G 1, 1981) and in conducting the tests (ASTM G 31, 1972). In most cases, the coupons were re-emplaced in the test solutions to accumulate additional exposure. To create an intentionally creviced area on the coupon (to evaluate localized corrosion susceptibility – see Section 7), slotted Teflon washers were used as part of the fastener and mounting assembly that supported the coupons. Any evidence of localized attack could therefore be observed in this specific area.

5.1 Oxidation and General Corrosion Tests

Results obtained from coupons immersed in Well J-13 water maintained at different temperatures show that the corrosion penetration rates were low (all substantially less than 1 μm/yr), with little variation during the exposure period. After more than 10,000 exposure

hours in Well J-13 water at different temperatures, general corrosion rates in the range 0.030-0.225 μm/yr were measured. Some representative data are summarized in Table 6. (Reviews of both the data collection process and technical validity were conducted. Irregularities were found in the data collection process. However, the technical validity of the results were confirmed in an independent review conducted by two scientists of the material traceability, overall test techniques, and consistency of results with literature data.) Data obtained at shorter exposure times have been summarized and discussed by Glass et al. (1984). Little change in the general corrosion penetration rate occurred with exposure time; for example, AISI 304L had a corrosion rate of 0.094 μm/yr after 3548 hr and 0.072 μm/yr after 10,360 hr in Well J-13 water at 100°C. The data in Table 6 from recently completed tests indicate that the general corrosion rate was approximately the same for all the alloys tested; alloying differences would only be distinguished in more aggressive environments. The trend of results indicates a small decrease in the corrosion rate with increasing temperature, which might be due to the formation of a slightly thicker passive film or to the decrease in dissolved oxygen and nitrate ion at the higher temperatures.

Corrosion tests performed on candidate austenitic stainless steel coupons in wet steam (saturated at the test temperature of 100°C and at atmospheric pressure) and dry steam (unsaturated at the test temperature of 150°C and at atmospheric pressure) also showed expected low general corrosion penetration rates, calculated to be comparable with those in the Well J-13 water. However, all the specimens tested in the dry steam showed weight gains, and specimens tested in the wet steam showed weight losses. For specimens that showed weight gains, the results are expressed in terms of the corresponding amount of metal that would have been converted to oxide to create the increase. Representative data are included in Table 6. More detailed data and experimental procedures from these experiments are covered in a series of laboratory reports that are in preparation.

General corrosion rates for the candidate materials have also been determined by Glass et al. (1984), using electrochemical techniques (Tafel extrapolation and linear polarization). These determinations require much shorter laboratory times and therefore permit a more convenient survey of additional environmental conditions. The general (uniform) corrosion rates

Table 6. General corrosion and oxidation rates of candidate austenitic stainless steels in Well J-13 water at different temperatures.

Alloy	Temp (°C)	Time (hr)	Medium	Corrosion rate (μm/yr)[a,b] Avg.	Std. dev.
304L	50	11,512	water	0.133	0.018
316L	50	11,512	water	0.154	0.008
825	50	11,512	water	0.211	0.013
304L	80	11,056	water	0.085	0.001
316L	80	11,056	water	0.109	0.005
825	80	11,056	water	0.109	0.012
304L	100	10,360	water	0.072	0.023
316L	100	10,360	water	0.037	0.011
825	100	10,360	water	0.049	0.019
304L	100	10,456	saturated steam	0.102	[c]
316L	100	10,456	saturated steam	0.099	[c]
825	100	10,456	saturated steam	0.030	[c]
304L	150	3,808	unsaturated steam	0.071	[c]
316L	150	3,808	unsaturated steam	0.064	[c]
825	150	3,808	unsaturated steam	0.030	[c]

[a] Average of three replicate specimens of each alloy in each condition.
[b] Reviews of both the data collection process and technical validity were conducted. Irregularities were found in the data collection process. However, the technical validity of the results were confirmed in an independent review conducted by two scientists of the material traceability, overall test techniques, and consistency of results with literature data.
[c] Not determined.

measured electrochemically were higher than the weight loss coupon test results, as expected (due to the time dependence of the weight loss test and the time independence of the electrochemical test). This is discussed in more detail in Section 7 with regard to localized corrosion susceptiblity.

Some corrosion tests have been performed on AISI 304L under irradiated environmental conditions. A 1-yr test was conducted at room temperature in partially aerated (5 ppm measured oxygen content) Well J-13 water containing crushed tuff, with an average gamma dose rate of 6×10^5 rads/hr (H_2O basis) (Juhas et al., 1984). An identical but non-irradiated test was conducted simultaneously for control. Preliminary chemical analysis of the water after 1 yr of testing indicates that many of the dissolved ionic species in the Well J-13 water were concentrated by a factor of approximately two in the irradiated vessel compared with the non-irradiated vessel. The irradiated solution was relatively depleted of oxidizing species (nitrate ion and dissolved oxygen) compared with the non-irradiated solution. However, weight loss measurements on the specimens showed barely detectable corrosion on both the irradiated and non-irradiated material. The non-irradiated coupons showed higher corrosion rates than comparable irradiated coupons, although the amount of corrosion penetration was very small in all cases. The AISI 304L was tested in both the annealed and the heat-treated (weld simulation) condition (this is explained more fully in Section 6). The heat treatment was 650°C for 1 hr, which had no effect on the general corrosion rate. No evidence of intergranular penetration was noted on specimens that were metallographically sectioned and examined. Specimens that had been placed in the bottom of the test vessels were embedded in the crushed rock; the purpose of this was to create crevice-like conditions on the metal surface and to discern whether preferential attack would occur at these locations. No evidence for preferred crevice attack was noted on the coupons. A summary of results from the irradiation test is given in Table 7.

Corrosion tests conducted in irradiated Well J-13 water environments at higher temperatures showed comparable results for a 2-mo test. These tests were conducted in air-sparged, pressurized autoclaves containing Well J-13 water and crushed tuff (again to provide a crevice-like surface condition on the embedded coupons) at 105 and 150°C, with respective radiation dose rates of 3×10^5 and 6×10^5 rads/hr. AISI 304L in both the annealed and the sensitized conditions was used. The results from individual coupons are given in Table 8.

Table 7. Corrosion test results for room temperature, irradiated and non-irradiated 304L coupons (8760-hr exposure)[a].

304L Stainless steel material condition	J-13 Water environment (28°C)	Corrosion rates (μm/yr) Vessel A (irradiated)	Vessel B (non-irradiated)
Solution annealed	rock and water	average: 0.0811[b]	0.242[c]
		range: 0.0690-0.0951	0.215-0.272
		std. dev.: 0.00959	0.0201
Solution annealed	water	average: 0.151	0.285
		range: 0.0817-0.299	0.138-0.451
		std. dev.: 0.0734	0.118
Weld simulation heat treatment[d]	rock and water	average: 0.123	0.249
		range: 0.111-0.142	0.165-0.322
		std. dev.: 0.0114	0.0522
Weld simulation heat treatment[d]	water	average: 0.116	0.283
		range: 0.092-0.142	0.203-0.452
		std. dev.: 0.0470	0.0980

[a] Source: Juhas et al. (1984).
[b] Averages of six coupons in each set.
[c] Maximum localized penetration measured = 0.010 μm in 8760 hr (approximately 1 yr).
[d] Heat treatment: 1 hr at 650°C.

Table 8. Oxidation test results for stainless steel coupons in irradiated environments (2-mo exposure data)[a].

Material	Environment	Corrosion penetration rate (μm/yr) 105°C[b] 3×10^5 rads/hr	150°C[c] 6×10^5 rads/hr
304L (solution annealed)	J-13 water	0.31; 0.31	0.36
	J-13 water and tuff	0.29; 0.32	0.31
304L (solution annealed and heat-treated condition)	J-13 water	0.23; 0.37	0.51
	J-13 water and tuff	0.25; 0.30	0.55

[a] Source: McCright et al. (1983).
[b] Tests conducted in Inconel 600 vessel.
[c] Tests conducted in titanium - Grade 2 vessel.

5.2 Summary and Analysis of General Corrosion and Oxidation Testing

In summary, the general corrosion rates of the candidate stainless steels listed in Table 6 are quite small and, thus far, do not seem to be significantly affected by: (1) alloy composition (AISI 304L with 19 wt.% Cr and 10 wt.% Ni to Alloy 825 with approximately 21 wt.% Cr and 40 wt.% Ni; several alloys contain 2-3 wt.% Mo and other elements); (2) temperature (28 to 150°C); (3) exposure time (up to 11,000 hr); (4) irradiation (background to more than 10^5 rads/hr); or (5) whether the environment was wet (fully immersed in Well J-13 water or in the wet steam above the water) or dry (in a steam chamber with the temperature above the atmospheric boiling point of water). A value of 0.2 μm/yr would appear to be adequate to describe conservatively the rate data so far acquired (Oversby and McCright, 1984). Extrapolation of these rates indicates that a container made of any of the candidate materials with a 1-cm thick wall would not be penetrated by general corrosion for well over a thousand years. This discussion is expanded in Section 9.

A model has been developed to predict barrier penetration due to uniform corrosion in the presence of high radiation fields (Urquidi-MacDonald, 1987). Radiolytic products are taken into account. Adjustable parameters have been determined by fitting the models to existing experimental data. This model also has relevance to processes occurring at the bottom of pits, as well as in cracks and crevices. Once the relative rates of anodic and cathodic processes are calculated, mixed-potential theory facilitates calculation of the corrosion potential. This particular model treats mass transport as a pseudo steady-state process (transient diffusion is not dealt with). This will probably be sufficient to allow prediction of pH suppression in pits, cracks, and crevices (Pickering et al., 1973). Also, it is noted that the local potential and pH determine whether or not an active metal surface will undergo repassivation.

6. INTERGRANULAR CORROSION AND INTERGRANULAR STRESS CORROSION CRACKING OF AUSTENITIC MATERIALS

Experience with the candidate austenitic materials has shown that they are, under certain environmental or metallurgical conditions, susceptible to stress corrosion cracking. The crack propagation path (intergranular or transgranular) is often an important indication of the causative mechanism for stress corrosion and therefore serves as the basis for modeling activities for projecting container lifetimes. In some cases, both intergranular and transgranular

crack paths occur but one or the other cracking pattern dominates. Cracking along intergranular paths (and intergranular attack without stress assistance) is the subject of this section.

Intergranular corrosion attack (IGA) and intergranular stress corrosion cracking (IGSCC) are most frequently associated with a sensitized microstructure as a precursor to attack. (Intergranular stress corrosion cracking has occurred in nonsensitized stainless steels in such media as polythionic acid and hot concentrated caustic, but these environments appear not to be relevant here.) A sensitized microstructure develops when chromium carbide precipitates from solid solution (austenite or gamma phase), leaving a region depleted in chromium in the vicinity of the precipitate. This precipitation occurs most frequently along grain boundaries, and it can lead to serious degradation when the precipitates and resulting chromium-depleted zones form a continuous network across the container thickness. The protective passive film (Cr_2O_3) on the sensitized grain boundary is not as stable as that on the bulk material, because the chromium content is lower (less than 12 wt.% in the boundary compared with 18 to 20 wt.% in the bulk). When the sensitized material is exposed to oxidizing aqueous environments, the grain boundary area tends to corrode preferentially, and the attack can proceed along the continuous network of chromium-depleted zones; hence, intergranular attack occurs. In the presence of applied stress on a sensitized stainless steel, preferential attack is favored under less aggressive environmental conditions and results in IGSCC.

There have been reported observations of IGSCC occurring in nonsensitized material. The most common occurrence is in conjunction with TGSCC in chloride-containing environments where the crack propagation path has both a transgranular and an intergranular component. This has been discussed by Cowan and Gordon (1977), primarily for AISI 304 in concentrated boiling $MgCl_2$ solutions. By far, the transgranular path is the dominant of the two paths in chloride-containing environments. The intergranular component appears to be favored more when the chloride concentration is low, when the temperature is low, and when alloying additions are made to the base material. As discussed in Section 7 on TGSCC of austenitic materials, the conditions that favor development of the intergranular path over the transgranular path are the same conditions that favor an overall increase in resistance to stress corrosion cracking regardless of the propagation path. Another environment in which both intergranular and transgranular crack propagation can occur in nonsensitized material is in hot concentrated caustic solutions (Wilson and Aspden, 1977). Polythionic acid is another reagent that occasionally causes stress corrosion cracking of nonsensitized stainless steel (Theus and

Staehle, 1977). These environmental conditions appear to be extremely unlikely to develop under any scenarios envisioned for the repository.

The experience in BWR cooling water does appear to be applicable, at least as a starting point, for material testing and modeling activities. AISI 304 is used for the recirculating piping around the reactor core, and many incidents of stress corrosion cracking have occurred. Most of the cracking has been intergranular, and all has been associated with sensitized microstructures occurring in the heat-affected zones in welded sections. However, there have been several cases of chloride-induced, crevice-induced, and cold-worked-induced cracking. Fracture modes were mixed intergranular and transgranular (Hale and Pickett, 1986). The mildly oxidizing characteristics of both the BWR cooling water and that of groundwater associated with the geological formation at the repository site suggest a comparison.

6.1 Detection of Sensitized Microstructures

Chromium carbide precipitation is favored by exposure of austenitic stainless steels to moderately high temperatures (generally in the 500 to 800°C range) for periods ranging from minutes to many hours. The carbon content of the stainless steel is an important factor in determining susceptibility to sensitization. Time-temperature-sensitization (TTS) curves have been generated for the austenitic stainless steels; an example (Shreir, 1976) is shown in Fig. 3. Historically, intergranular corrosion was first noted around welds in high-carbon austenitic stainless steels (such as AISI 302, with 0.15 wt.% C). During the post-weld cooling, the heat-affected zone near the weld can cool at a rate such that it enters the sensitized region ("nose") of the TTS curve. Lower carbon stainless steels (such as AISI 304 with maximum 0.08 wt.% C and AISI 304L with maximum 0.03 wt.% C) have been developed to resist sensitization. For these alloys, longer heating times will move the material into the nose. As a practical limit, the L grades with less than 0.03 wt.% C will not sensitize during most welding operations. Tests have been developed over the years by the steel industry to detect sensitization; these are collected under ASTM A 262 (ASTM, 1985).

Currently, five practices are recognized by the ASTM; the general features of these practices are exposure of the stainless steel to a strongly oxidizing solution (oxalic acid, concentrated nitric acid, acid cupric sulfate, acid ferric sulfate, or nitric/hydrofluoric acid mixtures) and then measurement of the weight loss or metallographic examination of the attacked surface. Of the ASTM A 262 standardized practices, Practices A (oxalic acid) and E

(acidified cupric sulfate) are used most often. By and large, these are go/no go types of tests that indicate whether a structure is sensitized or not, and the documentation is usually qualitative (sensitized structures show photomicrographs with heavily etched grain boundaries). A considerable amount of literature is available on the mechanisms of sensitization and the ways of detecting it (Streicher, 1978; Clarke et al., 1978).

Some difficulties are encountered in applying the ASTM tests to predict nuclear waste package container performance. First, the reagents used in the tests are much more aggressive than the chemical species expected in the repository. Second, the reagents discern sensitized areas after some growth of the carbide and chromium-denuded regions. Carbide precipitation is a nucleation and growth process, and the ASTM tests do not detect the carbide nuclei whose formation would occur at times and temperatures to the left of the nose in Fig. 3. The question is whether these subcritical precipitates would grow significantly during the time that the container is in the repository. Third, the ASTM tests rely on qualitative judgments by the researcher, particularly with regard to estimating the degree of sensitization for partially sensitized microstructures (e.g., estimating the percent of grain boundary showing ditching). More recently, tests involving electrochemical polarization of a specimen exposed to an acid thiocyanate solution have been developed. Sensitized microstructures give a polarization transient with a shape that is significantly different from that of nonsensitized structures, and integration of the area under the curve is quantitatively proportional to the amount of grain boundary area attacked. These electrochemical tests are called Electrochemical Potentiokinetic Reactivation (EPR) tests (Majidi and Streicher, 1984).

Materials and processes which lead to gross sensitization would not be used in waste packages, but partial sensitization occurring along a limited number of grain boundaries or other pathways might occur. The degree of partial sensitization and the time required to achieve this condition needs to be quantified in order to predict the degradation mode by intergranular mechanisms. Although the EPR technique and the ASTM A 262 test methods use environments that are considerably more aggressive than the expected service conditions, these techniques are useful for screening materials and conditions that could lead to IGA and IGSCC.

Figure 3. Time-temperature-sensitization curves for AISI 304 and 304L stainless steels (ss). Cross-hatched region indicates where sensitized microstructures develop as a function of heating time, heating temperature, and carbon content in the alloy. Sensitized microstructures occur when chromium carbides precipitate and deplete local areas of chromium (lower bound of hatched region); heating for longer periods of time restores original chromium content in these areas (upper bound of hatched region). Modified from Shreir (1977).

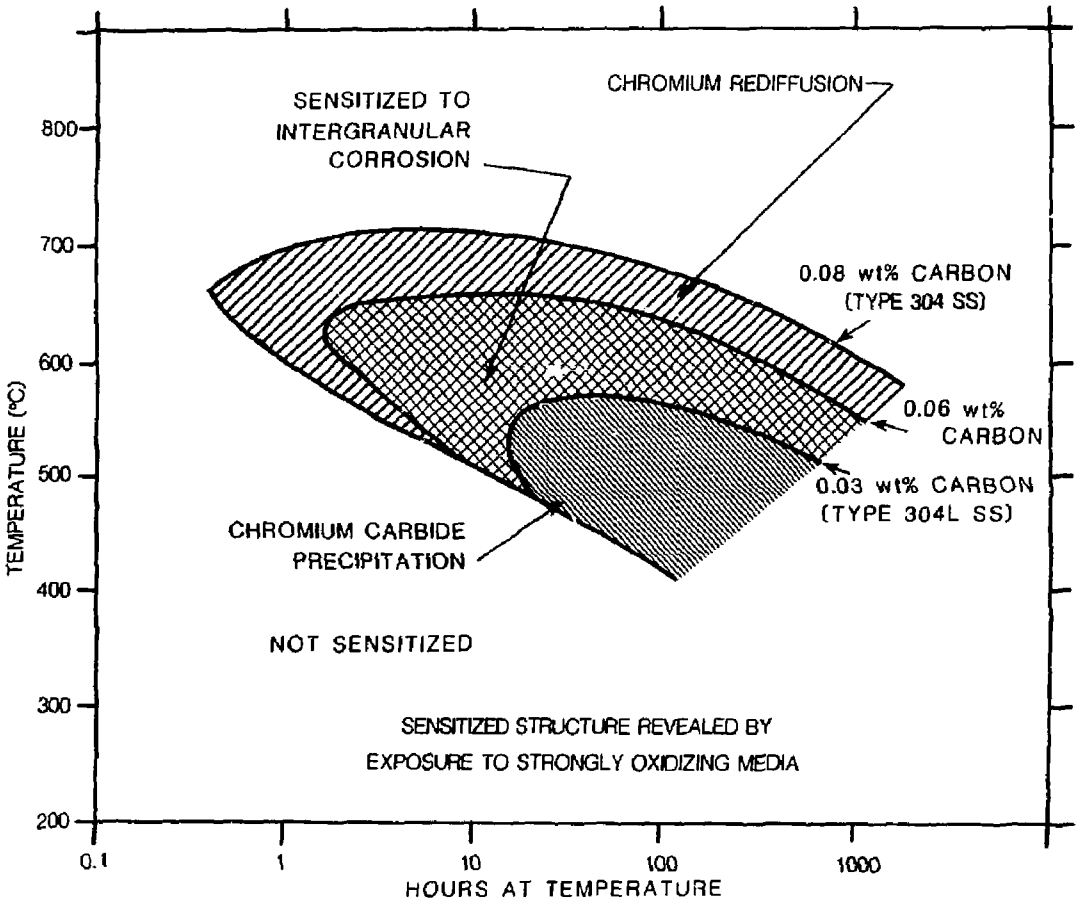

6.2 Tests to Detect IGSCC Susceptibility

Several intergranular stress corrosion cracking (IGSCC) tests have been performed with specimens of AISI 304, AISI 304L, AISI 316L, AISI 321, and Alloy 825 in various material conditions. Four-point loaded, bent-beam specimens (ASTM G 39, 1979) were machined from cold-worked plate in which a groove was machined and filled with weld material. The bent-beam configuration was chosen so that the base metal, weld zone, and heat-affected zone could all be simultaneously stressed at the same nominal level. Some specimens were given intentional heat treatments to develop a sensitized microstructure; then these specimens were stressed and exposed to Well J-13 water and to steam.

Specimens of readily sensitized AISI 304 were included in the test program to induce a stress-corrosion-susceptible condition for comparison with the more highly resistant materials and to illustrate the validity of the test technique in discerning the differences in the materials. One group of 72 specimens was given a sensitizing heat treatment after welding (700°C for 8 hr). Another group of 36 specimens remained in the cold-worked and as-welded condition with no subsequent heat treatment. When this treatment is used, the time at the specified temperature will produce a fully sensitized microstructure in the higher carbon stainless steels (e.g., AISI 304), but only a partial or nonsensitized condition in the L grade or stabilized stainless steels. The treatment over-tests what could happen in the heat-affected zone after multiple weld passes and prolonged slow cooling. It is difficult to envision that such a long time at elevated temperature would ever occur in container fabrication and welding. (Note that when much of this work was initiated, the NNWSI Project was considering the pour canister containing the vitrified waste forms as the primary containment barrier for defense and commercial reprocessed waste packages. The slow glass pouring and cooling operations would subject the canister to several hours at temperatures above 500°C. The reference designs for vitrified waste packages now include an outer metal container around the pour canister.) ASTM A 262 (ASTM, 1985) Practice A (electrolytic oxalic acid etching) revealed sensitization only in the AISI 304. The specimen configuration and test procedure corresponded to ASTM G 39 (ASTM, 1979) and are described by Juhas et al. (1984). Specimens were loaded to 90 percent of the room temperature yield stress and tested in Well J-13 water and in the saturated steam above the water at 100°C. This would put the actual projected stress slightly above yield at the test temperature. None of the specimens exhibited cracking after 2000 hr of testing for specimens having no post-weld heat treatment and after 4000 hr of testing for specimens given the post-weld sensitizing treatment. Additional specimens of the L grades that have been

given very lengthy heat treatments (1 wk at 600-700°C) were added after the tests were underway. The purpose of this heat treatment was to heavily sensitize the material.

Results from U-bend specimens of AISI 304 (0.063 wt.% C) and AISI 304L (0.017 wt.% C) exposed to irradiated Well J-13 water and water vapor have been discussed by Juhas et al. (1984). ASTM G 30 test procedures were followed. The self-loading nature of the U-bend permits its use in the small available working space in the irradiated autoclaves. Maximum stress levels in U-bends substantially exceed the yield stress. These materials were in the solution-annealed (15 min at 1050°C) and sensitized (24 hr at 600°C) conditions. Tests were performed in two autoclaves: one at 50°C and the other at 90°C, in a Co-60 irradiation facility at irradiation intensities of 6×10^5 and 3×10^5 rads/hr, respectively. Each autoclave was divided into three zones: water and rock (bottom), rock and vapor (middle), and moist air only (top). The air in the test vessel was purged daily with fresh air. The operating pressure in the vessel was essentially atmospheric so that the air space in the vessel was saturated with water vapor at the operating temperature. The intent of these experimental conditions was to accelerate cracking and provide some failed specimens in a reasonable test period. It should be noted that the high gamma dose rates and aqueous conditions are not expected to occur concomitantly in the repository environment. Specimens were examined after 1 and 3 mo of exposure, and the results are given in Table 9. In the 50°C test, two specimen failures were recorded: one after 1 mo of exposure and one after 3 mo of exposure. Both specimens were sensitized AISI 304, located in the vapor-only region of the autoclave. In the 90°C study, two sensitized AISI 304 specimens, both from the water-and-rock region, had failed after 1 mo of exposure. The 3-mo exposure inspection showed two additional failures: both were AISI 304, one in the vapor-only region and one in the vapor-and-rock region of the autoclave. Metallographic examination of the fractured specimens revealed IGSCC; an example is shown in Fig. 4.

The observed stress corrosion susceptibility of the sensitized AISI 304 was expected. None of the AISI 304L specimens have cracked intergranularly, but they have exhibited transgranular stress corrosion cracking (TGSCC) in subsequent inspections (Section 7). The larger number of failures occurring in the irradiated vapor phase suggests that a more severe environmental condition exists there, generated by radiolysis of the environment without dilution or buffering of the species produced. It is also possible that salts were deposited on

Table 9. Stress corrosion cracking test results from U-bend specimens exposed to irradiated J-13 water, crushed tuff rock, and water vapor. Results after 3-mo exposure[a].

	Environment					
	50°C (6 x 10^5 rads/hr)			90°C (3 x 10^5 rads/hr)		
Material	rock + water	rock + vapor	vapor	rock + water	rock + vapor	vapor
304	0/4	0/4	2/4	0/4	3/4	1/4
304L	0/4	0/4	0/4	0/4	0/4	0/4

[a] Source: Juhas et al. (1984) and Westerman et al. (1987).

given very lengthy heat treatments (1 wk at 600-700°C) were added after the tests were underway. The purpose of this heat treatment was to heavily sensitize the material.

Results from U-bend specimens of AISI 304 (0.063 wt.% C) and AISI 304L (0.017 wt.% C) exposed to irradiated Well J-13 water and water vapor have been discussed by Juhas et al. (1984). ASTM G 30 test procedures were followed. The self-loading nature of the U-bend permits its use in the small available working space in the irradiated autoclaves. Maximum stress levels in U-bends substantially exceed the yield stress. These materials were in the solution-annealed (15 min at 1050°C) and sensitized (24 hr at 600°C) conditions. Tests were performed in two autoclaves: one at 50°C and the other at 90°C, in a Co-60 irradiation facility at irradiation intensities of 6×10^5 and 3×10^5 rads/hr, respectively. Each autoclave was divided into three zones: water and rock (bottom), rock and vapor (middle), and moist air only (top). The air in the test vessel was purged daily with fresh air. The operating pressure in the vessel was essentially atmospheric so that the air space in the vessel was saturated with water vapor at the operating temperature. The intent of these experimental conditions was to accelerate cracking and provide some failed specimens in a reasonable test period. It should be noted that the high gamma dose rates and aqueous conditions are not expected to occur concomitantly in the repository environment. Specimens were examined after 1 and 3 mo of exposure, and the results are given in Table 9. In the 50°C test, two specimen failures were recorded: one after 1 mo of exposure and one after 3 mo of exposure. Both specimens were sensitized AISI 304, located in the vapor-only region of the autoclave. In the 90°C study, two sensitized AISI 304 specimens, both from the water-and-rock region, had failed after 1 mo of exposure. The 3-mo exposure inspection showed two additional failures: both were AISI 304, one in the vapor-only region and one in the vapor-and-rock region of the autoclave. Metallographic examination of the fractured specimens revealed IGSCC; an example is shown in Fig. 4.

The observed stress corrosion susceptibility of the sensitized AISI 304 was expected. None of the AISI 304L specimens have cracked intergranularly, but they have exhibited transgranular stress corrosion cracking (TGSCC) in subsequent inspections (Section 7). The larger number of failures occurring in the irradiated vapor phase suggests that a more severe environmental condition exists there, generated by radiolysis of the environment without dilution or buffering of the species produced. It is also possible that salts were deposited on

Table 9. Stress corrosion cracking test results from U-bend specimens exposed to irradiated J-13 water, crushed tuff rock, and water vapor. Results after 3-mo exposure[a].

	Environment					
	50°C (6 x 10^5 rads/hr)			90°C (3 x 10^5 rads/hr)		
Material	rock + water	rock + vapor	vapor	rock + water	rock + vapor	vapor
304	0/4	0/4	2/4	0/4	3/4	1/4
304L	0/4	0/4	0/4	0/4	0/4	0/4

[a] Source: Juhas et al. (1984) and Westerman et al. (1987).

Figure 4. Metallographic cross sections of sensitized Type 304 U-bend specimens showing IGSCC. Source: Juhas et al. (1984) and Westerman et al. (1987).

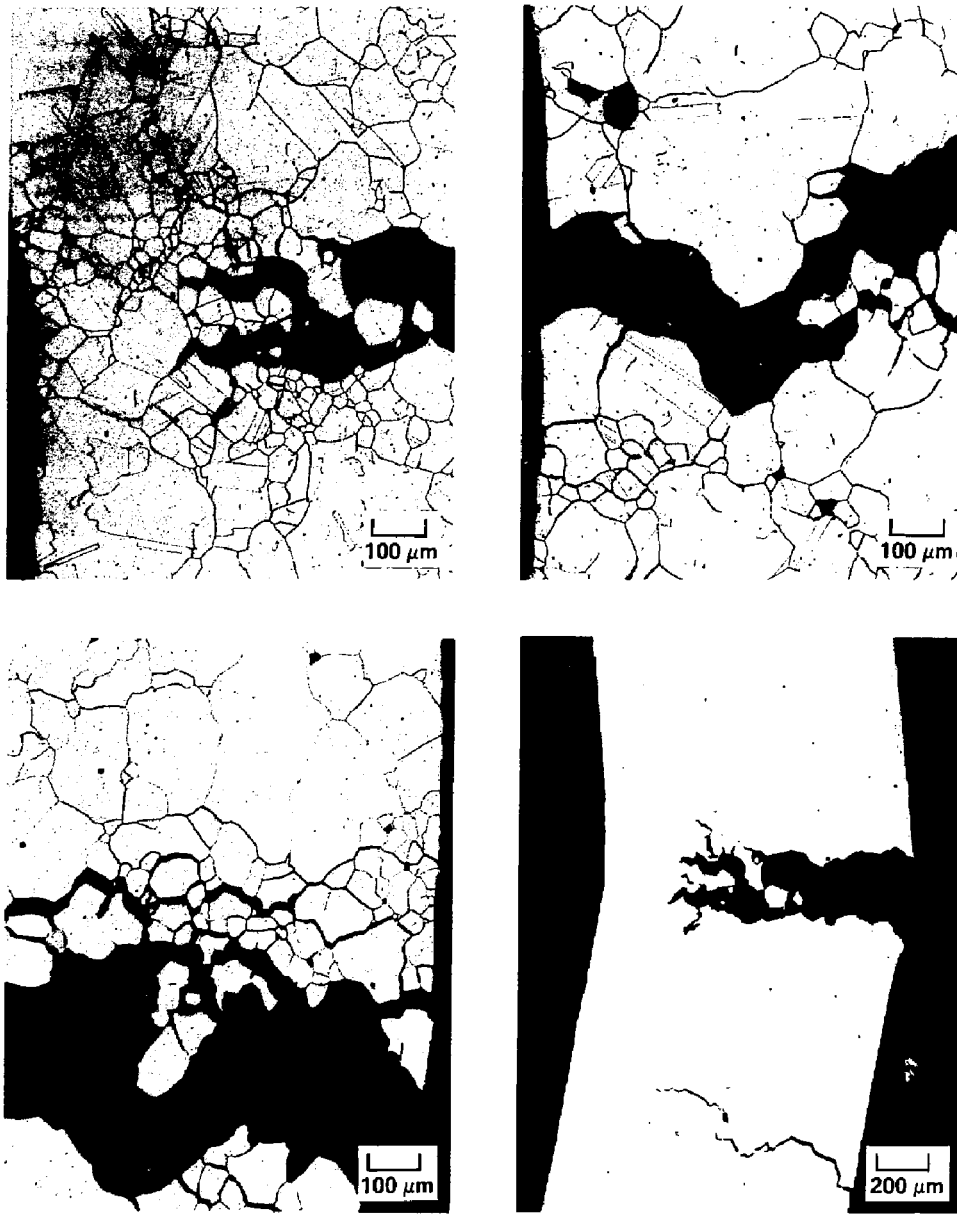

these specimens by aerosol generation during air sparging of the liquid. In the immersion condition, dilution and buffering would have occurred, moderating the severity of the environment.

Slow strain rate tests have been performed on AISI 304 and AISI 304L in Well J-13 water but not in the irradiated environments. The materials have undergone various heat treatments in attempts to produce conditions more susceptible to stress corrosion (Juhas et al., 1984). The slow strain rate technique and interpretation of test results have been discussed in papers by Parkins (1979) and Payer et al. (1979).

Essentially, the slow strain rate test is a determination of the effect of the environment on degradation of mechanical properties (yield strength, tensile strength, elongation, and reduction in area). A blank determination of these properties is made in air. Specimens are loaded until fracture occurs, and the fractured surface is examined, usually by scanning electron microscopy. A stress corrosion failure is indicated by a brittle fracture with evidence of grain facets and cleavage planes. In the absence of stress corrosion, the specimen fails by overload, and the failure is ductile, with characteristic heavy plastic deformation. In many respects, the slow strain rate test resembles a common tensile test, but the specimens are strained at slow crosshead speeds (less than 10^{-4} mm/mm/sec). Straining at these low rates allows study of the competition between the rate of slip-step emergence (creation of new surface by deformation of the metal specimen) and the rate of environmental interaction with this new surface, the interaction being the dissolution or the passivation of the new surface. Mechanisms of stress corrosion cracking in metals relate to the transition from passive to active behavior. Generally, some previous experimentation is required to determine the range of strain rates to use for a given metal/environment couple.

Results of testing the austenitic materials in 150°C aerated Well J-13 water are summarized in Tables 10 and 11 (Juhas et al., 1984; and Westerman et al., 1987). These initial tests were performed at this more elevated temperature to induce failure in some of the test specimens. The AISI 304 material contained 0.054 wt.% C and was tested in both the mill-annealed (as-received from the vendor) condition and in the solution-annealed and sensitized condition (1050°C for 15 min and water quench, followed by 600°C for 24 hr and air cool). The AISI 304L material contained 0.024 wt.% C and was tested in both the solution-annealed (1050°C for 15 min and water quench) and the solution-annealed and sensitized condition

Table 10. Results of slow strain rate tests of 304 stainless steel at 150°C[a].

Environment	Strain rate (per s)	Reduction of area (percent)	Elongation (percent)	Yield strength (ksi)	Ultimate strength (ksi)
			Mill-annealed specimens		
air	10^{-4}	80.2	48.0	37.4	74.4
air	2×10^{-7}	76.5	45.0	35.9	76.6
J-13[b]	10^{-4}	77.9	47.0	36.1	75.3
J-13	10^{-4}	79.6	46.0	36.3	74.9
J-13	2×10^{-7}	75.7	50.0	33.5	77.5
J-13	2×10^{-7}	76.4	47.0	35.1	77.0
			Solution-annealed and sensitized specimens		
air	10^{-4}	72.2	50.6	21.9	68.0
air	10^{-4}	66.5	51.5	26.0	68.8
J-13	10^{-4}	75.5	53.5	23.5	68.8
J-13	10^{-4}	74.9	51.0	23.5	69.0
J-13	2×10^{-7}	50.9	[c]	22.0	70.1
J-13	2×10^{-7}	26.4	[d]	20.7	64.5

[a] Source: Juhas et al. (1984) and Westerman et al. (1987).
[b] Air-sparged Well J-13 water.
[c] Not determined.
[d] Broke at gauge mark.

Table 11. Results of slow strain rate tests of 304L stainless steel at 150°C[a].

Environment	Sirain rate (per s)	Reduction of area (percent)	Elongation (percent)	Yield strength (ksi)	Ultimate strength (ksi)
		Solution-annealed specimens			
J-13[b]	10^{-4}	80.5	54.0	25.8	68.4
J-13	10^{-4}	78.4	52.0	27.1	68.2
J-13	2×10^{-7}	68.7	48.0	28.4	67.7
J-13	2×10^{-7}	72.9	46.3	26.7	68.2
		Solution-annealed and sensitized specimens			
air	10^{-4}	73.7	49.0	29.4	68.6
J-13	10^{-4}	72.2	49.6	[c]	[c]
J-13	10^{-4}	74.8	51.6	29.6	69.1
J-13	2×10^{-7}	76.0	49.0	26.6	68.8
J-13	2×10^{-7}	70.4	48.0	27.2	68.8

[a] Source: Juhas et al. (1984) and Westerman et al. (1987).
[b] Air-sparged Well J-13 water.
[c] Not determined.

(1050°C for 15 min and water quench, followed by 600°C for 10 hr and air cool). For the AISI 304 material (Table 10), the mill-annealed specimens had slightly lower ductility in the Well J-13 water than in air at the low strain rate; however, the changes in ductility were slight and do not indicate a susceptibility to stress corrosion cracking (SCC). The AISI 304 specimens in the solution-annealed and sensitized condition failed intergranularly with a significant drop in ductility when the strain rate was reduced from 10^{-4} to 2×10^{-7}/sec in Well J-13 water at 150°C. Cracks were found along the gauge section of these specimens, and the fracture surfaces showed clear evidence of intergranular fracture. The results of the AISI 304L tests are summarized in Table 11. Neither the solution-annealed nor the solution-annealed and sensitized treatments produced stress-corrosion-susceptible material under these test conditions.

Slow strain rate tests are continuing at other temperatures in Well J-13 water and in irradiated Well J-13 water. Specimens of AISI 316L are being investigated along with AISI 304L specimens that have been given lengthy heat treatments in the sensitization range.

6.3 Low Temperature Sensitization

Although the L grades of stainless steel appear to be nonsusceptible to sensitization for the length of time the container might remain in the 500-800°C temperature range, a long-term low temperature sensitization might occur during the tens to hundreds of years when the container will experience surface temperatures in the 100-250°C range after emplacement in the repository. The cumulative effects of time at temperature during welding and subsequent very long times at moderately elevated temperatures in the repository are additive in forming sensitized microstructures. This possibility of low temperature sensitization (LTS) was analyzed by Fox and McCright (1983), who concluded that heavily cold-worked AISI 304L (0.028 wt.% C) could develop a sensitized structure after as little as 10 yr at an isothermal surface temperature of 280°C. This analysis was based on extrapolating the results from the work of Briant (1982) in support of investigations on sensitized 300-series stainless steels under boiling water reactor (BWR) environmental conditions. Reduction of the container surface temperature in the repository could cause a significant increase in the time required to develop a sensitized microstructure; for instance, the stainless steel in Briant's work would take 120 yr to sensitize isothermally at 250°C and 4000 yr at 200°C. It should be noted that strains of this level produce microstructures atypical of those found in BWR pipes or those reasonably expected for waste package containers. The heat treatment was used only to accelerate the sensitization phemonenon. In reality, the container surface will cool continuously; therefore,

predictions based on isothermal conditions are very conservative. A subsequent analysis (Oversby and McCright, 1984) indicated that, at a peak surface temperature of 250°C followed by cooling at a rate predicted from a heat transfer code and assuming certain reference waste package conditions (Hochman and O'Neal, 1984), even the high-carbon, heavily cold-worked AISI 304L used in Briant's work would not sensitize. Results of this analysis are illustrated in Fig. 5.

Development of low temperature sensitization can be retarded in ways other than reduction of the peak surface temperature of the container. The mechanism for development of LTS is discussed by Povich (1978) and requires a highly cold-worked structure for nucleation of subcritical carbide precipitates that are formed in the usual sensitization temperature range (above 500°C) but are not discernible by any of the ASTM tests. These subcritical precipitates then grow when the specimen is exposed to temperatures below 500°C for prolonged periods. Obviously, reduction of the amount of cold work in the specimen vitiates development of LTS.

Work performed in response to the concerns of IGSCC in BWR piping indicates that the molybdenum-bearing AISI 316L was considerably more resistant to LTS (Mulford et al., 1983; Briant et al., 1982). The same group also tested special grades of AISI 316 (and AISI 304) with extra low carbon (<0.02 wt.%) and with intentionally high nitrogen content (>0.06 wt.%) and found that these compositions produced beneficial effects. Special nuclear grades of AISI 316 with high nitrogen and low carbon are recommended as replacement materials for AISI 304 piping in BWRs (Danko, 1984; Proebstle and Gordon, 1982). It appears that the molybdenum and nitrogen additions impede the diffusion of carbon atoms in austenitic stainless steels; therefore, the growth rates of carbide nuclei are slowed, and materials containing these alloy additions are considerably more resistant to sensitization both above and below 500°C.

Figure 5 shows an extrapolation of the LTS data from the BWR work and superposition of this on a typical time-temperature (plotted as log time vs. 1/T) profile for a spent fuel waste package in the thermal environment of a tuff repository (Oversby and McCright, 1984). The

Figure 5. Relationship between thermal history of emplaced nuclear waste containers and long-term sensitization of austenitic stainless steels. Modified from Oversby and McCright (1984).

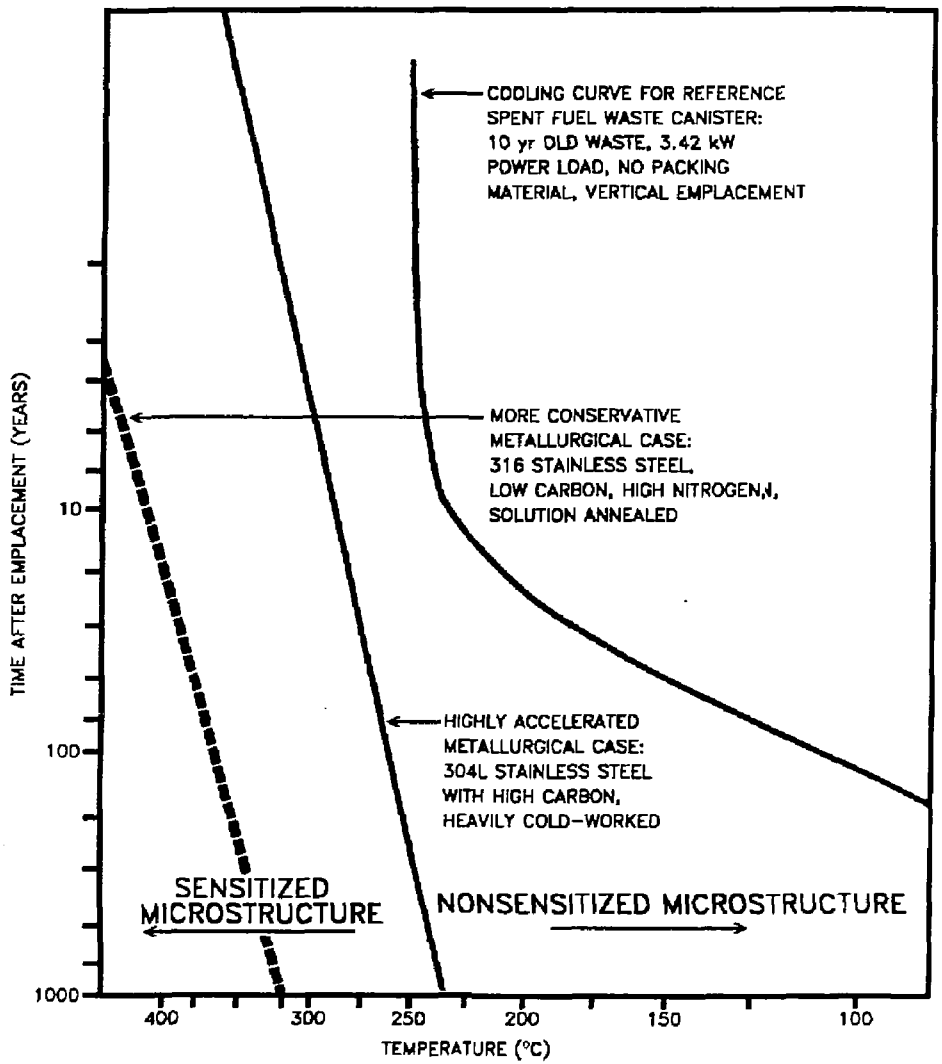

prediction from the superposition is that even the heavily cold-worked AISI 304L would not develop a sensitized microstructure (from the Briant et al., 1982 work cited above). However, a higher surface temperature on the container would move the temperature decay curve to the left so that it might possibly intersect the line corresponding to the extrapolation of time-to-sensitization for the alloy. The figure also indicates that a greater degree of conservatism would be obtained from using an AISI 316-type of stainless steel with higher nitrogen and lower carbon content because of the greater time required to attain a sensitized microstructure at a given temperature.

Some additional factors need to be considered to assess the possibility of developing a sensitized microstructure and resulting IGA and IGSCC. With sufficient time at temperature, chromium could rediffuse from the bulk to the depleted regions and restore a uniformly high chromium content throughout the alloy. This condition would eliminate any preference for localized attack due to the lack of chromium and the instability of the protective film at these locations. The activation energy for chromium diffusion is considerably higher than that for carbon diffusion so that the restoration process is slow. Chromium rediffusion is indicated in the series of curves on the top-right side of the TTS curves (Fig. 3). At very long times at lower temperatures (200-300°C), the series of curves bounding the sensitized region on the bottom and left in Fig. 3 could meet those bounding the series of curves on the right. Physically, this would mean that the carbide precipitates would be nucleated but the growth of these precipitates would be so slow that the chromium content would never be locally depleted. This situation would not produce a sensitized microstructure.

On the other hand, situations that would enhance carbon diffusion at lower temperatures (such as movement of carbon atoms along grain boundaries and dislocation pipes) could readily favor sensitization. Diffusion along dislocations is relatively more significant at lower temperatures, where matrix diffusion of atoms is very slow. This competition of different mechanisms was considered by Logan (1983), who applied a finite element analysis and concluded that AISI 304L would not sensitize under the projected repository thermal conditions. However, his analysis did not consider a full range of reported activation energies for the different diffusion processes. Other work (Kekkonen et al., 1985) cites measured activation energies for sensitization in 304 stainless steel and grouped these into "high" activation energy processes (diffusion of Cr in the matrix) and "low" activation energy processes (diffusion of Cr along grain boundaries). The respective activation energies were on the order of 220 kJ/mol and 100 kJ/mol. The interpretation of this work was that low temperature sensitization could occur

in real operating times (≤ 40 yr) at temperature in BWRs because of the domination of the low-activation energy process at temperatures less than approximately 350°C. However, as discussed in the paper by Smith, 1975 on diffusion in 316 stainless steel, the grain boundary diffusion mechanism operates only over a limited area so that the absolute amount of material moved by this mechanism is small and becomes smaller as the temperature decreases. This is in accord with the decreasing degree of sensitization measured at the lower temperatures. Another consideration for the vanishing amount of low temperature sensitization at BWR operating temperatures (288°C) and lower is that the growth rate of the carbide becomes controlled by the reaction kinetics forming the carbide at the austenite/carbide interface, and this is presumably a slow process at low temperatures (<250°C). Thus, arguments can be made that would hasten the sensitization effect at low temperatures with respect to extrapolations made from higher temperature data (diffusion along grain boundaries and along dislocation pipes in very heavily strained material), and arguments can be made that would retard the effect (interface control vs. diffusion control). Figure 5 indicates that if sensitization were to occur at all, it would be evident in a few to several years at temperatures in the range 200-300°C. This time period lies within the realm of experimental practicality.

6.4 Environmental Effects on IGSCC Susceptibility

In analysis of IGSCC, a sensitized microstructure is considered necessary for the phenomenon to occur in the absence of crevices. The chemical environmental conditions are also important. The phenomenon has been studied mostly under the thermal and chemical environmental conditions relevant to BWR coolant (250-300°C high-purity water on the order of 1 Mohm-cm resistivity, under pressure, with varying oxygen contents, usually ranging from 2 to 8 ppm). The general conclusion from this work is that the stronger the oxidizing potential of the environment, the greater the susceptibility for IGSCC in sensitized materials. The work of Fujita et al. (1981) indicated that gamma radiation (4.5×10^4 rads/hr) further increased the stress corrosion susceptibility of sensitized AISI 304 in high-purity water. They used the slow strain rate test to determine the SCC susceptibility and found that the fractures were all intergranular.

Unlike other corrosion degradation modes on stainless steel, susceptibility toward IGSCC is probably not so strongly affected by just the chloride ion. (Sulfate ions and heavy metal cations in small concentrations, as well as chloride ion, appear to favor IGSCC on susceptible materials in BWR environments.) Many theories of SCC consider a surface pit or

crevice to be the site of initiation, and the electrolyte content is important in establishing these sites (Staehle, 1971). It is also difficult to make valid extrapolations of results obtained in the BWR environment to predict the behavior of waste package containers, although the appearance of a phenomenon occurring after decades at the reactor operating temperature suggests that it could occur in the repository during longer time periods at somewhat lower and decreasing temperatures.

The analysis of Fox and McCright (1983) considered some of the mitigating effects that the environment might have, even on a sensitized stainless steel. First, the dominant environment for tens to hundreds of years after emplacement would be unsaturated steam at temperatures above 96°C. During this period, the gamma radiation field would be at its highest level. However, without an electrolyte present, there would be high electrical resistance between local anodic and cathodic sites and, consequently, slow rates of oxidation. Mechanisms for aqueous corrosion become operable when a continuous moisture film is present, which appears to occur only at or below the boiling point and at relative humidities greater than 50-60 percent (Shreir, 1977). By the time the container surface temperature cools to where condensation is possible, the radiation field would be less than approximately 500 rads/hr. At this level of radiation, radiolytically induced changes in the aqueous environment might not have significant effects on corrosion. Experimental work thus far completed has not indicated any intergranular stress corrosion initiation in the wet environment for the low-carbon austenitic stainless steels (McCright et al., 1983; and Juhas et al., 1984).

6.5 Stress Effects on IGSCC Susceptibility

Stress is also an important factor in assessing stress corrosion susceptibility. Work performed with regard to SCC of AISI 304 piping in BWR environments characteristically showed that a threshold stress on the order of the yield stress of annealed material and perhaps at 70 percent of the yield strength of cold-worked material is needed to initiate SCC, the actual threshold stress being a function of temperature, ionic concentrations, and degree of sensitization (Bruemmer and Johnson, 1984). The waste container body, including any assembly welds, could be annealed after forming to reduce residual stress. Reduction of the residual stress would also decrease the tendency for low temperature sensitization to occur during prolonged exposure to the thermal conditions of the repository, because the annealing or stress relief process on the container would have eliminated many potential high-diffusivity paths for carbide growth and chromium depletion. Any annealing or stress relieving to be performed

after the final closure weld is made would probably be impractical, and this region might retain a residual stress approaching the yield strength of the material. However, different processes leave the weld and heat-affected zones in different states of stress, and it is possible to choose a process that would leave at least the outside surface of the container in compression, to minimize the possibility of initiating SCC. The effects of different welding processes on increasing the resistance to SCC of AISI 304 in the BWR environment have been discussed by Iwasaki (1982). A leading process involves inductively heating the weld on one side and cooling it on the other to superpose a favorably oriented thermal stress on top of the weld stress, so that the surface that is exposed to the SCC causative environment is compressed. The ready accessibility of the container assembly welds is expected to make them amenable to nearly any process required to demonstrate a high level of assurance that SCC will not occur. However, the closure weld presents limitations on the choice of processes that can alleviate stress corrosion concerns. This point is discussed in greater detail in Section 8.

6.6 Alloying Effects on IGSCC Susceptibility

Another approach to minimizing sensitization is use of the stainless steel grades with additions of alloying elements to stabilize the carbides. These grades include AISI 321 (titanium addition) and AISI 347 (niobium addition). Titanium and niobium form carbides more readily than chromium; hence, the carbon in the stainless steel will preferentially precipitate with the titanium or niobium, leaving essentially all of the chromium in solid solution in the austenite. A considerable excess of the stabilizing element above that needed to stoichiometrically combine with the carbon is added, but, since titanium and niobium are ferrite-stabilizing elements, their contents must be carefully controlled to balance the phase distribution, particularly in welded regions. In practice, the stabilized stainless steel must undergo the proper time-at-temperature to assure formation of the titanium or niobium carbides and not the formation of the chromium carbides. The different carbides preferentially form at different temperatures; somewhat slower cooldowns after welding are preferred for the stabilized grades. An improperly heat-treated stabilized stainless steel is subject to knife-line attack in aggressive oxidizing environments, because some chromium carbide has formed in a very narrow region; this region subsequently undergoes intergranular attack. The additional alloying element presents additional concerns in many welding processes compared with AISI 304L and AISI 316L. These concerns are discussed in Section 8. To avoid IGSCC problems in the BWR environment, the stabilized grades (particularly AISI 347 and some modified versions of AISI 347) are the preferred construction materials, particularly for reactors in Europe. Recent

alloy developments combine the best features of the low-carbon grades with those of the stabilized grades of stainless steels (Abe et al., 1982). The high alloy content of Alloy 825, its low carbon content, and titanium stabilization of the carbides confer a very high degree of resistance to sensitization.

6.7 Summary of Testing and Analysis to Date

In summary, experimental work performed as of June 1987 has not shown any tendency for the L grades of stainless steels to stress corrosion crack intergranularly even when specimens are stressed to and beyond the yield strength and are given heat treatments that favor carbide precipitation. Exposure conditions have also been severe, including irradiated water and wet vapor, in which moderately to strongly oxidizing conditions are obtained. An analysis aimed at determining whether low temperature sensitization could occur in nuclear waste containers indicated that normally annealed AISI 304L with the expected time-temperature history during fabrication, welding, and subsequent storage in the repository would not sensitize. The combination of heavily cold-worked material due to a major fabrication error and a time-temperature history significantly different from the expected case might result in sensitization occurring during the containment period.

Viable alternatives to AISI 304L would be AISI 316 (with extra low carbon and high nitrogen modifications), AISI 321, and Alloy 825. Another possible modification includes addition of carbide-stabilizing elements to reduce development of a sensitized microstructure, but the stabilized grades might pose additional concerns in welding. Reduction of the peak surface temperature and stresses in the container would also alleviate intergranular stress corrosion susceptibility. This can be accomplished by reducing the residual stress from fabrication and welding of the container and also by reducing the peak temperature of the containers in the design of the waste package and the arrangement of waste packages in the repository. Although it is advantageous to maintain the container surface temperature above the boiling point for as long as possible, from the point of view of retarding sensitization it is advantageous to keep the surface temperature below approximately 250°C for the more susceptible materials.

A model is being developed to predict sensitization in austenitic stainless steels, and the model is being extended to high-nickel materials such as Alloy 825. The essential feature of this model is consideration of the chromium diffusion rate as established by the chromium thermodynamic activity gradient between the activity of chromium in the bulk and that at the carbide-austenite interface. This model considers temperature, strain, and compositional effects in materials (Mozhi et al., 1985).

7. PITTING CORROSION, CREVICE CORROSION, AND TRANSGRANULAR STRESS CORROSION CRACKING OF AUSTENITIC MATERIALS

These three corrosion degradation modes are governed principally by the composition of the aqueous environment when the concentration of certain ionic species in water exceeds some threshold amount. Discussion was advanced in Glassley (1986) on the waste package environment and what the expectations are on the amount and composition of the water that can enter the near-package environment. Concerns relative to the performance of austenitic stainless steel and high-nickel alloy container materials are briefly discussed in Section 4. But just as the attack itself is localized, the causative environment might be localized and might be considerably different from the bulk environment. In the majority of cases, the susceptibility to these degradation modes is dependent on the chloride ion concentration in the environment. A review paper by Nuttall and Urbanic (1981) discussed the levels of chloride ion needed to initiate pitting, crevice, and transgranular stress corrosion attack in AISI 304. Much of their documentation on critical chloride levels (as NaCl) was based on the observations of Truman (1977). Figure 6 was adapted from their work; the chloride content of Well J-13 water (approximately 7 ppm) is juxtaposed. Because of the similarity in composition of major alloying elements, AISI 304L is expected to behave similarly to AISI 304 with respect to these modes. AISI 316L (i.e., molybdenum-bearing stainless steels) and Alloy 825 (i.e., higher nickel materials) are markedly more resistant to chloride-induced corrosion degradation modes, because higher thresholds of chloride ion concentration are required to initiate and propagate the corrosion attack. It is important to note that pitting can be viewed as a nucleation and growth process. Therefore, instead of basing lifetime predictions solely on a "critical threshold," it might become necessary to use models for the prediction of incubation time as a function of chloride anion concentration and electrochemical potential (Okada, 1984).

Figure 6. Temperature-chloride concentration thresholds (for AISI 304) for initiation of localized corrosion phenomena in sodium chloride solutions. Crevice, pitting, and transgranular stress corrosion cracking initiate to the right of their respective threshold curves as determined by immersion corrosion tests. For comparison purposes, the chloride ion concentration of Well J-13 water is indicated. Modified from Nuttall and Urbanic (1981).

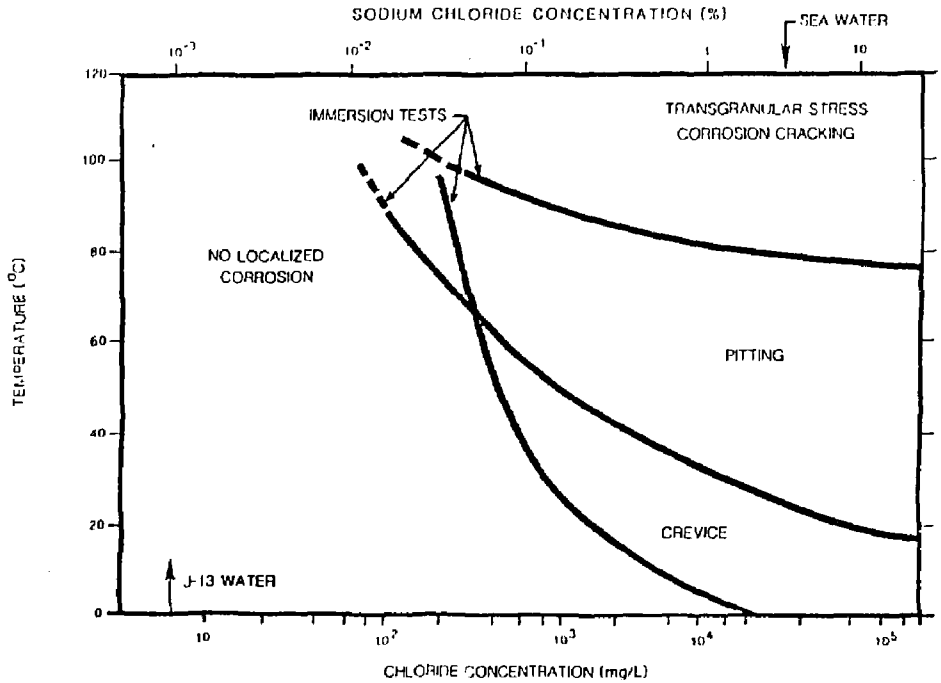

Although these degradation modes have some features in common, there are important differences, particularly in the initiation phase of each mode. A brief discussion is presented here, because the testing and analyses are based on aspects of the causative mechanisms; greater detail can be found in such reference texts as Fontana and Greene (1978) and Sedricks (1979).

Crevice corrosion is favored when differential concentration cells are established on a metal surface, particularly on a metal that shows active-passive behavior, as do stainless steels in many environments. The creviced area is starved for oxygen, and the passive film breaks down and cannot readily re-form. Dissolution of the metal occurs at this resulting local anodic site, the metal ions hydrolyzing with the water to form a more acidic environment than the bulk environment (Pickering and Frankanthal, 1972). Anionic species, especially the mobile chloride ions, migrate to the anode and generally increase the ionic strength in the local environment. The local pH in the crevice region decreases, and the concentration of anionic species (such as chloride) increases. These conditions do not favor repassivation of the alloy, and a high dissolution rate of the metal in the creviced region continues.

Pitting corrosion is initiated at weak points in the passive film. Pits form preferentially at locations such as inclusions (especially certain sulfide-rich inclusions) on the exposed metal surface, where the film readily breaks. Electrochemical differences between the inclusion and the bulk material stimulate local currents, and dissolution of the inclusion creates a local chemical difference that is aggressive toward the metal. Propagation of the pit occurs because of locally intense metal dissolution. The larger area of the metal surface remains passivated and cathodic. Many features of the propagation phase in pitting corrosion are similar to those for crevice corrosion.

Transgranular stress corrosion cracking (TGSCC) is due to the conjoint action of very localized anodic dissolution at the crack tips and applied or residual stress. The cracks frequently initiate around a crevice or pit, anodic dissolution at the crack tip is driven by cathodic processes occurring along the crack wall. Resistance to this kind of corrosion is obtained by adding alloying elements that decrease the electrochemical potential difference between bare areas (where the strain has transiently broken the protective passive film) and the areas still covered and protected by the film. Unlike the intergranular kind of SCC discussed in Section 6, these cracks propagate transgranularly, and the propagation is not affected appreciably by sensitization of the material. In high chloride solutions (on the order

of a few percent chloride ion), stresses on the order of 10% of the yield stress sustain cracking. The threshold stress decreases with increasing chloride ion concentration.

Pitting, crevice, and TGSCC are most significantly affected by the alloy composition (major alloying constituents: Cr, Ni, Mo; and to some extent the minor constituents: S, P, N, Mn) and the environmental composition. These degradation modes are particularly favored in concentrated solutions, since the high ionic strength of these environments support the electrochemical currents between local anodic and cathodic sites. Furthermore, species that tend to acidify the environment and species that cause breakdown of passive films favor these forms of corrosion. The primary role of the beneficial alloying additions is probably their effect on increasing the rate of film repassivation (Latanision and Staehle, 1969).

7.1 Electrochemical Testing to Determine Localized Corrosion Occurrence

A preliminary study by Glass et al. (1984) surveyed electrochemical parameters relating to general corrosion (e.g., corrosion potential and corrosion current) and to localized pitting and crevice corrosion (e.g., pitting potential and protection potential). These parameters were measured for the candidate materials in aqueous solutions that are believed to be characteristic of the repository site. In addition to using Well J-13 water, certain intentional additions were made to study the effect of chloride ion, and, in some cases, the ionic species in Well J-13 water were concentrated by boil-down. Test procedures and details are discussed by Glass et al. (1984). The principles and theory of electrochemical techniques for evaluating corrosion susceptibility of metals are described by Barnartt (1977), Mansfeld (1977), and Verink (1977).

To assess the susceptibility of the candidate materials to localized corrosion (pitting and crevice attack) in Well J-13 water at different temperatures, cyclic anodic polarization curves were obtained. The potential of the working electrode (which is the candidate material of interest) was scanned by enforcing potentials anodic to the corrosion potential (E_{corr}) and then reversing the direction of the scan back to more negative values. The scan rate was 1 mV/sec (to ensure reasonably steady-state conditions), and potentials were measured relative to a saturated calomel electrode (SCE) at room temperature. Current flowing through the working electrode was continuously monitored during the scan. Such a potential scan, whose waveform is triangular when the impressed potential vs. time is plotted, yields electrochemical values of interest such as the pitting potential (E_{pit}) and the protection potential (E_{prot}). The pitting

potential is the potential above which pits spontaneously initiate and grow. The protection potential is the potential below which previously initiated pits repassivate and no new pits form. At potentials between the pitting and protection potential, new pits are not initiated but previously initiated pits continue to grow. The values of the pitting and protection potential relative to the corrosion potential are indicative of the pitting susceptibility of the tested alloy in the tested environment.

The values of E_{pit}, E_{prot}, and E_{corr} depend on the technique used (particularly the potential scan rate). Slow scan rates approach the truly steady-state potentiostatic condition, and the pitting potential is usually observed to decrease at the slower scan rate values. For example, the pitting potential of AISI 316L in a 0.2 M NaCl solution is 0.429 V (SCE) at a potentiodynamic scan rate of 10 mV/sec. The pitting potential decreases to 0.397 V (SCE) at a rate of 1 mV/sec and to 0.391 V (SCE) at a rate of 0.1 mV/sec. Projections of localized corrosion performance are best made on the basis of the potentiostatic determination (that is, the scan rate approaching zero) of the pitting potential as well as the other important electrochemical parameters.

A typical anodic polarization curve for AISI 304L in 90°C Well J-13 water is shown in Fig. 7. The curve displays features common to all polarization curves obtained in Well J-13 water; the important electrochemical parameters are identified on the figure. When the stainless steel is scanned anodically starting from E_{corr}, the AISI 304L remains passive until the pitting potential is reached. At this characteristic potential, complete breakdown of the passive surface occurs and the anodic current density increases by several orders of magnitude. The closer E_{pit} is to E_{corr}, the more susceptible the alloy would be to pitting in the event that an increase in the oxidizing potential of the environment occurred. This might occur in a radiation field where radiolysis products would shift E_{corr} to more positive values. From plots like that in Fig. 7, tabulations of electrochemical parameters for some of the prospective container materials were made. Plots of these parameters are shown in Figs. 8 through 10 (AISI 304L, AISI 316L, and Alloy 825, respectively, in Well J-13 water at different temperatures). Over the range tested, no clear temperature dependence was found.

In all cases, the values of the pitting potential are sufficiently removed from those of the corrosion potential such that no spontaneous pitting of these alloys should occur in Well J-13 water. This result is also expected from the summary figure, Fig. 6. The other ionic species

Figure 7. Potentiodynamic anodic polarization curve for AISI 304L stainless steel in Well J-13 water at 90°C. Scan rate was 1 mV/s. Scan starts from E_{corr}. Line marked passive indicates that stainless steel remains passive until the pitting potential is reached. Modified from Glass et al. (1984).

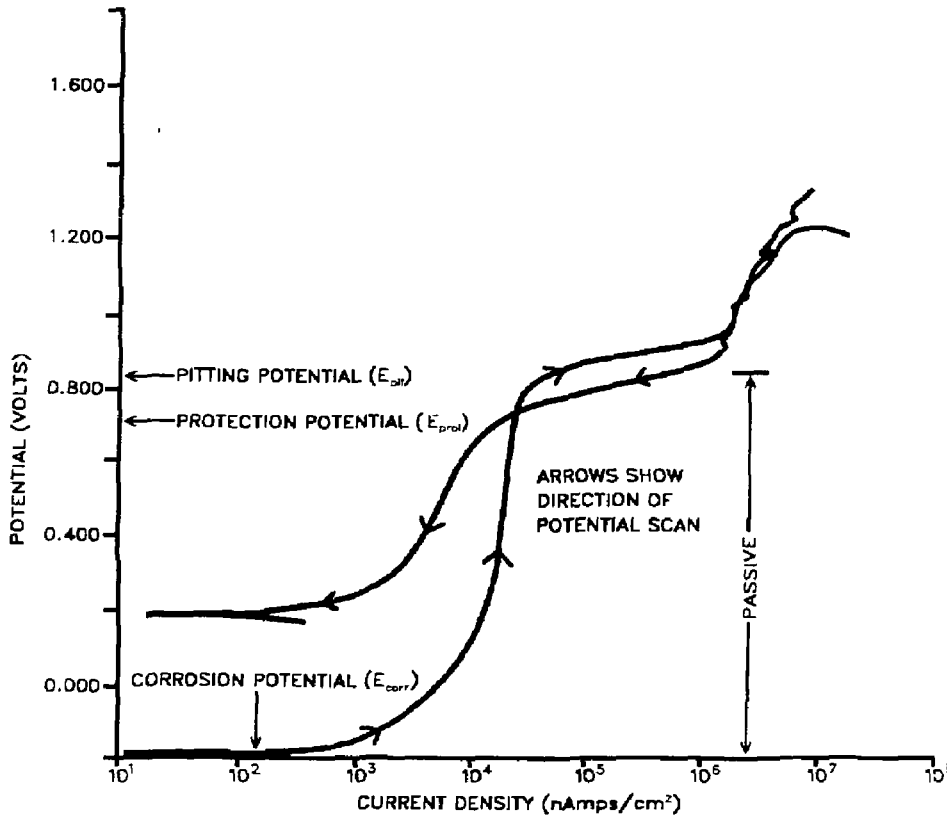

Figures 8, 9, and 10. Electrochemical parameters for AISI 304L , AISI 316L, and Alloy 825 in tuff-conditioned water from Well J-13 as a function of temperature. All potentials are referenced to a saturated calomel electrode at 25°C. Modified from Glass et al. (1984).

Figure 8

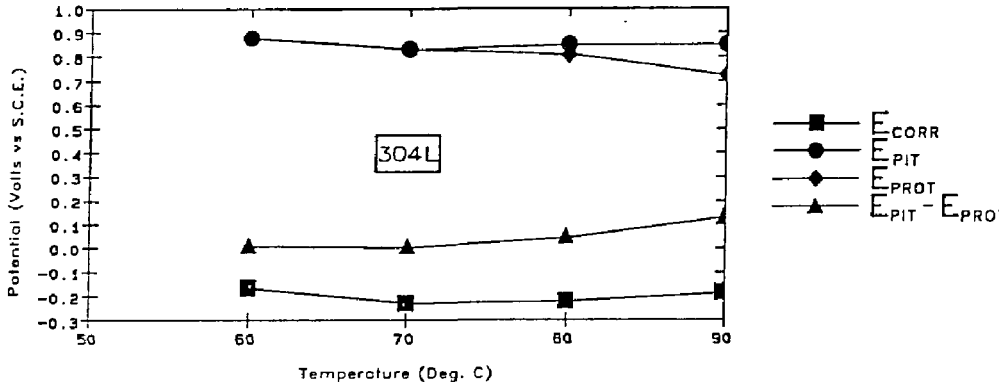

Figure 9

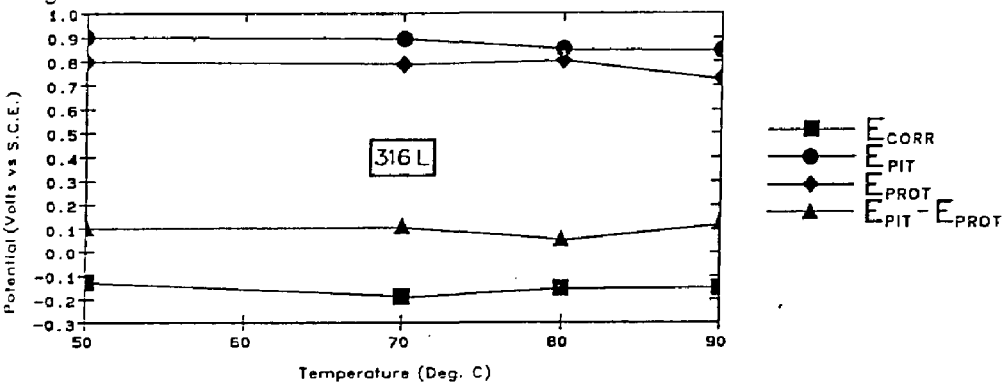

Figure 10

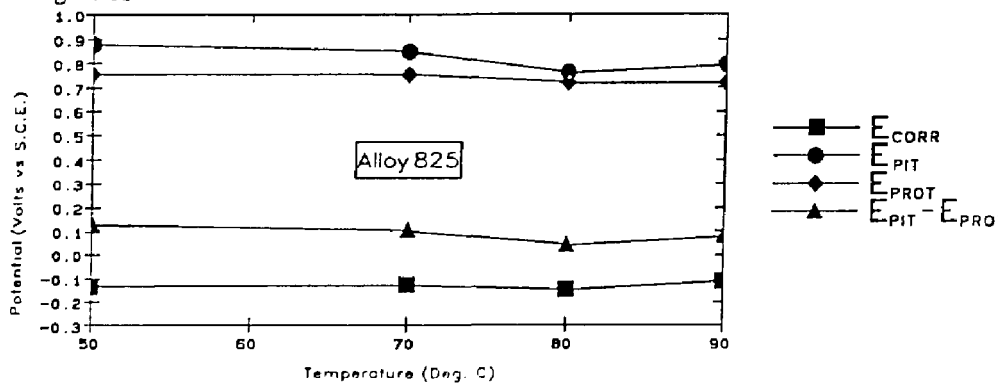

present in the Well J-13 water, if they have any effect at all, would tend to retard pitting, as the quantitative analysis by Szklarska-Smialowska (1974) has indicated. Although the halide ions (chloride and fluoride) increase the pit propagation rate, ions such as nitrate and bicarbonate tend to retard the propagation rate. The parameter (E_{pit} - E_{prot}) has been used previously by Wilde (1974) to evaluate alloys in terms of crevice corrosion resistance. As the value of (E_{pit} - E_{prot}) becomes larger, the resistance to crevice corrosion decreases. Also, greater difficulty in repassivating growing pits is indicated by larger values of (E_{pit} - E_{prot}). When the protection potential moves closer to the corrosion potential on the return scan, the metal surface is less easily repassivated, allowing localized attack to continue. In a crevice situation, the environmental conditions favor initiation of localized attack; therefore, the interest is in how rapidly the attacked surface can repassivate.

The data in Figs. 8 through 10 do not show any clear trends for changes in localized corrosion susceptibility. The curves for AISI 316L and Alloy 825 show the same trends as those for AISI 304L. As with the data for general corrosion, very little difference was noted for the candidate alloys in Well J-13 water over the 50-100°C temperature range tested.

As expected, when chloride ion is added to Well J-13 water, the pitting and protection potentials move closer to the corrosion potential for AISI 304L. Glass et al. (1984) showed that an addition of 1000 ppm NaCl to Well J-13 water moved the pitting potential to within 100 mV of the corrosion potential, so that spontaneous pitting of the specimen could be observed. Their results are consistent with the data presented in Fig. 6. The more highly alloyed AISI 316L and Alloy 825 show more resistance in this environment, as would be expected, because of the well-documented role of molybdenum (and to a lesser extent nickel) in increasing the resistance to chloride-ion effects on inducing localized corrosion (Bingham, 1974).

Another consideration in predicting localized corrosion susceptibility is the surface condition of the alloy. The containers are expected to experience a high-temperature air/steam environment for a significant time after emplacement, with temperatures up to approximately 250°C (spent fuel packages). Some preliminary results (Glass et al., 1984) on AISI 304L specimens with thermally formed oxide films indicate that these specimens were somewhat more resistant to pitting (lower current densities near the pitting potential) in 90°C Well J-13 water with 1000 ppm chloride addition than those that were not preoxidized. However, once these specimens started to pit and the applied potential was then shifted cathodically, the thermally oxidized specimens did not repassivate any more rapidly than those that were not

previously oxidized; thus, the beneficial effects can be lost once pitting initiates. The work of Bianchi et al. (1974) indicates that, at some temperatures, oxides are formed that are more susceptible to pitting corrosion because of changes in the semiconducting properties of the oxide. Additional work is needed to resolve the effects of thermally grown films on the subsequent localized corrosion susceptibility.

7.2 Localized Corrosion Testing in Gamma-Irradiated Environments

The combination of a concentrated aqueous environment and a sufficiently high gamma dose rate to promote radiolysis of the water might pose one of the more demanding of the possible situations on the container. Relatively little previously published work exists in this area. The coexistence of a high gamma field on a wet container surface is not an anticipated condition, because the gamma dose rate is expected to be at a relatively low level (<100 rads/hr) when the container surface cools to the boiling point of water for the majority of the containers (Glassley, 1986). However, waste packages placed at the periphery of the repository will cool more rapidly, and it is conceivable that these could become wet while the radiation level is high enough to radiolyze the aqueous environment.

Glass et al. (1985) measured the corrosion potentials of austenitic stainless steels in irradiated Well J-13 water environments. Upon imposition of the gamma field (3×10^6 rads/hr), the corrosion potentials of both AISI 304L and AISI 316L in a series of electrolytes related to Well J-13 water shifted in the positive (oxidizing) direction, typically by 150-200 mV. The results for AISI 316L in 10x and 100x concentrated Well J-13 water are shown in Figs. 11 and 12. The 10x and 100x concentrated electrolytes were prepared by boiling down Well J-13 water to reach the desired level of concentration. In these figures, "on" refers to lowering the test cell into the center of the gamma source assembly (cobalt-60), and "off" refers to raising the cell approximately 1.5 m above the source assembly where the cell is shielded by the water in which the source assembly is submerged. Several on/off cycles are shown. Similar positive potential shifts upon imposition of the gamma field were observed for AISI 316L in plain Well J-13 water and for AISI 304L both in plain Well J-13 water and in its concentrated versions. As expected, the gamma radiation field made the environment more oxidizing. Part of this was shown to be very probably due to the production of hydrogen peroxide from radiolysis of the Well J-13 water. Chemical analysis of the irradiated solution and a demonstration experiment

Figure 11. Corrosion potential behavior for 316L stainless steel in 10x concentrated Well J-13 water under gamma irradiation. The solution was not exposed to irradiation prior to initiation of the first "on/off" irradiation cycle. Source: Glass et al. (1985).

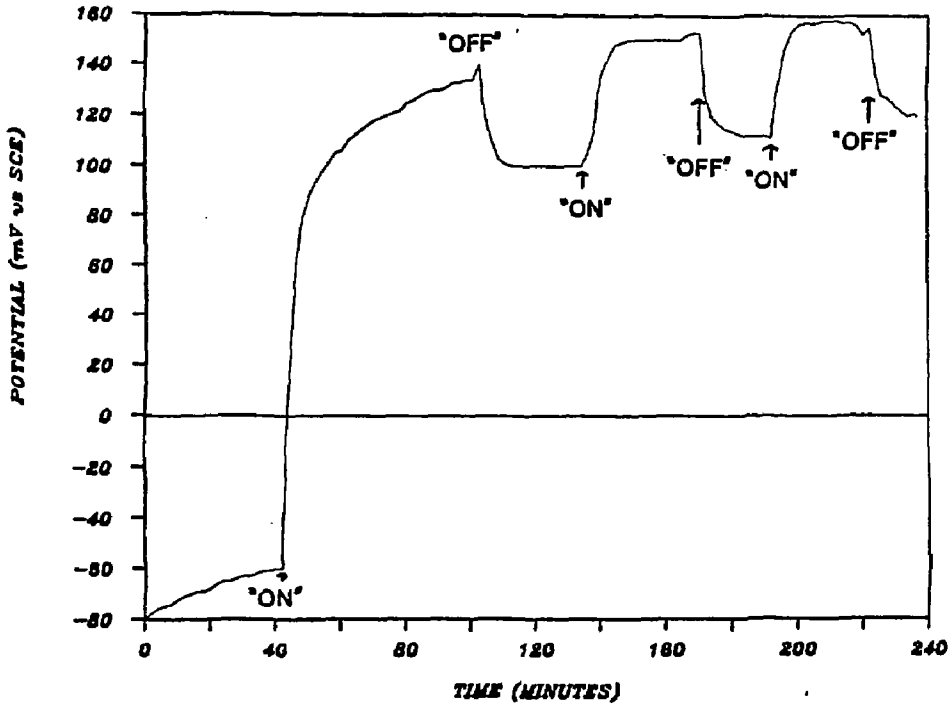

Figure 12. Corrosion potential behavior for 316L stainless steel in 100x concentrated *Well J-13* water under gamma irradiation. The solution was not exposed to irradiation prior to initiation of the first "on/off" irradiation cycle. Source: Glass et al. (1985).

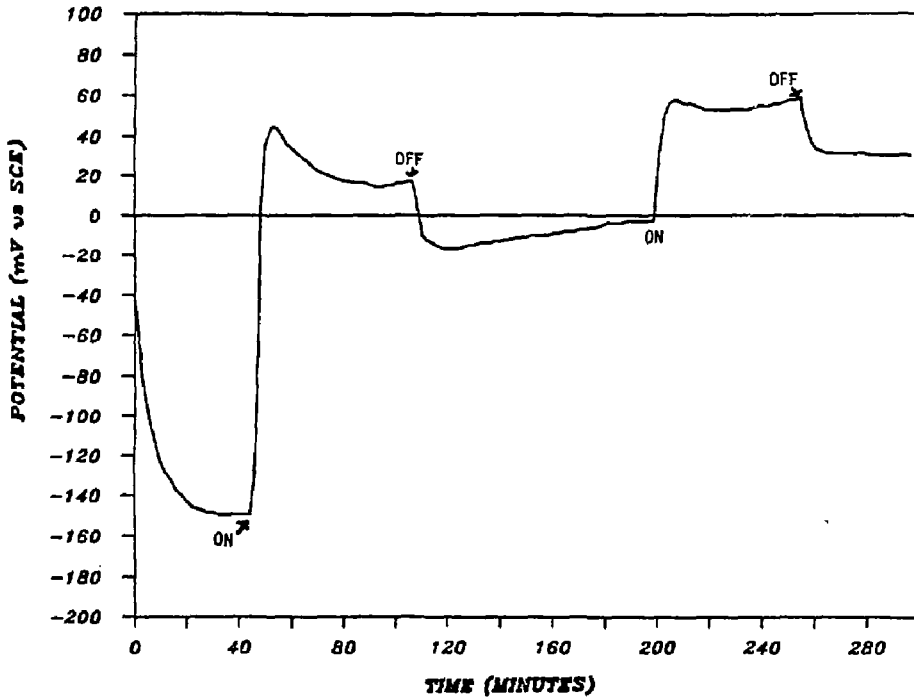

in which drops of H_2O_2 were added to the solution with simultaneous monitoring of the corrosion potential confirmed that the hydrogen peroxide concentration was in the range of 0.14 to 0.49 mM.

Polarization curves were determined for some of the candidate stainless steels (AISI 304L and AISI 316L) in irradiated Well J-13 water. Results indicated that both the pitting potential and the corrosion potential were shifted in the positive direction by approximately the same amount. Thus, irradiation does not appear to increase the susceptibility to localized corrosion in unaltered Well J-13 water. Some preliminary work by Glass et al. (1985) in which AISI 316L was exposed to a solution of 650 ppm chloride (prepared by dissolving NaCl in deionized water) indicated a susceptibility of the material to pitting and crevice corrosion under those conditions. In this case, the protection potential (on the reverse scan) lies at more negative values than the corrosion potential. In the same solution but without irradiation, the protection potential lies at more positive potentials than the corrosion potential, a situation indicating that localized corrosion is not predicted. These polarization curves are depicted in Fig. 13. These curves were obtained in deionized water with NaCl additions; the mitigating ionic species normally present in the Well J-13 water were absent. This kind of work is being continued on other materials and at different concentrations and temperatures.

An important benefit of the work described in this section is its application to conducting long-term tests at predetermined controlled potentials. The goal of these tests is either to accelerate or to retard localized corrosion, depending on the choice of the controlled potential and its relative position to the critical pitting and protection potentials, as an important aspect of the modeling effort for localized corrosion. This effort also relates to the work discussed under general corrosion (Section 5), where a model to predict the long-term changes in the corrosion potential is being developed. The chemical effects of gamma radiation can then be related to the change in corrosion potentials and critical potentials. Future work is especially needed for a range of gamma dose rates and temperatures to define the ranges of these electrochemical parameters.

7.3 Localized Corrosion Testing with Creviced Specimens

Metal-insulator-metal sandwich-type creviced specimens are being exposed for long periods of time to Well J-13 water and to its concentrated versions with and without

Figure 13. Comparison of the potentiostatic anodic polarization behavior for 316L stainless steel in 650 ppm Cl^- solution in deionized water with and without gamma irradiation. The polarization curves were scanned anodically starting from the corrosion potential in each case. Upon reaching the anodic limit, the scans were reversed to more negative potentials. In this figure, E_{corr} and E_p represent values of the corrosion potential and pitting potential, respectively, for the unirradiated case. The corresponding values for the irradiated experiment are indicated on the figure as $^*E_{corr}$ and $^*E_p$. Source: Glass et al. (1985).

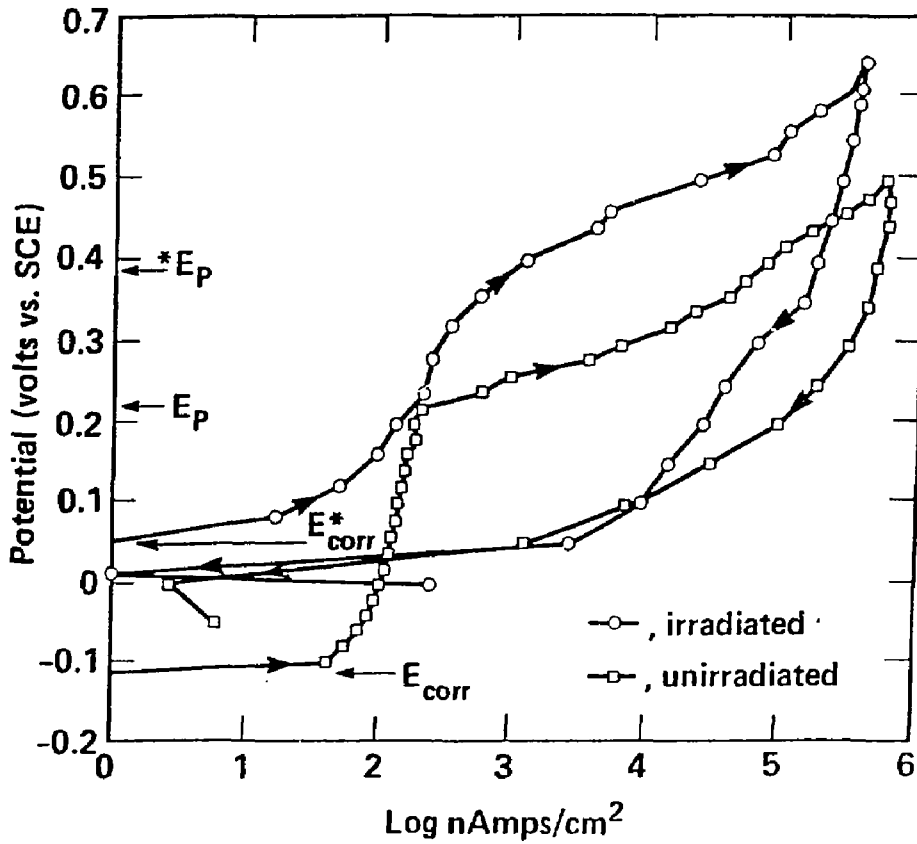

irradiation. The electrochemical polarization approach is useful to identify metal/environment combinations that might induce localized forms of corrosion, but confirmation tests such as these are needed. Further, the initiation phase can require long exposure times in rather benign environments (such as what Well J-13 water appears to be). An example of the type of testing used is found in Glass et al. (1985). They exposed (without any applied potential) 5 cm x 5 cm plates of stainless steel, bolted together with Teflon shims as spacers, for 54 days in noncirculating 35°C water with 10,000 ppm chloride. They found an average of 7.7 percent of the area of AISI 304L specimens was attacked, and 1.3 percent of the area of AISI 316L specimens was attacked. The penetration depth was irregularly distributed over the attacked area and was not measured.

Along with the general corrosion tests, discussed in Section 5, Teflon-metal crevices were created to observe whether preferential attack would occur there. These crevices were created with slotted washers that were used with the fastener assembly to support the coupons in the test environment. These tests have been described by McCright et al. (1983). After exposure to the test environment, the creviced area (approximately 1 cm^2 on each face of the coupon) was examined for preferential attack designated as crevice attack, while the bold area (the noncreviced remainder of the area -- approximately 12 cm^2 on each face) was examined for preferential attack, designated as pitting attack. The ASTM G 46 evaluation and examination procedure was followed and depths of any localized attack points were determined by a focusing microscope. The data obtained so far indicate that a tarnishing phenomenon is occasionally observed around the creviced area. After more than 10,000 hr, the deepest attack in a crevice on AISI 304L occurred in 90°C Well J-13 water and was estimated at 0.3 μm, and the deepest attack in a crevice on AISI 316L occurred in 70°C Well J-13 water and was estimated at 0.5 μm. The other stainless steels showed similar results. (As was the case for general corrosion, the differences between localized corrosion behaviors of the different grades of stainless steel would not be expected to be apparent in the benign environment of Well J-13 water and steam. In more concentrated electrolytic environments, however, the different grades would behave differently.) Pitting attack as measured on the bold surface area was even less extensive than the crevice tarnish attack. The aspect ratio (ratio of depth of attack to the width of attack) was less than 1. In true pitting of stainless steels, the aspect ratio is significantly greater than 1. Expressed on an annualized basis, these localized corrosion rates are of comparable magnitude to the general corrosion rate and are consistent with the conclusions drawn from the electrochemical polarization work. No enhancement of localized corrosion appears to occur in the unmodified Well J-13 water under the conditions so far tested.

In general, even in a corrosion situation where uniform corrosion mechanisms dominate, the attack pattern is rarely completely uniform. The localized contribution to the general attack is treated as a roughening effect to make an engineering estimate of the metal wastage. The general corrosion is multiplied by the roughening factor (typically a factor of 3 to 5 for calculating an effective corrosion allowance). Calculating the ratio of the localized corrosion rate to the general corrosion rate is one method for determining the roughening factor. In the case of austenitic stainless steels exposed to Well J-13 water, this roughening factor appears to be close to unity. Of course, localized corrosion initiation is expected to be slow under these environmental conditions; therefore, additional exposure time is necessary before definitive conclusions can be drawn.

Another approach to measuring the initiation condition for crevice corrosion in the laboratory is to expose the specimens in a tightly controlled crevice, to apply a constant potential on the specimen surface, and then to measure the current-time transient. At each increment of potential application (potentials are applied step-wise in the anodic or more oxidizing direction), the current is allowed to decay to steady state before the next potential is applied. When the applied potential is below the critical potential for crevice corrosion initiation, the current decays in a regular and rapid pattern to steady state. When the applied potential is at or exceeds the critical potential, the current transient rises sharply and decays much more slowly. From the pattern of current transients, the approximate value of the critical potential is established; the accuracy of the value will depend on the magnitude of the potential steps, and results are often reported as a range at which the current transients are observed to show the beginning of a rise and slow decay behavior. As an example of this approach, the critical potential values in Table 12 were obtained. In this study, the crevice corrosion behavior of standard grades of AISI 304L and AISI 316L were compared in an acid chloride solution; three different grades of 316LN (extra-low carbon, nitrogen-fortified) material from different manufacturers were also tested. The nitrogen levels ranged from 0.011 to 0.016 in the LN grades. These materials differed primarily in the amount of inclusions, and, as expected, the cleaner materials exhibited the highest critical potentials for initiation of crevice corrosion in the aggressive solution used for the test. The sulfur levels in the three 316LN materials were 140 ppm (316LNU), 60 ppm (316LN), and 30 ppm (316LNF). The highest critical potentials were obtained for the material with the lowest sulfur (and therefore the lowest inclusion) content. Similarly, the sulfur contents in the two 304L materials in Table 12 were 150 ppm (304L) and 70 ppm (304LN).

Table 12. Critical potentials for crevice corrosion in 0.1M HCl.

Alloy	E_{crit} (mV vs. SCE)
304L	-20 to 0
304LN	20 to 40
316L(NU)	50 to 80
316LN	125 to 150
316LN(F)	300 to 350

7.4 Activities to Determine Transgranular Stress Corrosion Cracking Susceptibility

In the discussion on intergranular stress corrosion cracking (Section 6), it was reported that some of the U-bend specimens exposed to irradiated Well J-13 water and water vapor showed transgranular cracking. Although this particular test had been designed primarily to show IGSCC susceptibility, broken specimens were examined to determine the crack propagation path. The following were the important test conditions: two vessels were exposed in a gamma radiation pit, one at 50°C and the other at 90°C. The radiation dose rates were 5×10^5 and 3×10^5 rads/hr, respectively. The specimens were arranged in three zones within each vessel. One third of the specimens were exposed to Well J-13 water with crushed tuff in the bottom of the vessel, another one-third were exposed to the wet vapor and crushed tuff in the middle of the vessel, and the top one-third were exposed to the vapor only. As pointed out previously in the discussion on intergranular cracking, these environmental conditions, particularly the combination of high gamma dose rate and aqueous chemical conditions, are aggressive. After 14 mo of exposure in the 90°C test, two specimens of AISI 304L that had been given a sensitizing heat treatment showed transgranular cracking. One of the cracked specimens was located in the vapor-only zone, and the other was located in the vapor-and-rock zone. Subsequent inspections (after 23 mo of exposure) revealed that other specimens of both sensitized AISI 304 and AISI 304L and annealed AISI 304 and AISI 304L cracked transgranularly in the 90°C test. No specimens cracked transgranularly in the 50°C test although intergranular cracking was noted for sensitized AISI 304 material in this test. These observations are discussed in greater detail by Westerman et al. (1987).

Three major points should be made before considering the results. First, when the research began, the tuff rock available was from the Topopah Spring surface outcropping. Rock-water interaction studies by Oversby and Knauss (1983) show that this rock contains soluble salts such as caliche or evaporite material as a result of its location on the surface. It was found that the tuff taken from the depth proposed for the repository did not contain such material (Oversby, 1985). Consequently, the electrolyte concentrations present in these tests (peak chloride concentration of 600 ppm) were considerably higher than would be expected in the proposed repository. This is particularly important in the case of chloride because of its role in stress corrosion cracking. Second, these tests were viewed as corrosion tests rather than chemical experiments, and emphasis was placed upon maintaining an open system, sparged daily with fresh air, to simulate repository conditions. Attempts were not made to keep track

of the total amount of water added or the final volumes of solution remaining. Third, the temperature control in the intended 90°C experiment was unsatisfactory for the first month, which led to repeated boil-off of the solution and plugging of the access line. The temperature and the time history of the physical state of the corrosion medium are therefore uncertain for this period.

In view of these factors, it appears that these tests were considerably more severe than the repository application would be. Nevertheless, they provide a bounding case for comparison.

The TGSCC suggests that chloride ion effects were a contributing factor. Analysis from water samples taken over the course of the test gave widely fluctuating values for the chloride ion (and other ionic species). A peak value of 600 ppm chloride was measured at the 7-mo exposure period. Other ionic species also showed very high values. As mentioned, in the early part of this test some operational difficulties were encountered in keeping the liquid level constant, and new Well J-13 water had to be added. Leaching from the rock might have been a source of ionic species. Corrosion products were analyzed from the specimens which showed TGSCC, but no particularly high content of chloride was measured on these surfaces.

It appears that the TGSCC resulted from the presence of a more concentrated electrolyte on the metal surface; however, the evidence is insufficient to fully support this explanation. A level of 600 ppm chloride exceeds the threshold concentration for initiating SCC (Fig. 6). In addition to purging the system of the radiolytically produced hydrogen and oxygen gas, the sparging (depending on how high a flow rate was used) could have blown the liquid up into the vapor space or produced aerosols of the dissolved solutes, which then could deposit on the metal sample surfaces located in the vapor phase. One of the difficulties in conducting experimental work in gamma radiation pits is the confined working space of the vessel and the difficulty in isolating experimental artifacts, especially during the relatively long time period (2 yr).

By whatever means the chloride concentrated (assuming that chloride ion is the species responsible for the cracking), the effect of chloride ion in initiating cracking is increased when the environment becomes more oxidizing. Gamma radiation makes the environment more oxidizing. It is well established that the threshold levels of chloride to initiate cracking in 18-8 types of austenitic stainless steels are lowered when the environment is made more oxidizing.

Williams (1957) showed that chloride levels as low as 2 ppm initiate TGSCC when the oxygen content is high (20 ppm) and that higher chloride concentrations are required to initiate cracking when the oxygen content is lower. However, this work was performed in a boiling environment of wet steam with intermittent wetting; therefore, it is likely that the real causative levels of chloride-induced cracking were higher.

The results of this test are consistent with the frequent observation that if environmental and metallurgical conditions are favorable for both morphologies of stress corrosion cracking, the intergranular crack propagation path is initiated before the transgranular propagation path.

In another experiment, a series of 40 U-bend specimens of AISI 304 and AISI 304L, both in the solution-annealed and sensitized condition, were exposed to non-irradiated Well J-13 water at 200°C in an autoclave (Westerman et al., 1987). The autoclave was cycled so that the specimens were exposed to the hot liquid water under pressure for a week; then the liquid was allowed to boil to dryness by reducing the pressure while maintaining the temperature. New water was then added and the system was returned to pressure and the cycle repeated. The intent of this experiment was to allow concentration of ionic species in Well J-13 water to accumulate on the metal specimen surfaces. After 50 cycles (1 yr) of alternate wetting and drying, only the sensitized AISI 304 specimens cracked, and these cracked intergranularly, even though the experiment was planned primarily as one for investigating and accelerating transgranular cracking. Water analyses showed that, after 1 yr, the chloride content had reached 90 ppm and the fluoride content had reached 19 ppm in the water. The expectation is that some of the AISI 304 and AISI 304L specimens will show TGSCC, particularly those in the annealed condition (which are not expected to fail intergranularly).

Although rather extreme (in contrast to the expected) environmental conditions are needed to reveal localized corrosion tendencies of the candidate materials, recent publications (Bandy and van Rooyen, 1985) indicate that nitrogen additions to stainless steel and nickel-base materials combat localized corrosion. These additions are also beneficial in increasing the resistance to sensitization, and they combat forms of corrosion associated with that phenomenon. Because a desirable feature of the waste package design is technical conservatism, the nitrogen-fortified stainless steels might have a number of attributes in their favor. Sulfur helps to provoke attack in stainless steels susceptible to localized corrosion; therefore, reduction of this residual element might provide even further assurance.

The above experiments were conducted in environmental conditions that are not anticipated in the Yucca Mountain repository. In particular, a concomitant high radiation field and aqueous environment are not expected. However, the susceptibility of the AISI 304L to cracking due to either an increase in the electrolyte content or an increase in the oxidizing potential of the environment does need to be determined. Thus, testing of AISI 316L and Alloy 825 to discern comparative susceptibility to TGSCC under similar accelerating conditions is planned. Future work will involve use of precracked specimens to eliminate the apparently long incubation time needed to initiate cracking in Well J-13 water or in the concentrated boiled-down modification of this water. Some of these precracked specimens will be maintained at constant applied potentials either to accelerate or to retard crack growth.

7.5 Environmental Considerations in Localized Corrosion Initiation

As discussed in Glassley (1986), the amount of water that could enter into the near-waste package environment is expected to be small because of the low precipitation in the Nevada desert and the small fraction of the precipitation that actually percolates to the depth where the repository would be located. The heat generated from the radioactively decaying waste would vaporize incoming water when the package environment is above 96°C. During this period, it is possible that repeated evaporative processes (i.e., a refluxing operation) could leave behind salt deposits inside the 96°C isotherm in the rock that would later be dissolved by water at a lower temperature as the isotherm moves toward the container. The result would be that water with higher concentrations of ionic species could contact the metal container. Another scenario for concentrating ionic species directly on a container would be repeated dripping on the hot container surface from a fracture located above the container so that a highly ionic residue is left on the container, to become wetted later. Although even more unlikely than the preceding scenarios, it is possible that flooding of a portion of the repository could occur by a series of events such as a fracture admitting a surge of water to enter the waste package environment combined with plugging of the fractures below the container (a bathtub effect), with consequent boiling away of the water and concentration of the ionic salts. Repeated occurrences of this event would be required to build up a significant concentration of the important species affecting metallic corrosion. Although the events that can produce concentrating effects are the subject of study in the repository environment task, performing corrosion tests in these concentrated environments is important in selecting container materials.

One analysis that has been conducted in this regard is that of Morales (1985). This analysis concluded that the dripping water on the hot metal surface scenario could not realistically occur in the repository because the thermal output from the container would evaporate any liquid water at a distance well away from the container. With regard to the scenario of repeated evaporation of downward infiltrating water and eventual resaturation of this water when the boiling point isotherm has moved to the container surface, this analysis concluded that a conservative maximum of 20x the ionic salt content in the Well J-13 water could occur during the dry-out period. The subsequent scenario would be that resaturation of the dry-out zone could result in an effective 20x salt content of Well J-13 water reaching the containers as a burst, or the more gradual redissolution of the accumulated salt in the rock over a longer period of time, resulting in a slightly more concentrated salt solution than Well J-13 water reaching the containers.

To project the numbers of containers that could eventually perforate by localized corrosion attack or transgranular stress corrosion cracking, models will be built around the rates of attack for different concentrations of salt in groundwater of the Well J-13 type. It is recognized that eventual cooling of the repository will allow for hydration of the environment with potential for access of the aqueous solution to the container surface. However, this does not appear to be possible until late in the containment period, several hundred years after the repository closure. A more precise statement of the time is dependent on many features of the waste package and repository design and the thermal projections based on these designs. These are described more fully in O'Neal et al. (1984).

An additional factor affecting the accessibility of water to the container material is the possible intervention of the borehole liner and/or radiation shield plug. As discussed in Section 11, if carbon steel is used as the liner material, it will likely be sacrificial to the container material, and in any event will probably contact the water first. If the liner were breached and all other considerations were assumed to be the same for the two emplacement plans, horizontal emplacement of the container would create a more vulnerable condition for the propagation of localized corrosion than would vertical emplacement, because more surface area would be exposed to incoming water from above, and it is known that initiated pits will grow more favorably in the direction of gravity. Furthermore, the bottom side of the horizontally emplaced container will have a comparatively larger contact area with the platform or other under-structure (to emplace, support, and retrieve the waste package). This contact area can act as a "crevice" site for initiating localized attack.

7.6 Summary of Testing for Pitting, Crevice, and Transgranular Stress Corrosion Cracking

In summary, the candidate stainless steels appear to be sufficiently resistant to pitting, crevice attack, and transgranular stress corrosion cracking in the unmodified Well J-13 water and in steam generated from the water. Even if the highest measured localized corrosion rate is added to the general corrosion rate, container service life far exceeds the maximum containment requirement. However, if concentration of the ionic species in the water were to occur, these might result in much more aggressive environmental conditions in which the candidate stainless steels would show quite different behavior. It appears that the combination of concentrated electrolyte and irradiation is the most severe environment so far tested, and even AISI 316L might pit and crevice corrode under these conditions. Scenarios that could result in such environmental conditions are unlikely; however, assessing container behavior under unanticipated processes and events is necessary in order to develop radionuclide source term estimates for low probability scenarios.

8. PHASE STABILITY AND EMBRITTLEMENT OF AUSTENITIC MATERIALS

In this section, the stability of the austenitic structure over long periods of time is discussed. Possible phase transformations of concern include the formation of ferrite, martensite, and sigma phase in some of the candidate stainless steels. A concern is whether these phases could adversely affect the long-term fracture toughness and result in a more brittle (and in some cases less corrosion resistant) structure than the parent structure. Some transformation products, such as martensite, are more susceptible to hydrogen embrittlement when exposed to environmental situations where atomic hydrogen is produced. Many of these phase instability concerns are closely related to microstructural features of the weld and heat-affected zones and thus to the processes used for fabricating and welding the container material structure.

8.1 Phase Stability

Many austenitic stainless steels possess a tendency for transformation of some austenite to ferrite. The austenite-stabilizing alloying elements are balanced against the ferrite-

stabilizing elements in alloy development. In welding processes using filler materials, a certain amount of delta-ferrite (typically 3-5 wt.%) is sought in the fusion zone to mitigate against hot cracking. For this reason, the higher chromium content AISI 308 material is specified for the filler material in welding AISI 304L, the extra chromium content (approximately 2 wt.%) favoring ferrite retention. According to some researchers, carbides that might have grown due to low temperature sensitization will most likely reside at austenite-ferrite boundaries (DaCasa et al., 1969; and Duhaj et al., 1968). Duplex stainless steels (dual phase) appear to be more resistant to high temperature sensitization and perform quite well under conditions where completely austenitic stainless steels crack intergranularly and by stress corrosion (Hochman et al., 1977), probably due to the high Cr content in the ferrite phase. Whether retained delta-ferrite or subsequent transformation of austenite to alpha-ferrite would be harmful to the corrosion performance of a stainless steel nuclear waste container has not yet been demonstrated.

Another concern with retained ferrite is its possible transformation to hard, brittle, sigma phase when held at moderately elevated temperatures. Although most studies show the nucleation time of sigma phase from delta-ferrite to be quite long, some sigma-phase nuclei have been observed after exposure at 750°C for only approximately 5 min (Wegrzyn and Klimpel, 1981). As with the study of low temperature sensitization, the expected prolonged exposure of the container to temperatures in the 100-280°C range in the repository raises the question of whether a small amount of sigma phase would form at these relatively elevated temperatures for very long times (hundreds of years). A content of just 2 wt.% sigma phase reduces the fracture toughness (impact strength) of stainless steel by one-half. Fracture toughness is most important as a material property for the first 50 yr when retrievability of the waste package is a requirement; impact loads on the container during retrieval could conceivably rupture an embrittled material. Molybdenum additions (ferrite stabilizer) as in AISI 316L slightly increase the tendency toward sigma-phase formation (and also enhance formation of brittle chi and Laves phases). Thus, the beneficial qualities offered by the AISI 316 series in improving resistance to localized corrosion and resistance to sensitization effects might be offset by a greater tendency to form brittle phases over long periods of time. These factors need to be addressed in future work. Also, cold deformation appears to speed up the kinetics of sigma-phase transformation. Although most of the container surface could be stress relieved, the area around the final closure weld would appear to be subject to retention of residual stress.

Residual cold work in the container could also favor transformation of the austenite to martensite with attendant loss in fracture toughness. As in sigma-phase formation, this transformation would be expected to occur at a local level. Further, a martensite transformation would allow more carbon to become available for chromium carbide formation, and subsequent sensitization would be more likely to occur. Generally, the molybdenum-bearing stainless steels are more resistant to martensite transformations; therefore, in this situation, the AISI 316 series would be more resistant than the AISI 304 series. This transformation could be avoided if the container were annealed.

8.2 Hydrogen Embrittlement

Although the face-centered cubic austenitic structures are ordinarily regarded as highly resistant to hydrogen-embrittling effects, the long-term interaction with a hydrogen-producing environment must be considered a possible degradation mode. Martensite transformation from the austenite results in a phase that is much more susceptible to hydrogen embrittlement, and strain-induced martensite could form in a heavily cold-worked AISI 304L material. As discussed earlier, a source of hydrogen is the radiolytic decomposition of water vapor (during the containment period, when the radiation field is high) or the electrochemical decomposition of water resulting from corrosion reactions on a container surface. The former source would only be significant if the environment becomes saturated while the radiation field is high.

Of the candidate materials, AISI 304L is the most susceptible to martensite formation if the material is very highly strained. A rough calculation of the M_d (deformation of martensite transformation) temperature at 30% strain for a typical AISI 304L composition indicates that significant martensite forms when the temperature drops to approximately 85°C. This calculation was based on the expression given in the review article by Novak (1977). Higher strains will elevate the temperature, and alloying additions will lower the temperature. This result suggests that hydrogen embrittlement of a martensitic structure would be of concern at a late period in locally highly strained areas when the container surface cools below this critical temperature and when an aqueous environment could access the container surface. It therefore is of no concern with respect to retrieval.

One potential problem area that has not yet been explored is hydrogen embrittlement in the duplex structure of weld metal for austenitic stainless steels. The ferrite phase has the

potential for trapping hydrogen. In this case, no martensite transformation is required as a prerequisite condition. Although hydrogen could enter the stainless steel from radiolytic decomposition of the water vapor, the relatively high temperatures would tend to mitigate against trapping effects (the hydrogen could diffuse out as readily as it diffuses in). Also, the oxidizing nature of the environment will tend to combine oxidizing radicals with atomic hydrogen as it is produced. One possible source of hydrogen produced by radiolytic decomposition of water vapor could develop inside the waste package container from water-logged spent fuel rods. Because the spent fuel waste packages will likely be filled with an inert gas (e.g., argon), atomic hydrogen might have a longer residence time in this kind of environment. Thus, there exists the possibility that this hydrogen could enter and permeate into the metal container. However, these effects will need to be investigated to determine whether hydrogen is produced and whether it can permeate into the metallic structure.

3.3 Welding Considerations

The integrity of the weld region of the container and the propensity of weld-processing variables for producing microfissures in the weld require evaluation of the state-of-the-art techniques for nondestructive post-weld inspection of the container.

In welding processes using filler materials, a certain amount of delta ferrite (e.g., 3-5 wt.%) is generally sought in the fusion zone to mitigate against hot cracking. For this reason, the higher chromium content AISI 308 is often specified for the filler material in welding AISI 304L. However, the intentional presence of delta ferrite in the weld microstructure and its effect (beneficial or detrimental) on long-term corrosion resistance need to be considered in the full characterization of the container material.

Molybdenum additions (such as those made to AISI 316L) slightly increase the tendency to form brittle phases such as sigma. Thus, the beneficial qualities of AISI 316L (including improved resistance to localized corrosion and sensitization) might be somewhat offset by the greater tendency to form brittle phases over long periods of time. These factors need to be addressed in future work. Also, cold work appears to increase the kinetics of sigma formation. Although most of the container could be stress relieved, the area around the final closure weld would appear to be subject to retention of residual stress.

Care must be taken in welding Alloy 825. This alloy is purely austenitic and lacks the formation of delta-ferrite in the weld zone; the advantage of delta ferrite is to soak up harmful impurities (such as sulfur) that cause hot cracking. This means that more careful control of the alloy chemistry (and filler material if a weld process using filler material is eventually selected) is required. The higher nickel materials are sufficiently unlike the austenitic stainless steels that different welding parameters should be used to ensure sound welds.

8.4 Summary of Work on Phase Instability and Embrittlement

Relatively little work has addressed issues of phase instability for some of the candidate materials and problems of embrittlement that might be associated with the phase instability. The embrittlement might be purely mechanical due to the loss of fracture toughness by formation of sigma phase or other brittle intermediate phases, or the embrittlement might be due to hydrogen produced by the environment, the hydrogen favoring martensite and possibly ferrite formation. Further study of the long-term physical metallurgical stability of the different grades of austenitic stainless steels in repository-relevant thermal and chemical environments is needed. The high nickel Alloy 825 is apparently immune to transformation of austenite, but the possibility (apparently remote) of detrimental hydrogen embrittlement would need to be addressed. Reduction of sulfur (and probably phosphorus) to as low a level as practicable appears to be a universal benefit in all of the candidate materials (reduce hot cracking of welds, reduce inclusion content for nucleation of pits and stress corrosion cracks, and eliminate a possible site for chromium carbide nucleation). So-called premium grades with careful control of interstitial elements in the melting process might be justified to increase the certainty of avoiding undesirable degradation modes.

9. PROJECTIONS OF CONTAINMENT LIFETIMES USING AUSTENITIC MATERIALS

The purpose of this section is to project a lifetime for the container based on corrosion data obtained to date. The performance assessment of the container is a composite of the different assessments of each potential mode of degradation. These individual assessments are generally not additive; environmental or metallurgical conditions will determine which mode is operative (and exclusive to the others), and, as these conditions change, different degradation modes might become operative.

9.1 Time Periods and Relevance of Degradation Modes

As discussed in Section 3, the function of the metal container depends on the time period when the repository is in operation and the various time periods following permanent closure of the repository. The first 300- to 1000-yr post-closure period is the period of containment by the metal barrier. The metal barrier is relied upon to demonstrate substantially complete containment for that period of time. The subsequent 1000- to 10,000-yr period is one of controlled release by the waste form. Because a large quantity of the metal barrier is expected to be present at that time, the metal barrier will influence the controlled release rate; therefore, characterization of the corrosion modes through this period is necessary. Because a dry environment is likely for the first 300 yr (and likely beyond that period), low temperature oxidation appears to be the only operational degradation mode during the minimum containment period. As the environment resaturates when the container temperature cools, various kinds of aqueous corrosion can begin to operate during the later part of the containment period and into the controlled release period.

Thus far, oxidation is the only experimentally measurable degradation mode for the candidate stainless steels under anticipated environmental conditions that are expected to be significant during the minimum containment period. Significant here means that the environmental conditions will endure for long periods of time (tens to hundreds of years) and that the majority of the 25,000 to 50,000 waste package containers will experience these conditions. General aqueous corrosion will occur when the container surfaces become wet; as discussed in O'Neal et al. (1984) and in Glassley (1986), this condition is not expected during the minimum containment period, but it might develop around some of the containers during the succeeding 300- to 1000-yr post-closure period. The time for hydration of the rock to occur will depend strongly on the configuration of containers in the repository and on the average thermal loading per container and the aereal power density maintained for the configuration. A typical corrosion rate in unsaturated steam is 0.07 μm/yr, and this increases to 0.10 μm/yr in saturated steam and to 0.2 μm/yr in water immersion. Even with full water immersion during the entire maximum containment millenium, the projected amount of metal wastage would predict complete containment for container lifetimes (assuming 10,000 μm thickness) in excess of 10,000 yr. If the high value of 0.51 μm/yr (measured on AISI 304L in irradiated Well J-13 water at 150°C -- a physically impossible condition here but an example for mechanistic arguments) were used, a high crevice corrosion rate of 0.5 μm/yr (based on actual measured localized corrosion rates of immersed AISI 316L) were coupled to this, and the results projected, the

wastage would be only one-tenth of the container thickness. Sustained localized corrosion rates of several micrometers per year would be needed before this form of corrosion would seriously limit the containment objectives. Rates of this magnitude would not be expected to occur in unsaturated steam. Because sustained immersion of substantial areas of the containers appears to be highly improbable, higher corrosion rates are not expected.

One nonuniform mode of corrosion that does appear to offer some limitations on containment life is development of a sensitized microstructure during the containment period and subsequent wetting of the affected area to produce intergranular stress corrosion cracking. The time-to-sensitization decreases substantially with an increase in the peak temperature of the container. For example, a very heavily cold-worked AISI 304L (with 0.028 wt.% C) is predicted to sensitize in as little as 120 yr at isothermal conditions of 250°C but as long as 4000 yr at 200°C. AISI 304 did exhibit cracking in irradiated Well J-13 water and saturated vapor; the question remains whether the lower carbon content in the L grades can confer immunity or at least a high resistance to the phenonmenon. Proper selection of the thermomechanical processing of the container can confine this phenomenon to the area around the final closure weld; proper selection of the alloy, its physical microstructure, and control of microconstituents can further reduce the susceptibility to achieve a situation that is compatible with substantially complete containment with a high level of assurance. The more highly alloyed materials and those stabilized with carbide-forming elements offer improvement in this regard, because of either the kinetic hindrances on chromium diffusion to form chromium carbide or prior formation of another carbide.

The metastability of austenite in the 300-series candidate austenitic materials might be a second issue of concern during the containment period, since sigma (or another brittle) phase might form from either the austenite or from retained delta ferrite in the duplex weld material. A further embrittlement problem during the containment period might be hydrogen embrittlement at the austenite/ferrite interface or in the ferrite phase if sufficient hydrogen forms from radiolysis of the environment and permeates the metallic structure during this time period.

Other degradation modes to consider as limiting containment would be transgranular stress corrosion cracking, pitting, and crevice corrosion. These modes would only occur if some unusual event happened during the minimum containment period when the container is above the boiling point of the vadose water. Their occurrence becomes considerably more probable

when aqueous conditions occur by eventual water infiltration to the cooling container surface in the later periods. These modes would be promoted by lengthy immersion time (to build up and sequester electrolyte concentration in the local geometry) or influx of a more concentrated electrolyte than the reference Well J-13 water environment, neither of which are expected conditions for a Yucca Mountain repository. Oxidizing species in the water, including those produced by whatever gamma flux exists at that time, are expected to axacerbate effects of chloride and other ionic species. Again, metallurgical remedies (use of more premium grades of the common AISI 304 or AISI 316 types of stainless steel) can alleviate the problem. In the extreme case where a salt solution is postulated to intrude, at least at a very local level, the highly alloyed (and consequently more expensive) Alloy 825 might be the best recourse.

Alloy 825 is considered to be the most resistant of the candidate materials to virtually every form of corrosion that might occur in a geological repository in tuff. The alloy is low in carbon, and titanium stabilized to render it highly resistant to sensitization. The austenitic structure is stable at all temperatures. The alloy is quite resistant but not immune to chloride-induced pitting, crevice attack, and transgranular stress corrosion cracking [localized attack does occur in very aggressive solutions that are low in pH, very high in chloride, and strongly oxidizing (such as 10 percent $FeCl_3$ solutions)]. Although the metallurgical stability and the chemical stability in the Yucca Mountain environment all appear to be quite favorable to Alloy 825 as a container material, some developmental work will be needed to assure its good weldability, should this material be selected for the advanced designs. Metallurgical studies to confirm phase stability in the welded condition as well as resistance to localized corrosion are being planned.

9.2 Long-Term Performance Projections and Selection of Container Materials for Advanced Designs

Corrosion testing including program planning and execution, has been on-going for four years (as of June 1987). A principle of corrosion engineering is that a corrosion test can never be run for too long a time; Fontana and Greene (1978) ascribe a rule of thumb that the minimum time to complete a corrosion test (in hours) is 2000/expected corrosion rate in mils/year, which means that corrosion test times of more than 30,000 hr (more than 3 yr) are needed. This time period attempts to eliminate surface effects and artifacts that can dominate the corrosion behavior in the early periods (these effects are more important when the corrosion rates are very small).

In addition, experience has shown that parametric studies involving the key species in the medium (in this case, J-13 water chloride, nitrate, oxygen etc. content) can provide valuable information useful in projecting results from relatively short-term tests out to very long times. We plan to conduct these tests in the future.

Understanding the governing mechanisms for the different corrosion processes is the basis for long-range predictions of performance. To this end, estimates of the changes in the corrosion potential for the different candidate stainless steels are modeled on changes in environmental conditions. Initiation of mechanisms for localized and stress-assisted forms of corrosion is based on the corrosion potential exceeding a characteristic critical potential (for each form of corrosion) that corresponds to the threshold causative environmental conditions for that particular corrosion mode. When this critical potential is at or below the corrosion potential, then the particular form of localized or stress corrosion is operative. If the critical potential lies above the corrosion potential, then general corrosion is the operating mode. The performance assessment model of the waste package is composed of individual performance assessment models for the different waste package components. The overall corrosion model for the waste package container is based on which particular corrosion model (general, pitting, crevice, stress, etc.) operates for a given set of environmental conditions. During the entire 10,000-yr period of concern for characterization of the corrosion performance of container materials, different individual corrosion models can operate according to the particular environmental conditions, and the overall corrosion model will account for the situations where individual models are operative. Performance predictions ultimately involve a mapping activity between the phenomenology observed during the testing activities and an understanding of the mechanisms that govern the phenomenology.

The research and development effort on metal barriers is driven by the need to select a container material that will provide substantially complete containment for the requisite time period. Thus, a large effort is placed on assessing the chemical stability of the different candidate metals in the projected thermal and geochemical environment of the repository, and failure of these candidate materials is assumed to occur by corrosion. A good deal of effort will be placed on the particular corrosion effects in and around the welds, and some of the special limitations imposed by making the final closure weld by remote processes will need to be addressed.

Regardless of the material chosen for container fabrication, the integrity of the welds is a critical issue. Weld integrity is a function of what process is used, how these processes are carried out, and what inspection techniques are used to detect flaws. From the point of view of container material selection, good weldability is sought. The practical definition of weldability is that it is a measure of the degree to which the metal is amenable to joining by a variety of techniques, with a high degree of latitude (forgiveness) in the amount of control required to obtain a fully sound weld. This quality will play an important role in determining which metal will be selected for the advanced design, but much of the weld process specification for the chosen metal will be left to a future date for decision.

9.3 Experience with AISI 304L in the Climax Test

Although the discussion in Section 9.2 centered on some of the deficiencies of the reference material (AISI 304L), experience with AISI 304L as the container material for the Climax Spent Fuel Test in granite illustrates some qualities for long-term geological disposal of nuclear waste. This experience is described by Weiss et al. (1985). One of the canisters in the Climax test was unintentionally exposed to groundwater when a leak developed in the carbon steel liner. The particular canister held spent fuel (some of the canisters in the Climax test contained only heaters to simulate the thermal output of the spent fuel); therefore, the ensuing environment contained a combination of potentially adverse conditions. One was intrusion by groundwater with an ionic content that included 30-160 ppm chloride ion concentration, a concentration substantially higher than that expected for the groundwater associated with the Yucca Mountain repository in tuff. Two other adverse conditions were the presence of a radiation field around the canister and the presence of assembly welds on surfaces exposed to the water. Portions of the canister are believed to have been exposed to the water for approximately 8 mo; the canisters were located in the Climax mine for 3 yr. Selected areas of the exposed canister were sectioned and examined microscopically, particularly for evidence of localized corrosion. No discernible corrosion was noted on any of the canister surfaces including the areas around the weld. Interestingly, some of the welds did not show full penetration. Although conditions obviously differ between Climax and Yucca Mountain, the excellent performance of AISI 304L in the Climax spent fuel test speaks well for its prospects in the tuff repository. If significant corrosion had been observed, there would have been cause for serious concern; it is reassuring that none was found.

10. COPPER-BASE MATERIALS

The work on the three copper-base candidate materials is less extensive than that on the austenitic materials, having started at a later time. We have published two reports on a feasibility assessment on the use of copper-base waste package container materials, covering work performed in FY 1985 (McCright, 1985) and FY 1986 (Acton and McCright , 1986). Although only limited testing was possible during this short time frame, a considerable amount of information was obtained, and the copper-base materials were assessed to be feasible as a container material, based on what was learned during the two-year period. Some questions remained about the effects of gamma radiation on the corrosion behavior, and longer-term tests were judged to be needed to conclusively determine the feasibility.

Other concerns regarding copper-base alloys include potential dealloying effects over very long times as well as the significance of a ductility minimum at 250°C for pure copper. These questions will be the subject of studies we are currently planning.

10.1 Literature Review

One of the first steps in assessing the feasibility of copper-based materials for waste packages was to review available information in the literature that appeared to be relevant. A report was published (Myers, 1986) that summarized what was found about the oxidation and corrosion behavior of the three candidate materials (CDA 102, CDA 613, and CDA 715) in air, steam, and a variety of aqueous solutions at temperatures between ambient and 300°C. Some information was also found about copper corrosion in irradiated moist air. The chief results from the literature review were as follows.

Oxidation studies of copper and the candidate alloys in air and dry steam environments indicate that the amount of metal lost is small even for many years of exposure to these environments in the 100-300°C range, regardless of the kinetic law followed by the oxide growth. No evidence was noted in the literature review of a spalling or exfoliation phenomenon occurring in this temperature range. The oxidation rate of alloys containing aluminum is very much less than the rate for pure copper. This was a major reason for including aluminum bronze as a candidate material in the testing program.

The preponderance of data found in the literature survey indicated that steam is relatively noncorrosive to copper [rates less than 0.1 mil/yr (2.5 μm/yr)], but that the presence of noncondensible gases such as O_2 and CO_2 increases the corrosion rate in condensing steam. Corrosion rates of approximately 10 mils/yr (250 μm/yr) occur when the ratio of CO_2 to O_2 in the condensate is high and the pH of the solution becomes acidic (ASM, 1961). These atmospheric gases will be present in the repository environment; the distribution of these gases in the condensate could significantly differ from their distribution in the atmosphere, depending on the temperature and the presence or absence of pH-buffering species in the liquid phase.

The general corrosion rates for copper and its alloys in natural and industrial waters depend on the temperature, dissolved gas content, pH, and ionic species present in the water. By extension of the available data, one would conclude that water of a composition similar to that of Well J-13 water should not be particularly corrosive to copper. At temperatures approaching the boiling point, the water is likely to be less corrosive than it is at lower temperatures because of the lower solubility of oxygen at the higher temperatures.

Sparse information exists on the radiation effects on corrosion and oxidation in these environments. It is known that irradiation of moist air at room temperature produces nitric acid and ozone. Copper has been found to be coated with basic cupric nitrate (Gerhardite) when subjected to irradiated moist air. In irradiated liquid water, the main stable species are H_2 and H_2O_2. Furthermore, copper is known to be a strong catalyst for the decomposition of H_2O_2. Irradiation of a two-phase air-water system results in the fixation of nitrogen from the air into the water as nitric and nitrous acids, which are corrosive to copper. In addition, under low-oxygen conditions, ammonium ions can be formed, which would also be detrimental to copper. Ammonia significantly increases the general corrosion rate of copper and causes transgranular stress corrosion cracking of copper and many of its alloys. [For copper-aluminum alloys, general corrosion rates of 50 mils/yr (approximately 1 mm/yr) are reported in moist ammoniacal environments, and stress corrosion time to failures are reported to be on the order of days (Thompson and Tracy, 1944).]

One reference cited in the literature review indicated transgranular stress corrosion cracking of copper in concentrated (1 M), aerated, sodium nitrite solutions (Benjamin et al., 1983). The relevance of this work is that Well J-13 water contains nitrate ions in concentrations less than 15 ppm. Thermal decomposition of some of the nitrate and the presence of the metal

will likely favor some nitrite ion formation in the water (also less than 15 ppm). Nitrite would also be formed as a radiolysis product. The conditions of temperature, aeration, and concentration in which the materials underwent SCC suggest that cracking will not occur when the nitrite concentration is less than 0.001 M (70 ppm) in the anticipated repository temperature range. The uncertainty of this threshold and its extrapolation to long times is not established. These researchers did not investigate SCC in copper-base alloys.

Some aluminum bronzes are reported (Klement et al., 1959) to be susceptible to intergranular stress corrosion cracking in saturated steam environments in the temperature range relevant to the repository. These investigators also report that the addition of tin (0.2 to 0.3 percent) to the aluminum bronze prevents SCC susceptibility. This observation resulted in the development of the CDA 613 material. On the other hand, CDA 613 is susceptible to transgranular stress corrosion cracking in ammonia vapor.

Well J-13 water does not contain significant concentrations of species that are known to favor pitting attack on copper-base materials (e.g., ferric ion, manganese ion). The relatively high ratio of bicarbonate to sulfate is expected to mitigate against localized attack. Sulfide ion is another potentially harmful species in inducing localized attack on copper and copper-base alloys, but the expected oxidizing conditions in the repository should preclude formation of this species. Development of selective leaching attack does not appear to be a likely degradation mode in waters similar to Well J-13 water.

One investigation cited in the literature review found susceptibility of laboratory binary (not commercial) copper-nickel alloys to intergranular corrosion and intergranular stress corrosion cracking in 300 and 350°C water and steam in autoclave tests (Sato and Nagata, 1974). A similar kind of cracking has not been observed in commercial copper-nickels, such as CDA 715. The 0.5 percent iron addition in commercial material, which is beneficial in reducing susceptibility to other forms of corrosion, might be responsible for the difference in behavior between laboratory and commercial materials.

In view of the results of this literature search and the limited time available for the feasibility study, we decided to focus our efforts on key areas that were specific to our application and for which little data were available:

1. Calculation of the expected external gamma dose rates for various container wall thicknesses.

2. Thermodynamic analysis of the copper-air-water system that contains species produced by irradiation.

3. Electrochemical measurements of the behavior of copper-base materials under non-irradiated and irradiated conditions.

4. Corrosion and oxidation tests of copper-base materials in Well J-13 water, air with saturated steam, and air with unsaturated steam, all under gamma irradiation.

5. Corrosion interaction tests between copper and Zircaloy in Well J-13 water under irradiation.

In the future we will expand these studies to include dealloying and ductility as well as an evaluation of parametric variation in key species such as chloride and nitrate in the J-13 water.

10.2 Gamma Dose Rate Calculations

Under cooperation with Rockwell Hanford Operations, preliminary calculations of gamma dose rates outside the waste package during the containment period were made for two waste forms: consolidated spent fuel rods and West Valley reprocessed waste (Reed and Underberg, 1986). The calculations were done using the QAD shielding code of Science Applications, Inc.

Calculations were performed for consolidated PWR spent fuel with 33,000 MWd/MTU at 10, 30, 100, and 300 yr after removal of the fuel from the reactor. One calculation was done using spent fuel with 60,000 MWd/MTU burnup for comparison. The container was modeled at 100 percent copper for several thicknesses.

Figure 14 shows dose rate as a function of (1) distance from the container and (2) wall thickness of the container. The error in the dose rates calculated might be as high as 50 to 100 percent. This is a function of detector location, material composition, and time, but is primarily due to the use of a single build-up factor for all the materials present in the system studied. Other possible contributions to the error in the calculations are the assumed homogeneity of the gamma source and the mesh size used in the calculations.

Figure 14. Calculated initial irradiation dose rate as a function of distance from container and thickness of the container (10-yr-old spent fuel at 33,000 MWd/MT burnup) (Reed and Underberg, 1986).

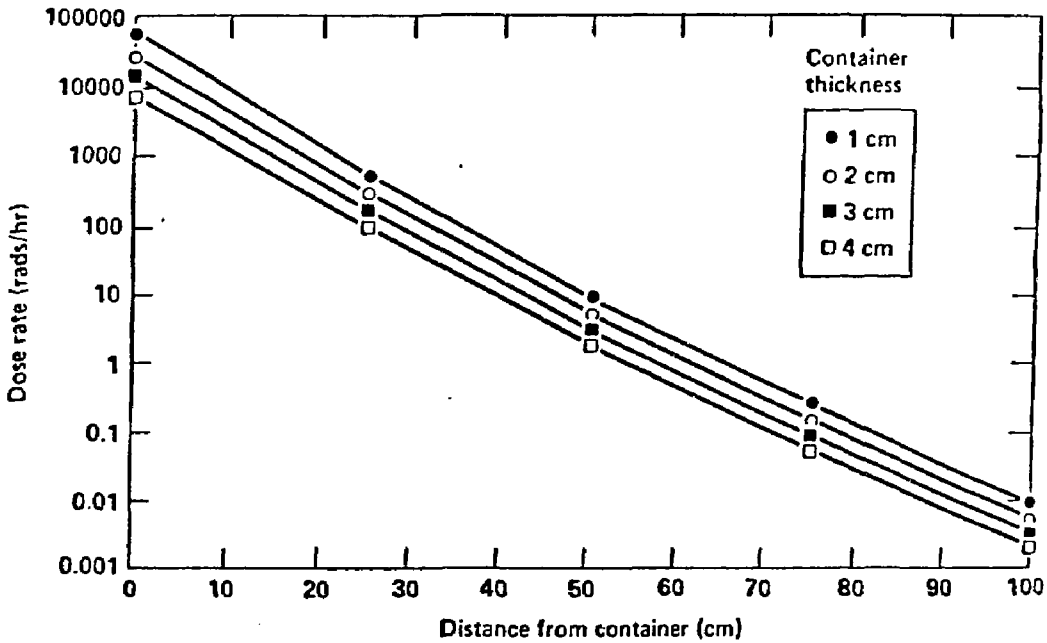

The dose rates used in accelerated corrosion screening tests and scoping studies were much higher than the estimated actual irradiation dose rates calculated here; for example, 3.3 x 10^6 rads/hr in the case of tests by Glass et al. (1986) and 1 x 10^5 rads/hr in the case of Yunker (1986). This confirms that the experimental conditions used in the screening tests are conservative in relation to the radiation conditions anticipated in the repository.

10.3 Thermodynamic Analysis

Under subcontract with the Copper Development Association, Inc., studies were conducted by Verink (McCright, 1985) in an effort to make preliminary predictions as to stable species that might be formed on copper exposed to irradiated Well J-13 water at temperatures up to 95°C in the presence of Yucca Mountain tuff rock. Pourbaix diagrams were calculated to estimate the thermodynamic equilibrium relationships for copper in non-irradiated and in irradiated Well J-13 water. The influence of varying the irradiated water composition and the influence of the additional presence of NO_3^- in concentrations up to 0.1 M were examined, based on calculations indicating that such a concentration might be reached if Well J-13 water exposed to sufficient atmospheric air were irradiated with a total dose of 10^{10} rads. The studies based on room temperature data indicated that no change in the features of the Cu-H_2O Pourbaix diagram should be expected at room temperature even with large increases in concentrations of the chemical species present in oxygen-saturated, irradiated (3.3 x 10^6 rads/hr) Well J-13 water. If estimates of NO_3^- concentration of 0.1M in irradiated Well J-13 water are accurate, questions surface regarding the passive behavior of copper. The thermodynamic study assumed formation of $Cu(NO_3)_2 \cdot Cu(OH)_2$ as a stable species. The domain of stability was found to be significant at room temperature. The protectiveness of this species was not examined in this preliminary work.

It should also be noted that $Cu(OH)_3NO_3$ scales (identified by x-ray diffraction) have been observed on copper surfaces in vapor spaces above Well J-13 water and crushed tuff (Smith, 1987).

10.4 Electrochemical Measurements

Akkaya and Verink (1986) experimentally investigated the three candidate materials in terms of their electrochemical corrosion behavior in non-irradiated 0.1 N $NaNO_3$ solutions at 95°C. Anodic polarization experiments were conducted to determine the passive current

densities, pitting potentials, etc., together with cyclic current reversal voltammetry (CCRV) tests to evaluate the stability and protectiveness of the passive oxides formed. X-ray diffraction and Auger electron spectroscopy were used for identification of the corrosion products as well as scanning electron microscopy for the surface morphology studies.

Even though all three materials appeared at first to be susceptible to pitting to a certain extent in 0.1 N $NaNO_3$ at 95°C at high (oxidizing) potentials near the breakdown potential, stable and protective passive films formed on the surface of the alloys, which provided resistance to both general and localized (pitting) corrosion. Near the breakdown potential, oxidation of the environment and breakdown of protective films contributed to an extremely aggressive condition on the polarized metal surface. It is significant to note that CDA 102 showed better resistance to both general and localized (pitting) corrosion than did CDA 613 and CDA 715, and these results on uniformity of attack are consistent with those obtained under gamma-irradiated conditions, as discussed in the Section 10.5.

Electrochemical measurements under irradiated conditions have been performed at LLNL by Glass et al. (1985). For this work, an electrochemical cell was constructed for use in a ^{60}Co irradiation facility, Fig. 15. The upper portion contains a reference electrode (SCE) placed in a reservoir containing saturated KCl. The upper and lower chambers are connected by a Luggin probe, also filled with saturated KCl. The lower portion, the cell itself, contains the Luggin probe, the working electrode, a coiled platinum counter electrode, and a port for deaeration. The reference electrode is therefore isolated from the gamma sources, which consist of ^{60}Co pencils arranged in a cylindrical pattern around the cell. At the center of the cylinder the dose rate was 3.3 Mrads/hr (±20 percent). All experiments were performed at 30°C (±5°C). The 3.3 Mrads/hr field strength is approximately 70 times stronger than that calculated for the container surface 10 yr after discharge from the reactor. When the temperature drops below the boiling point in the repository, the field at the container surface will be more than 4 orders of magnitude lower than that used in these experiments.

Figure 16(a) shows the corrosion potential vs. time behavior of CDA 102 in Well J-13 water when subjected to gamma radiation. Upon initiation of irradiation, the corrosion potential instantly jumps in the anodic direction by approximately 100 mV, then rapidly decays to more negative values. If allowed to decay to steady state, the shape suggests that it would probably reach nearly the same level as that prior to irradiation (Glass et al., 1986).

Figure 15. Schematic of the electrochemical cell (Glass et al., 1985).

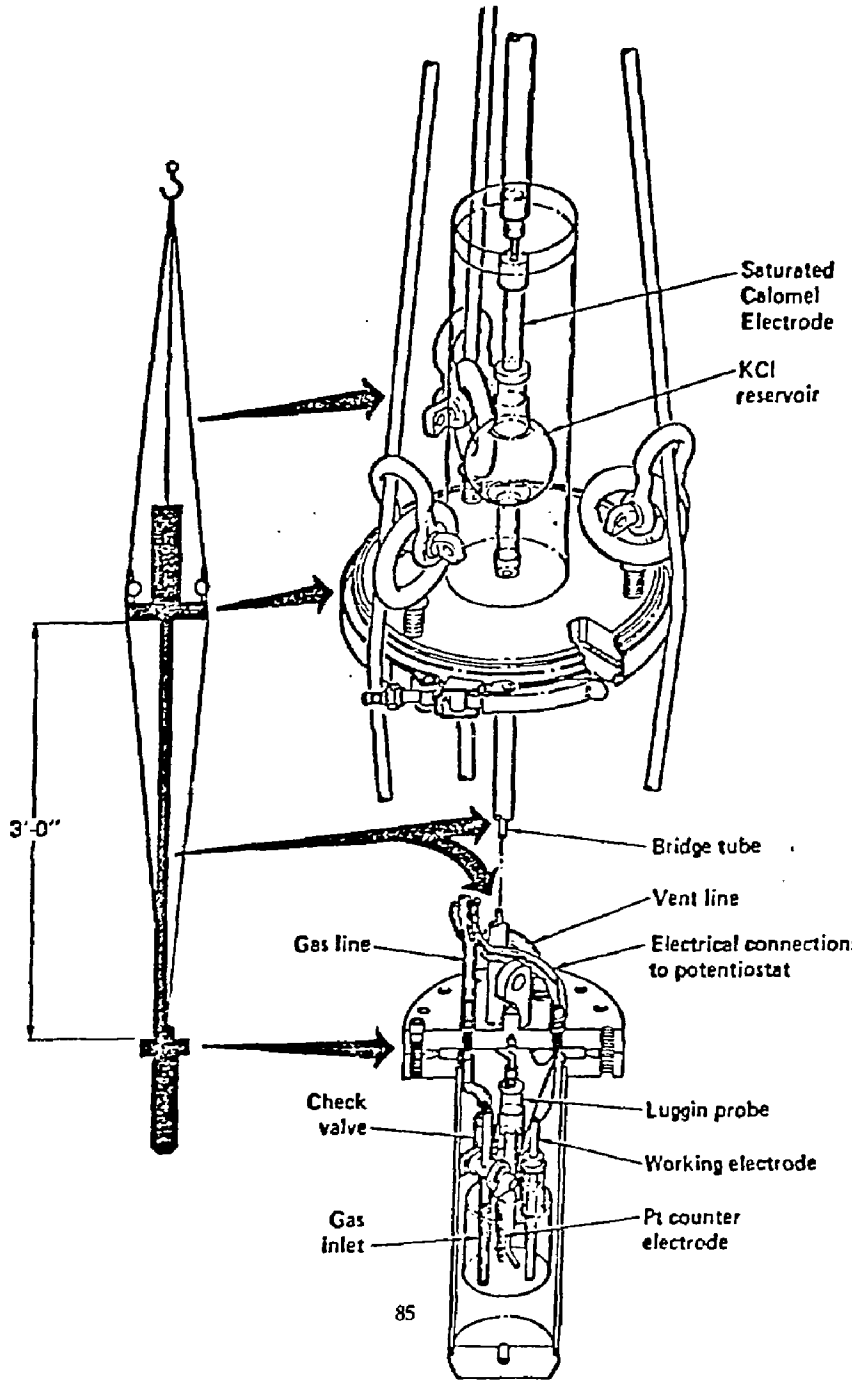

Figure 16. Corrosion potential response behavior for CDA 102. (A) Irradiated in Well J-13 water at 3.3 Mrads/hr; (B) in non-irradiated Well J-13 water to which one drop of 30% H_2O_2 solution was added (0.5 mM); stirred as indicated (Glass et al., 1986).

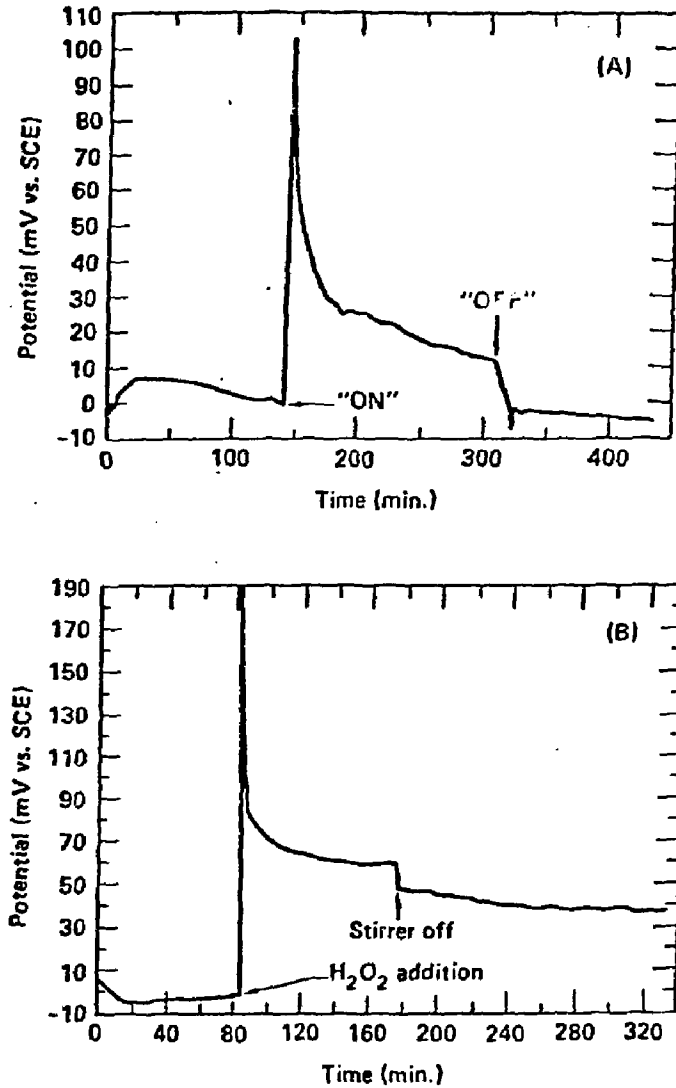

The same effect can be simulated by adding small quantities of hydrogen peroxide to non-irradiated Well J-13 water. Figure 16(b) demonstrates the simulation. This strongly suggests that H_2O_2 is the dominant radiolysis product affecting the electrochemical behavior of copper in irradiated aqueous environments. The enhanced decomposition of H_2O_2 by the catalytic effect of a copper surface was shown to account for the rather rapid decline of the corrosion potential when the test specimen was removed from the gamma source. The catalytic decomposition of H_2O_2 by copper tends to offset the increasing oxidizing characteristics of the environment caused by the formation of this species. The result is that the corrosion rate of copper does not increase by as much as first expected.

Results similar to those for pure copper were also observed for the copper-base alloys. However, the limited results with copper-base alloys indicate that return to the initial steady state value of potential might be somewhat slower than with pure copper. This might be related to the rates of peroxide decomposition and the growth of oxide films. When the Well J-13 electrolyte is concentrated (e.g., to 20x), the potential shifts for pure copper are larger and appear to be longer lasting. Qualitatively, the same effects are observed when irradiation is simulated with peroxide additions. Representative polarization curves for pure copper in 20x concentrated Well J-13 water at 90°C are shown in Fig. 17. Little difference can be observed between the irradiated and non-irradiated curves except that the irradiated curve shows a somewhat more positive corrosion potential. The breakdown potentials are the same in both cases (Glass et al., 1986).

10.5 Corrosion and Oxidation Tests of Copper-Base Materials Under Gamma Irradiation

Glass et al. (1986) conducted one short-term (15-day) 30°C exposure test on a pure copper rod exposed to a 3.3 Mrads/hr gamma field while half-immersed in Well J-13 water, with the top half in contact with moist air. Oxidation occurred on both halves, but the top half experienced more severe attack. X-ray diffraction analysis revealed that the oxide phase formed was Cu_2O. No basic cupric nitrate was found.

More extensive irradiated tests were performed by Yunker at Westinghouse Hanford Co. (Yunker, 1986; and Yunker and Glass, 1987). In this work, weight-loss, crevice, and welded

Figure 17. Polarization curves for CDA 102 in 20x Well J-13 water at 90°C, both out of and in a gamma radiation field. The dose rate in the field was 1 x 10^5 rads/hr. Both scans were run at 1 mV/s starting from the most cathodic potential (Glass et al., 1986).

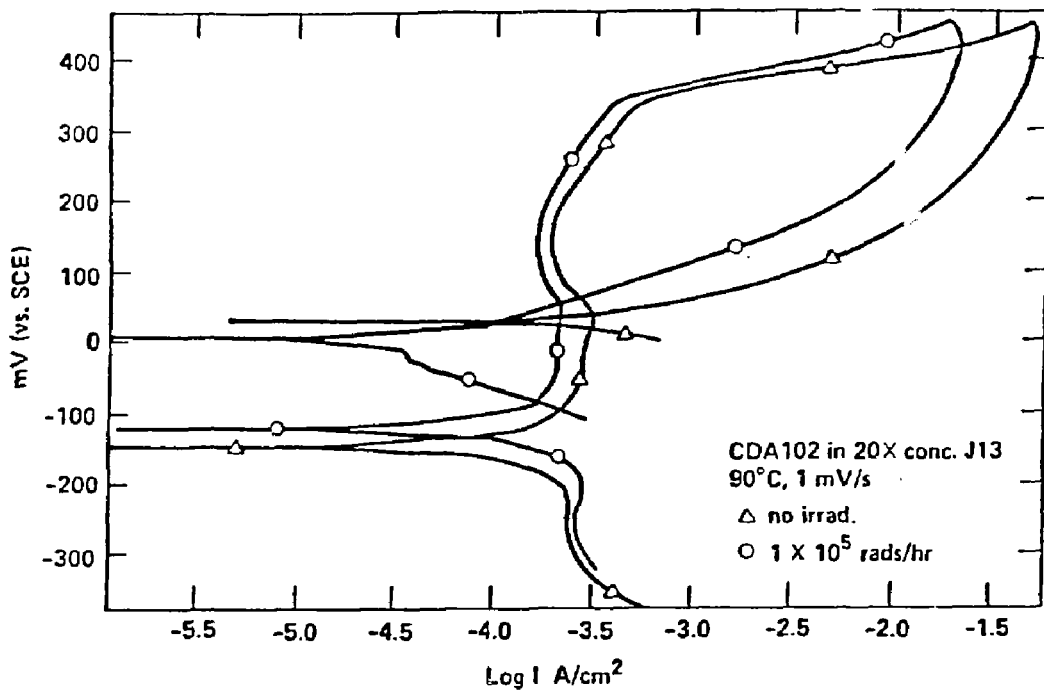

stressed teardrop-shaped samples were exposed to a ^{60}Co gamma radiation field of approximately 1 x 10^5 rads/hr for several thousand hours. CDA 101 (essentially the same as CDA 102), CDA 613, and CDA 715 were tested in 150°C air-water vapor (dry steam), Well J-13 water at 95°C, and water-vapor saturated air at 95°C. Dry or unsaturated steam is a condition where the partial pressure of H_2O vapor is considerably less than the equilibrium vapor pressure at a given temperature, as indicated on a pressure-temperature diagram for water. By comparison, a wet steam or saturated steam environment is one in which the partial pressure of the water vapor is essentially the equilibrium vapor pressure so that the steam condenses on exposed surfaces. A wet steam environment is therefore defined as an aqueous environment, from the standpoint of corrosion.

After exposure, the specimens were examined visually. Then the corrosion films were removed with deaerated hydrochloric acid solution at room temperature. After being rinsed and dried, the specimens were again examined visually at 10x magnification. Weights were measured for the weight-loss specimens. The teardrop specimens were examined for microcracks using fluorescent dye penetrant. Selected specimens were examined by x-ray diffraction and Auger electron spectroscopy. Gas and water compositions were analyzed.

In the initial visual examination of the specimens, the CDA 715 material was found to be covered with a dark, thick layer which had a tendency to spall, leaving small craters in the layer. The crevice corrosion around the support washers on this material was the most severe of that found on any of the specimens. The presence of a copper-colored phase was clearly visible in many of the pits.

A variety of features was observed on the metal surfaces after the corrosion films were removed. Pitting was seen on specimens of each of the three materials, filiform-like (underfilm) corrosion was apparent on a number of the CDA 613 specimens, and enrichment of component metals was common on the surfaces of alloys CDA 613 and CDA 715 (the copper-colored areas were very apparent). The metal surfaces of the CDA 715 specimens were the roughest. Rows of pits and enrichment of component metals (copper-colored regions) were seen along the fusion welds of most of the CDA 613 teardrop specimens. No evidence of stress-assisted cracking was seen in the dye penetrant examination of the teardrop specimens, nor was there any evidence of crevice corrosion on the interior surfaces of the crevice specimen pairs (smooth, flat plates bolted tightly together) or under their tightly fitted alumina support washers. There was evidence of crevice corrosion under the loosely fitting alumina support

washers used on the weight loss specimens and where the alumina support tubes contacted the sides of the teardrop specimens.

Table 13 is a summary of the weight loss and uniform corrosion rate data from 54 specimens. It is important to note that not all of these specimens corroded uniformly, and crevice corrosion was found under some of the support washers. Thus the term "uniform" is used with reservation. For the pure copper specimens, the ranges of values of x in Cu_xO were calculated from the values of metal loss and oxide film weight. The combined uncertainties for these mass values is ±0.12 mg. The ranges of values in Table 14 indicate the effect of this uncertainty on the calculated value of x (i.e., the smallest sample of oxide has the most uncertainty in x). These estimates are not affected by the non-uniform oxide coverage found on some specimens.

For a number of the corrosion films, both electron spectra and profiles of element composition vs. depth were obtained (at Westinghouse Hanford) with an Auger Electron Spectrometer. At the beginning of an analysis, the surfaces of the metal oxide specimens normally show an adsorbed layer containing carbon, chlorine, and occasionally nitrogen. Usually, after a 3- to 5-min sputtering period, most of this surface contamination was gone. The shapes of the concentration vs. depth profiles for oxygen and the metals varied among the different types of specimens. The profile in a thin film on an exposed CDA 613 specimen showed a distinct layer enriched in aluminum, positioned between the outer surface of the oxide and the base metal. The profiles of an oxide film on exposed CDA 715 showed a layer high in nickel content over a layer relatively high in copper content. In the case of pure copper (CDA 101), the AES data provided a measurement of metal-to-oxygen ratio of the film. Values of this ratio, measured near the middle of the films, are included in Table 14.

X-ray diffraction (XRD) analyses were made of the corrosion films on specimens exposed for 1 and 3 mo. Results are summarized in Table 15. These analyses were made with the films intact on the base metal.

It can be seen from Table 13 that the highest corrosion rates for all three materials were observed on the specimens exposed to the air-saturated steam phase at 95°C. A comparison with corrosion rates observed without radiation (Table 16) showed little difference for the CDA 101 and CDA 613, but substantial increases were seen in the corrosion rates of CDA 715 due to irradiation.

Table 13. **Weight loss and uniform corrosion rates.**

	Exposure		Range[a] of	
	Temperature (°C)/phase	Time (hr)	Metal loss (mg)	Corrosion rate (mil/yr)
CDA 101				
	150/gas	836	3.2-3.3	0.068-0.070
		2334	4.3-4.6	0.032-0.035
		4392	7.8	0.031
		10,078	10.2-21.6	0.017-0.018
	95/gas	720	10.5	0.26
		2280	27.13	0.21
		5016	46.2	0.161
	95/liquid	720	4.4-6.6	0.108-0.162
		2280	10.9	0.084
		5016	23.0	0.080
CDA 613				
	150/gas	836	1.1-1.7	0.026-0.040
		2334	2.3	0.019-0.020
		4392	2.6-3.4	0.012-0.015
		10,078	3.6-5.8	0.0071-0.010
	95/gas	720	7.9	0.217
		2280	9.21	0.080
		5016	17.9	0.071
	95/liquid	720	2.7-3.2	0.074-0.088
		2280	8.4	0.073
		5016	11.0	0.044
CDA 715				
	150/gas	836	7.0-10.0	0.015-0.021
		2334	8.4-11.7	0.063-0.088
		4392	7.6-10.5	0.031-0.042
		10,078	18.0-27.6	0.032-0.048
	95/gas	720	19.2	0.47
		2280	70.6	0.54
		5016	64.3	0.22
	95/liquid	720	3.4-4.8	0.083-0.12
		2280	17.7	0.14
		5016	25.7	0.090

[a]Ranges are for a maximum of three specimens.

Table 14. Stoichiometry estimates of Cu_xO[a].

Exposure Temperature (°C)/phase	Exposure Time (mo)	Mole Cu/Mole O
150/gas	1	— [2.4]
	3	1.5-2.9; [2.2]
	6	1.8-2.6
95/gas	1	1.5-1.8
	3	1.6-1.7; [2.3]
	7	1.3-1.4
95/liquid	1	1.4-2.2
	3	0.9-1.0
	7	0.6

[a]The values [x] are from AES measurements in the "bulk" film.

Table 15. Summary of XRD analyses.

	Exposure		
	Temperature (°C)/phase	Time (mo)	Phases identified[a]
CDA 101			
	150/gas	1	Cu_2O, CuO
	150/gas	3	Cu_2O, CuO
	95/gas	1	Cu_2O, CuO
	95/gas	3	M = CuO, tr = Cu_2O
	95/liquid	1	Cu_2O, CuO
	95/liquid	3	Cu_2O, CuO
CDA 613			
	150/gas	1	Al, CuO
	150/gas	3	Al, CuO
	95/gas	1	Al, CuO
	95/gas	3	Al, CuO
	95/liquid	1	Al, CuO
	95/liquid	3	Al, CuO
CDA 715			
	150/gas	1	CuO
	150/gas	3	--
	95/gas	1	CuO
	95/gas	3	S = CuO
	95/liquid	3	M = CuO

[a]All phase entries are at trace levels, unless shown. S = secondary; M = minor; tr = trace. Major copper not shown.

Table 16. Comparison of corrosion rates for copper and copper-base alloys in irradiated and non-irradiated environments, mils/yr (Yunker, 1986 and McCright, 1985).

Alloy	Non-irradiated unsaturated steam, 150°C (~4 mo)	Irradiated unsaturated steam, 150°C (~6 mo)	Non-irradiated saturated steam, 100°C (~8 mo)	Irradiated saturated steam, 95°C (~7 mo)	Non-irradiated Well J-13 water, 100°C (~8 mo)	Irradiated Well J-13 water, 95°C (~7 mo)
CDA 101/102	0.061	0.031	0.124	0.161	0.083	0.080
CDA 613/614	0.014	0.013	0.090	0.071	0.059	0.044
CDA 715	0.002	0.036	0.014	0.22	0.040	0.090

The order of the time dependence of the corrosion process (n) was determined from the slope of the logarithm of the weight loss vs. the logarithm of time. The values of n were found to be 0.59 and 0.45 for CDA 101 and CDA 613, respectively, at 150°C. The data for CDA 715 at 150°C were ambiguous. More data will be required to clarify the order for this case and for the 95°C cases.

The most uniform corrosion was observed on the CDA 101 specimens. Pitting was observed on two specimens of pure copper that had been exposed to the gas phase at 95°C. The most severe attack seen so far on this material appears to be associated with the presence of liquid water and with foreign particles and materials that were embedded in the specimen surface during its manufacture (and not removed by the surface pretreatment). The amount of corrosion on this material appeared to be between the amounts on the two alloys in all three environments. From the AES and XRD studies, the stoichiometries observed in the oxide layers of CDA 101 seemed to be closer to Cu_2O in the oxides produced in the gas phase and closer to CuO for those produced in the liquid phase. On the alloys, only the CuO phase was detected by XRD.

The overall oxidation process is apparently slower for CDA 613 than for CDA 101. The AES data showed a layer of oxidized aluminum between the surface of the oxide layer and the base metal. After removal of the oxide, pitting and filiform-like corrosion (characteristic of aluminum corrosion) were seen in the surface of the metal. Copper-colored phases were clearly visible near many of the pits. From the corrosion pattern found in the welds of the teardrop specimens, it appeared that there also might have been some enrichment of component metals during the process of fusion welding of this material.

The CDA 715 alloy showed severe roughening of the metal surfaces under the oxide layer from corrosion at 95°C in the gas phase. It is not completely clear why CDA 715 behaved as it did. Apparently the layer of corrosion products that forms on this material under irradiated air-steam conditions is not very protective. In past experiments involving irradiation of pure nickel in moist air at 40°C, it was found that hydrated nickel nitrate was formed (Primak and Fuchs, 1954 and 1955). This species is very soluble, and has a low melting point (56.7°C) and a low boiling point (136.7°C) (Weast, 1976).

The observation that the 95°C air and saturated steam environment was the most corrosive under irradiation for CDA 715 probably resulted from the formation of nitric acid and

acid forming nitrogen oxides in the gas phase, which deposited in the liquid films on the specimens that were located in this phase, making their environment more corrosive. In the case of the specimens in the 95°C liquid water phase, the acid concentration never exceeded the buffering capacity of the bicarbonate. In the case of the 150°C gas phase specimens, the temperature was too high for a liquid film to be present on the samples, and also too high for nitric acid to be thermodynamically stable. The increased oxidation rate of irradiated CDA 715 in this region must then have been due to nitrogen oxides, ozone, and/or oxidizing free radicals. The radiation chemistry of the air/Well J-13 water system has been discussed by Van Konynenburg (1986).

The order n of the corrosion process is difficult to interpret. Under non-irradiated conditions at higher temperatures (>200°C), copper exhibits parabolic (n=0.5) oxidation behavior because copper ions diffuse through a cation-deficient protective oxide layer to form new oxide near the external surface of the layer. The oxide phase Cu_2O is thermodynamically stable under normal atmospheric conditions. At lower temperatures, however, migration of the cations is controlled by the gradient of the electric field within the oxide lattice. The theory is discussed by Smeltzer and Young (1975). The oxidation is logarithmically time-dependent up to approximately 150°C, has a cubic time dependence at increased temperatures, and is parabolic at 200°C and above (Kubaschewski and Hopkins, 1962).

Although the details of the corrosion and oxidation behavior of the copper-base materials in irradiated environments are not understood completely, it can be seen from Tables 13 and 16 that the rates are nevertheless low, and these materials remain viable candidates.

11. BOREHOLE LINER MATERIALS

This section is concerned with the performance of a borehole liner that can be designed to achieve at least a 50-yr service life after emplacement of the waste packages, as required in 10CFR60.110, for possible retrieval of the waste packages. Of concern is the effect that the presence of the borehole liner could have on the waste package container. This effect can be favorable (assuming that the liner would sacrificially corrode and protect the container) or unfavorable (soluble corrosion products migrate to the container surface and intensify the attack on this component). On the other hand, if the borehole liners are made of carbon steel, the corrosion products could form ferric silicates which could accelerate the dissolution of the glass

waste forms. Another consideration is that the liner might act as a physical shield to prevent an unanticipated surge of water from coming into contact with the container. The effect of liner corrosion products on radionuclide transport properties is also important. Although these effects are not part of the designed functions of the liner, its presence in the waste package environment can influence the ultimate performance assessment of the container. Initial attention has been paid to carbon steel as a liner material. However, upon further evaluation it is quite possible that the liner material might have to match that of the container. Alternatives such as chromized, aluminized, or other products might also be considered and evaluated.

11.1 Test Results on Carbon Steel

Some corrosion testing of carbon steels and other ferrous materials has been performed in Well J-13 water and in steam (McCright and Weiss, 1985). Results indicate that the general corrosion rates of carbon steel (AISI 1020 steel tested under ASTM A 36) are 27-30 μm/yr in Well J-13 water at 100°C (5000-hr exposure). The corrosion rates decrease with time. In saturated steam at 100°C, the rates are 10-13 μm/yr; in unsaturated steam at 150°C, the rates are 0.4-0.6 μm/yr. Maximum corrosion rates occurred where the accessibility to oxygen was highest, the accessibility being determined by the combination of oxygen solubility and diffusivity. The corrosion attack pattern indicates some localized penetration, but the attack could be better described as surface roughening since the diameters of the pits exceeded their depths. The surface-roughening factor under the tested environmental conditions can be as high as 10-15, but it appears to decrease with increased exposure time. The measured general corrosion rate multiplied by this roughening factor can be used to establish a corrosion allowance for wastage (the effective penetration rate for the material). Stressed bent-beam carbon steel specimens, including welded specimens, have not failed by stress corrosion cracking after more than 10,000 hr of exposure to Well J-13 water. When the different corrosion rates are weighted with regard to the amount of time the carbon steel would be exposed to each environmental condition, it appears that a 1-in.-thick liner would last for 50 yr. Grouts used to secure the liner to the rock might make the environment more alkaline. The corrosion rate of carbon steel characteristically decreases with increases in pH and attains very low levels in the pH range 10-12. No corrosion testing has been performed in Well J-13 water that has been chemically modified by the presence of the grout.

The presence of radiation in the environment is expected to enhance the corrosion rate of carbon steel because of the production of additional oxidizing species. However, some experimental work performed in irradiated Well J-13 water indicated a corrosion enhancement factor of only 1.5. Nonquantitative observations from the spent fuel test in the Climax mine indicated that the liners used around the canisters containing spent fuel showed considerably greater corrosion than those canisters that contained only thermal simulators (Weiss et al., 1985). These differences might be attributable to different environmental conditions. Radiolysis products in the Well J-13 water immersion corrosion tests could be diluted and buffered by the relatively large amount of water used in the tests (crushed rock was also present). In the Climax test, only a limited amount of water was present around the liner (out of contact with the rock formation), and a considerable amount of air was irradiated; therefore, the environmental conditions in the Climax test could have become significantly more aggressive than the environmental conditions in the laboratory tests. More work is needed in a variety of irradiated environments.

11.2 Interaction Effects Between the Borehole Liner and the Container

Interaction of the carbon steel liner with the NNWSI waste package container (austenitic materials or a copper-base material) can occur by: (1) direct metal-to-metal contact, possibly creating a galvanic cell; or (2) the modification of the environment by the corroding metal from one component and transport of the corrosion products to the other component. These interactions are predicated on the presence of water between the components. Carbon steel is the likely anodic component in any galvanic coupling of different metal components, and its corrosion would cathodically protect the other. This protection also would reduce the likelihood of any localized and stress corrosion of the container material, since the cathodic protection provided by the carbon steel would lower the potential on the container material to below the critical potentials for these non-uniform modes of corrosion. Austenitic stainless steels and copper are very resistant to hydrogen embrittlement; therefore, making them the cathode in a galvanic couple should not be detrimental. Although the ferric ions that can be produced by corrosion of the carbon steel liner could induce pitting corrosion attack in either container material, the pH of the groundwater would tend to cause precipitation of the Fe^{+3} as ferric hydroxide so that no enhancement of container corrosion should occur. The opposite effect is that contact of the container with the liner could shorten the service life of the liner by acceleration of its corrosion rate. It is highly unlikely that water intrusion will occur between

the liner and the container during the early years after emplacement, but these interaction effects will need to be addressed and experimentally tested.

As a way of reducing the possible interactions among the waste package and repository components, NNWSI is considering use of a borehole liner made from a material in the same alloy family as the container. In this consideration, the liner material would not need to be fabricated from exactly the same material as the container, but the two materials should have comparable general corrosion rates and little galvanic interaction.

ACKNOWLEDGMENTS

It is a pleasure to thank the present staff members of the Metal Barrier Selection and Testing Task and those individuals who have previously worked on this task for all of their contributions. Several publications by the staff members have been cited in the references. In addition to the staff members co-authoring this report, other staff members have helpfully reviewed drafts of the text and offered valuable suggestions. The work performed by many subcontracting organizations is also appreciated and cited in the references. Last, we wish to thank Sandy Wander of KMI Associates for her diligence in processing the manuscript.

12. REFERENCES

Abe, S., T. Ogawa, S. Iwasaki, K. Hattori, M. Akashi, and R. Kume, 1982. "Development of SCC Resistant 347LP," Predictive Methods for Assessing Corrosion Damage to BWR Piping and PWR Steam Generators, Hideya Okada and Roger Staehle (eds.), National Association of Corrosion Engineers, Houston, TX, pp. 179-186.

Acton, C.F., and R. D. McCright, 1986. FY1986 Final Report to Congress on the Feasibility Assessment of Copper-Base Waste Package Container Materials in a Nuclear Waste Repository, UCID-20847, Lawrence Livermore National Laboratory, Livermore, CA.

Akkaya, M., and E. D. Verink, Jr., 1986. "Electrochemical Corrosion Studies on Copper-Base Waste Package Container Materials in Unirradiated 0.1 N $NaNO_3$ at 95°C," Copper Development Association Inc., Greenwich, CT.

ASM (American Society for Metals), 1961. Metals Handbook, 1, Properties and Selection of Metals, Committee on Corrosion of Copper, Ohio, pp. 983-1005.

ASTM (American Society for Testing and Materials), 1972. Recommended Practice for Laboratory Immersion Corrosion Testing of Metals, G 31-72(1985), ASTM Annual Book of Standards, American Society for Testing and Materials, Philadelphia, PA.

ASTM (American Society for Testing and Materials), 1973. Recommended Practice for Performing Stress-Corrosion Cracking Tests in a Boiling Magnesium Chloride Solution, G 36-73(1981), ASTM Annual Book of Standards, American Society for Testing and Materials, Philadelphia, PA.

ASTM (American Society for Testing and Materials), 1979. Practice for Preparation and Use of Bent-Beam Stress-Corrosion Specimens, G 39-79(1984), ASTM Annual Book of Standards, American Society for Testing and Materials, Philadelphia, PA.

ASTM (American Society for Testing and Materials), 1981. Recommended Practice for Preparing, Cleaning, and Evaluating Corrosion Test Specimens, G 1-81, ASTM Annual Book of Standards, American Society for Testing and Materials, Philadelphia, PA.

ASTM (American Society for Testing and Materials), 1984. Specification for Ni-Fe-Cr-Mo-Cu Alloy (UNS N08825 and N08821) Plate, Sheet, and Strip, B 424-84, ASTM Annual Book of Standards, American Society for Testing and Materials, Philadelphia, PA.

ASTM (American Society for Testing and Materials), 1984. Specification for Stainless and Heat-Resisting Chromium-Nickel Steel Plate, Sheet, and Strip, A 167-84, ASTM Annual Book of Standards, American Society for Testing and Materials, Philadelphia, PA.

ASTM (American Society for Testing and Materials), 1985. Recommended Practices for Detecting Susceptibility to Intergranular Attack in Austenitic Stainless Steels, A 262-85, ASTM Annual Book of Standards, American Society for Testing and Materials, Philadelphia, PA.

Bandy, R., and D. van Rooyen, 1985. "Properties of Nitrogen-Containing Stainless Alloy Designed for High Resistance to Pitting," Corrosion, Vol. 41, pp. 228-233.

Barnartt, S., 1977. "Electrochemical Nature of Corrosion," Electrochemical Techniques for Corrosion, R. Baboian (ed.), National Association of Corrosion Engineers, Houston, TX, pp. 1-10.

Benjamin, L. A. , D. Hardie, and R. N. Parkins, 1983. "Investigation of the Stress Corrosion Cracking of Pure Copper," Report No. SKBF-KBS-TR-83-06, University of Newcastle upon Tyne, England.

Bianchi G., A. Cerquetti, F. Mazza, and S. Torchio, 1974. "Pitting Corrosion of Austenitic Stainless Steels and Properties of Surface Oxide Films," Localized Corrosion NACE-3, R. W. Staehle, B. F. Brown, J. Kruger, and A. Agrawal (eds.), National Association of Corrosion Engineers, Houston, TX, pp. 399-409.

Bingham, R. J., 1974. "Pitting and Crevice Corrosion Resistance of Commercial 18% Cr Stainless Steels," Materials Performance, Vol. 13, pp. 29-34.

Briant, C. L., 1982. Effects of Nitrogen and Cold Work on the Sensitization of Austenitic Stainless Steels, Final Report NP-2457, EPRI Research Project 1574-1, Palo Alto, CA.

Briant, C. L., R. A. Mulford, and E. L. Hall, 1982. "Sensitization of Austenitic Stainless Steels I. Controlled Purity Alloys," Corrosion, Vol. 38, pp. 468-477.

Bruemmer, S. M., and A. B. Johnson Jr., 1984. "Effect of Chloride, Thiosulfate, and Fluoride Additions on the IGSCC Resistance of Type 304 Stainless Steel in Low Temperature Water," Proceedings of International Symposium on Environmental Degradation of Materials in Nuclear Power Systems-Water Reactors, August 22-25, 1983, Myrtle Beach, SC, National Association of Corrosion Engineers, Houston, TX, pp. 571-582.

Clarke, W. L., R. L. Cowan, and W. L. Walker, 1978. "Comparative Methods for Measuring Degree of Sensitization in Stainless Steel," Intergranular Corrosion of Stainless Alloys, ASTM STP 656, R. F. Steigerwald (ed.), American Society for Testing and Materials, Philadelphia, PA, pp. 99-132.

Cowan, R. L., II, and G. M. Gordon, 1977. "Intergranular Stress Corrosion Cracking and Grain Boundary Composition of Fe-Ni-Cr Alloys," Stress Corrosion Cracking and Hydrogen Embrittlement of Iron Base Alloys NACE-5, R. W. Staehle, J. Hochmann, R. D. McCright, and J. E. Slater (eds.), National Association of Corrosion Engineers, Houston, TX, pp. 1023-1070.

DaCasa, C., V. B. Nileshwar, and D. A. Melford, 1969. "M23C6 Precipitation in Unstabilized Austenitic Stainless Steel," Journal of the Iron and Steel Institute, pp. 1325-1332.

Danko, J., 1984. "Recent Observations of Cracks in Large Diameter BWR Piping: Analysis and Remedial Actions," Proceedings of the International Symposium on Environmental Degradation of Materials in Nuclear Power Systems -- Water Reactors, National Association of Corrosion Engineers, Houston, TX, pp. 209-222.

Duhaj, P., J. Ivan, and F. Makovicky, 1968. "Sigma Phase Precipitation in Austenitic Steels," Journal of the Iron and Steel Institute, pp. 1245-1251.

Evans, U. R., 1976. The Corrosion and Oxidation of Metals, Second Supplementary Volume, Butler & Tanner Ltd., Frome and London.

Fontana, M. G., and N. D. Greene, 1978. Corrosion Engineering, McGraw-Hill, New York, NY.

Fox, M. J., and R. D. McCright, 1983. An Overview of Low Temperature Sensitization, UCRL-15619, Lawrence Livermore National Laboratory, Livermore, CA.

Fujita, N., M. Akiyama, and T. Tamura, 1981. "Stress Corrosion Cracking of Sensitized Type 304 Stainless Steel in High Temperature Water Under Gamma Ray Irradiation," Corrosion, Vol. 37, National Association of Corrosion Engineers, Houston, TX, pp. 335-341.

Glass, R. S., G. E. Overturf, R. E. Garrison, and R. D. McCright, 1984. Electrochemical Determination of the Corrosion Behavior of Candidate Alloys Proposed for Containment of High Level Nuclear Waste in Tuff, UCID-20174, Lawrence Livermore National Laboratory, Livermore, CA.

Glass, R. S., G. E. Overturf III, R. A. Van Konynenburg, and R. D. McCright, 1985. Gamma Radiation Effects on Corrosion: I Electrochemical Mechanisms for the Aqueous Corrosion Processes of Austenitic Stainless Steels, UCRL-92311, Lawrence Livermore National Laboratory, Livermore, CA.

Glass, R. S., R. A. Van Konynenburg, and G. E. Overturf, 1986. "Corrosion Processes of Austenitic Stainless Steels and Copper-Based Materials in Gamma-Irradiated Aqueous Environments," presented at Corrosion/86, Houston, Texas, March 1986, National Association of Corrosion Engineers; also Lawrence Livermore National Laboratory, Livermore, CA, UCRL-53726.

Glassley, W. E., 1986. Reference Waste Package Environment Report, UCRL-53726, Lawrence Livermore National Laboratory, Livermore, CA.

Gordon, G. M., 1977. "Physical Metallurgy of Fe-Cr-Ni Alloys," Stress Corrosion Cracking and Hydrogen Embrittlement of Iron Base Alloys, NACE-5, National Association of Corrosion Engineers, Houston, TX.

Hale, D. A., and A. E. Pickett, 1986. "Materials Performance in a Startup Environment – Final Technical Report, May 1981-June 1984," G. E. Report NEDC-31335.

Hochmann, J., A. Desestret, P. Jolly, and R. Mayoud, 1977. "Properties of High-Chromium Ferritic Stainless Steels and Austeno0Ferritic Stainless Steels," Stress Corrosion Cracking and Hydrogen Embrittlement of Iron Base Alloys, NACE-5, National Association of Corrosion Engineers, Houston, TX.

Hockman, J. N., and W. C. O'Neal, 1984. Thermal Modeling of Nuclear Waste Package Designs for Disposal in Tuff, UCRL-8920 Rev. 1, Lawrence Livermore National Laboratory, Livermore, CA.

Iwasaki, S., 1982. "Methods for Preventing and Ameliorating Cracks in BWR Piping," Predictive Methods for Assessing Corrosion Damage to BWR Piping and PWR Steam Generators, H. Okada and R. Staehle (eds.), National Association of Corrosion Engineers, Houston TX, pp. 144-152.

Juhas, M. C., R. D. McCright, and R. E. Garrison, 1984. Behavior of Stressed and Unstressed Specimens in Tuff Repository Environmental Conditions, UCRL-91804, Lawrence Livermore National Laboratory, Livermore, CA.

Kekkonen, T., P. Aaltonen, and H. Hanninen, 1985. "Metallurgical Effects on the Corrosion Resistance of a Low Temperature Sensitized Welded AISI Type 304 Stainless Steel," Corrosion Science, Vol. 25, No. 8/9, pp. 821-836.

Klement, J. F., R. E. Maersch, and P. A. Tully, 1959. "Licking the Problem of Stress Corrosion Cracking," Metal Progress, 75, No. 2, p. 82.

Kubaschewski, O. and B. E. Hopkins, 1962. Oxidation of Metals and Alloys, Butterworths, London, pp. 249-253.

Latanision, R. M., and R. W. Staehle, 1969. "Stress Corrosion Cracking of Iron-Nickel-Chromium Alloys," Proceedings of Conference: Fundamental Aspects of Stress Corrosion Cracking, National Association of Corrosion Engineers, Houston, TX, pp. 214-307.

Logan, R. W., 1983. Computer Simulation of Sensitization in Stainless Steels, UCID-20000, Lawrence Livermore National Laboratory, Livermore, CA.

Majidi, A. P., and M. A. Streicher, 1984. "Potentiodynamic Reactivation Method for Detecting Sensitization in AISI 304 and 304L Stainless Steels," Corrosion, Vol. 40, National Association of Corrosion Engineers, Houston, TX, pp. 393-408.

Mansfeld, F., 1977. "Polarization Resistance Measurements – Experimental Procedure and Evaluation of Test Data," Electrochemical Techniques for Corrosion, R. Baboian (ed.), National Association of Corrosion Engineers, Houston, TX, pp. 18-26.

McCright, R.D., 1985. FY 1985 Status Report on Feasibility Assessment of Copper-Base Waste Package Container Materials in a Tuff Repository, UCID-20509, Lawrence Livermore National Laboratory, Livermore, CA.

McCright, R. D., and H. Weiss, 1985. Corrosion Behavior of Carbon Steels Under Tuff Repository Environmental Conditions, Mat. Res. Soc. Symp. Proceedings, Vol. 44, Materials Research Society.

McCright, R. D., H. Weiss, M. C. Juhas, and R. W. Logan, 1983. Selection of Candidate Canister Materials for High-Level Nuclear Waste Containment in a Tuff Repository, UCRL-89988, Lawrence Livermore National Laboratory, Livermore, CA.

Morales, A., 1985. Technical Correspondence in Support of the Final Environmental Assessment, SAND85-2509, Sandia National Laboratories, Albuquerque, NM.

Mozhi, T. A., W. A. T. Clark, K. Nishimoto, W. B. Johnson, and D. D. MacDonald, 1985. "The Effect of Nitrogen on the Sensitization of AISI 304 Stainless Steel," Corrosion–NACE, Vol. 41, No. 10, National Association of Corrosion Engineers, pp. 555-559.

Mulford, M. A., E. L. Hall, and C. L. Briant, 1983. "Sensitization of Austenitic Stainless Steels II. Commercial Purity Alloys," Corrosion, Vol. 39, National Association of Corrosion Engineers, Houston, TX, pp. 132-143.

Myers, J. R., 1986. "Corrosion and Oxidation of Copper and Selected Copper Alloys in Air, Steam, and Water at Temperatures up to 300°C: A Review of the Literature," Copper Development Association Inc., Greenwich, CT.

Novak, C. J., 1977. "Structure and Constitution of Wrought Austenitic Stainless Steels," Handbook of Stainless Steels, D. Peckner and I. M. Bernstein (eds.), McGraw-Hill, New York, NY.

Nuttall K., and V. F. Urbanic, 1981. "An Assessment of Materials for Nuclear Fuel Immobilization Containers," AECL-6440, Atomic Energy of Canada Limited, Pinawa, Manitoba, CANADA, pp. 94-102 and pp. 107-111.

Ogard, A. E., and J. F. Kerrisk, 1984. Groundwater Chemistry Along Flow Paths Between a Proposed Repository Site and the Accessible Environment, Los Alamos National Laboratory, Los Alamos, NM, LA-10188-MS.

Okada, T., 1984. "Halide Nuclei Theory of Pit Initiation in Passive Metals," J. Electrochem. Soc., Vol. 131, No. 2, pp. 241-247.

O'Neal, W. C., D. W. Gregg, J. N. Hockman, E. W. Russell, and W. Stein, 1984. Preclosure Analysis of Conceptual Waste Package Designs for a Nuclear Waste Repository in Tuff, UCRL-53595, Lawrence Livermore National Laboratory, Livermore, CA.

Oversby, V. M., 1985. The Reaction of Topopah Spring Tuff with J-13 Water at 150°C -- Samples from Drill Cores USW G-1, USW GU-3, USW G-4, and UE-25h#1, UCRL-53629, Lawrence Livermore National Laboratory, Livermore, CA.

Oversby, V. M., and K. G. Knauss, 1983. Reaction of Bullfrog Tuff with J-13 Well Water at 90°C and 150°C, UCRL-53442, Lawrence Livermore National Laboratory, Livermore, CA.

Oversby, V. M., and R. D. McCright, 1984. Laboratory Experiments Designed to Provide Limits on the Radionuclide Source Term for the NNWSI Project, UCRL-91257, Lawrence Livermore National Laboratory, Livermore, CA.

Parkins, R. N., 1979. "Development of Strain-Rate Testing and Its Implications," Stress Corrosion Cracking -- The Slow Strain-Rate Technique, ASTM STP 665, G. M. Ugiansky and J. H. Payer (eds.), American Society for Testing and Materials, Philadelphia, PA, pp. 5-25.

Payer, J. H., W. E. Berry, and W. K. Boyd, 1979. "Evaluation of Slow Strain-Rate Stress Corrosion Test Results," Stress Corrosion Cracking -- The Slow Strain-Rate Technique, ASTM STP 665, G. M. Ugiansky and J. H. Payer (eds.), American Society for Testing and Materials, Phildelphia, PA, pp. 61-77.

Pessall, N., and J. I. Nurminen, 1974. "Development of Ferritic Stainless Steels for Use in Desalination Plants," Corrosion, Vol. 30, p. 381.

Pickering, H. W., and R. P. Frankenthal, 1972. J. Electrochem. Soc., Vol. 118, No. 10, pp. 1297-1304.

Povich, M. J., 1978. "Low Temperature Sensitization of Welded Type 304 Stainless Steel," Corrosion, Vol. 34, National Association of Corrosion Engineers, Houston, TX, pp. 60-65.

Primak, W., and L. H. Fuchs, 1954. "Transportation of Matter and Radioactivity by Ionized Air Corrosion," Physics Today, Vol. 7, p. 15.

Proebstle, R. A., and G. M. Gordon, 1982. "Overview of Predictive Testing for BWR Piping Corrosion," Predictive Methods for Assessing Corrosion Damage to BWR Piping and PWR Steam Generators, Hideya Okada and Roger Staehle (eds.), National Association of Corrosion Engineers, Houston, TX, pp. 19-30.

Reed, D. T., and G. L. Underberg, 1986. "Shielding Analysis in Support of the OCRWM Status Report on Copper: Scoping Calculations for NNWSI," personal communications, Rockwell International, Richland, WA.

Russell, E. W., R. D. McCright, and W. C. O'Neal, 1983. Containment Barrier Metals for High-Level Waste Packages in a Tuff Repository, UCRL-53449, Lawrence Livermore National Laboratory, Livermore, CA.

SAE (Society of Automotive Engineers, Inc.), 1977. Unified Numbering System for Metals and Alloys, Publication SAE HSIU 86a, Warrendale, PA.

Sato, S., and K. Nagata, 1974. "Stress Corrosion Cracking of Cu Alloys in Pure Steam and Water at High Temperatures," Corros. Eng., Vol. 23, p. 125.

Sedricks, A. J., 1979. Corrosion of Stainless Steels, John Wiley & Sons, New York, NY, Chapter 2.

Shreir, L. L., 1977. Corrosion, Volume 1, Metal/Environment Reactions, Newnes-Butterworths, London, England.

Smeltzer, W. W. and D. J. Young, 1975. "Oxidation Properties of Transition Metals," Progress in Solid-State Chemistry, Vol. 10, Part 1, pp. 17-54.

Smith, A. F., 1975. "The Diffusion of Chromium in Type 316 Stainless Steel," Metal Science, Vol. 9, pp. 375-378.

Smith, H. D., 1987. "An Experimental Investigation of Copper-Zircaloy Interactions Under Potential Tuff Repository Conditions," Westinghouse Report No. HEDL-7619 (in preparation).

Staehle, R. W., 1971. "Stress Corrosion Cracking of the Fe-Cr-Ni Alloy System," The Theory of Stress Corrosion Cracking in Alloys, J. C. Scully (ed.), National Atlantic Treaty Organization Scientific Affairs Division, Brussels, Belgium.

Stoecker, J. G., and D. H. Pope, 1986. "Study of Biological Corrosion in High Temperature Demineralized Water," Materials Performance, Vol. 25, pp. 51-56.

Streicher, M. A., 1978. "Theory and Application of Evaluation Tests for Detecting Susceptibility to Intergranular Attack in Stainless Steels and Related Alloys -- Problems and Opportunities," Intergranular Corrosion of Stainless Alloys, ASTM STP 656, R. F. Steigerwald (ed.), American Society for Testing and Materials, Philadelphia, PA, pp. 3-84.

Szklarska-Smialowska, S., 1974. "The Pitting of Iron-Chromium-Niclel Alloys," Localized Corrosion NACE-3, R. W. Staehle, B. F. Brown, J. Kruger and A. Agrawal (eds.), National Association of Corrosion Engineers, Houston TX, pp. 312-341.

Theus, G. J., and R. W. Staehle, 1977. "Review of Stress Corrosion Cracking and Hydrogen Embrittlement in the Austenitic Fe-Cr-Ni Alloys," Stress Corrosion Cracking and Hydrogen Embrittlement of Iron-Base Alloys, National Association of Corrosion Engineers, Houston, TX, pp. 845-892.

Thompson, D. H., and A. W. Tracy, 1944. Trans. AIME, Vol. 185, p. 100.

Truman, J. E., 1977. "The Influence of Chloride Content, pH and Temperature of Test Solution on the Occurrence of Stress Corrosion Cracking with Austenitic Stainless Steel," Corrosion Science, Vol. 17, pp. 737-746.

Uhlig, H. H., 1963. Corrosion and Corrosion Control. An Introduction to Corrosion Science and Engineering, John Wiley & Sons Inc., New York, NY.

Urquidi-MacDonald, M., D. D. MacDonald, and S. Lenhart, 1987. "Mathematical Models for the Redox Potential and Corrosion Potentials for High Level Nuclear Waste Canisters in Tuff Environments," Final Report, SRI Project PYD-8292.

Van Konynenburg, R. A., 1986. "Radiation Chemical Effects in Experiments to Study the Reaction of Glass in a Gamma-Irradiated Air, Groundwater, and Tuff Environment," Lawrence Livermore National Laboratory, Livermore, CA, UCRL-53719.

Verink, E. D., Jr., 1977. "Application of Electrochemical Techniques in the Development of Alloys for Corrosive Environments," Electrochemical Techniques for Corrosion, R. Baboian (ed.), National Association of Corrosion Engineers, Houston, TX, pp. 43-52.

Weast, R. C., 1976. Handbook of Chemistry and Physics, 57th ed. CRC Press, Inc., Cleveland, OH.

Wegrzyn J., and A. Klimpel, 1981. "The Effect of Alloying Elements on Sigma Phase Formation in 18-8 Weld Metals," Welding Journal, pp. 146S-154S.

Weiss, H., R. A. Van Konynenburg, and R. D. McCright, 1985. Metallurgical Analysis of a 304L Stainless Steel Canister from the Spent Fuel Test--Climax, UCID-20436, Lawrence Livermore National Laboratory, Livermore, CA.

Westerman, R. E., S. G. Pitman, and J. H. Haberman, 1987. Corrosion Testing of Type 304L Stainless Steel in Tuff Groundwater Environments, PNL-5829 (in preparation), Pacific Northwest Laboratories, Richland, WA.

Wilde, B. E., 1974. "On Pitting and Protection Potentials: Their Use and Possible Misuses for Predicting Localized Corrosion Resistance of Stainless Alloys in Halide Media," Localized Corrosion NACE-3, R. W. Staehle, B. F. Brown, J. Kruger, A. Agrawal (eds.), National Association of Corrosion Engineers, Houston, TX, pp. 342-352.

Williams, W. L., 1957. "Chloride and Caustic Stress Corrosion of Austenitic Stainless Steel in Hot Water and Steam," Corrosion, Vol. 13, p. 539t.

Wilson, I. L. W., and R. G. Aspden, 1977. "Caustic Stress Corrosion Cracking of Iron-Nickel-Chromium Alloys," Stress Corrosion Cracking and Hydrogen Embrittlement of Iron-Base Alloys, National Association of Corrosion Engineers, Houston, TX, pp. 1189-1204.

Yunker, W. H., 1986. "Corrosion of Copper-Base Materials in Gamma Radiation," Hanford Engineering Development Laboratory, Richland, WA, HEDL-7612.

Yunker, W., and R. Glass, 1987. Long-Term Corrosion Behavior of Copper-Based Materials in a Gamma-Irradiated Environment, in Materials Research Society Symposium Proceedings, Vol. 84, pp. 579-590, Boston, MA (December 1-5, 1986); also available as UCRL-94500, April 1987, Lawrence Livermore National Laboratory, Livermore, CA.